

**STABILIZATION OF MARGINAL LATERITIC SOIL BY  
HIGH CALCIUM FLY ASH BASED GEOPOLYMER  
WITH CALCIUM CARBIDE RESIDUE AND  
GROUND GRANULATED BLAST  
FURNACE SLAG AS ADDITIVES**



**A Thesis Submitted in Partial Fulfillment of the Requirements for the  
Degree of Doctor of Philosophy in Construction  
and Infrastructure Management  
Suranaree University of Technology  
Academic Year 2015**

การปรับปรุงดินลูกรังด้วยคุณภาพด้วยเถ้าลอยแคลเซียมสูงจีไอโพลีเมอร์ผสม  
กากแคลเซียมคาร์ไบด์และตะกรันเตาหลอมบดย่อย



วิทยานิพนธ์นี้เป็นส่วนหนึ่งของการศึกษาตามหลักสูตรปริญญาวิศวกรรมศาสตรดุษฎีบัณฑิต  
สาขาวิชาการบริหารงานก่อสร้างและสาธารณูปโภค  
มหาวิทยาลัยเทคโนโลยีสุรนารี  
ปีการศึกษา 2558

**STABILIZATION OF MARGINAL LATERITIC SOIL BY HIGH  
CALCIUM FLY ASH BASED GEOPOLYMER WITH CALCIUM  
CARBIDE RESIDUE AND GROUND GRANULATED BLAST  
FURNACE SLAG AS ADDITIVES**

Suranaree University of Technology has approved this thesis submitted in partial fulfillment of the requirements for the Degree of Doctor of Philosophy

Thesis Examining Committee

---

(Prof. Dr. Arul Arulrajah)

Chairperson

---

(Prof. Dr. Suksun Horpibulsuk)

Member (Thesis Advisor)

---

(Assoc. Prof. Dr. Avirut Chinkulkijniwat)

Member

---

(Assoc. Prof. Dr. Panich Voottipruex)

Member

---

(Dr. Cherdasak Suksiripattanapong)

Member

---

(Prof. Dr. Sukit Limpijumnong)

Vice Rector for Academic Affairs  
and Innovation

---

(Assoc. Prof. Flt. Lt. Dr. Kontorn Chamniprasart)

Dean of Institute of Engineering

อิทธิกร ภูมิพันธ์ : การปรับปรุงดินลูกรังด้วยเถ้าลอยแคลเซียมสูง  
จีโอโพลิเมอร์ผสมกากแคลเซียมคาร์ไบด์และตะกรันเตาหลอมบดย่อย (STABILIZATION  
OF MARGINAL LATERITIC SOIL BY HIGH CALCIUM FLY ASH BASED  
GEOPOLYMER WITH CALCIUM CARBIDE RESIDUE AND GROUND  
GRANULATED BLAST FURNACE SLAG AS ADDITIVES) อาจารย์ที่ปรึกษา :  
ศาสตราจารย์ ดร.สุขสันต์ หอพิบูลสุข, 177 หน้า

โดยทั่วไปแล้ววัสดุที่ด้วยคุณภาพหรือไม่ผ่านมาตรฐานสำหรับงานก่อสร้างทางนั้น จะทำการปรับปรุงคุณภาพด้วยปูนซีเมนต์ อย่างไรก็ดี ตามกระบวนการผลิตปูนซีเมนต์จะใช้พลังงานในกระบวนการผลิตสูงและยังปล่อยก๊าซคาร์บอนไดออกไซด์ขึ้นสู่ชั้นบรรยากาศเป็นจำนวนมาก ดังนั้น จีโอโพลิเมอร์จึงเป็นวัสดุทางเลือกที่ดี เป็นมิตรกับสิ่งแวดล้อม มีคุณสมบัติด้านวิศวกรรมที่ดีหลายอย่าง รวมทั้งการให้กำลังและความทนทานสูง วิทยานิพนธ์นี้ จะศึกษาความเป็นไปได้ของการปรับปรุงดินลูกรังด้วยเถ้าลอยจีโอโพลิเมอร์ และใช้กากแคลเซียมคาร์ไบด์และตะกรันเตาหลอมบดย่อย เป็นสารเพิ่มเติมลงในระบบ เพื่อให้บรรลุเป้าหมายดังกล่าว วิทยานิพนธ์นี้ประกอบด้วยสามส่วนหลัก ส่วนแรกนำเสนอปัจจัยของตัวเร่งปฏิกิริยาและระยะเวลาการบ่มที่มีอิทธิพลต่อกำลังอัดและโครงสร้างทางจุลภาคของดินลูกรังที่ปรับปรุงด้วยเถ้าลอยแคลเซียมสูงจีโอโพลิเมอร์ ซึ่งเป็นนวัตกรรมใหม่ทางด้านวิศวกรรมงานทาง สารละลายตัวเร่งปฏิกิริยาเป็นส่วนผสมของโซเดียมซิลิเกตและสารละลายโซเดียมไฮดรอกไซด์ ในสัดส่วนต่างๆ ผลการศึกษาในส่วนแรกพบว่ากำลังอัดเพิ่มขึ้นตามระยะเวลาการบ่ม และกำลังอัดที่อายุ 7 วัน ของตัวอย่างทั้งหมดผ่านเกณฑ์มาตรฐานงานชั้นรองพื้นทางและชั้นพื้นทางของหน่วยงานด้านงานทางของประเทศไทย กำลังอัดสูงสุดที่อายุบ่ม 7 วัน พบได้จากตัวอย่างที่ผสมด้วยสัดส่วนโซเดียมซิลิเกตต่อสารละลายโซเดียมไฮดรอกไซด์ 90:10 และกำลังอัดสูงสุดที่อายุบ่ม 90 วัน พบที่สัดส่วนโซเดียมซิลิเกตต่อสารละลายโซเดียมไฮดรอกไซด์ 50:50

งานวิจัยในส่วนที่สอง นำเสนอกำลังอัดและลักษณะ โครงสร้างทางจุลภาคของดินลูกรังที่ปรับปรุงด้วยเถ้าลอยจีโอโพลิเมอร์กับกากแคลเซียมคาร์ไบด์ ภายใต้ปัจจัยที่มีอิทธิพลแตกต่างกัน (อายุการบ่ม สัดส่วนของโซเดียมซิลิเกตต่อสารละลายโซเดียมไฮดรอกไซด์ และสัดส่วนของกากแคลเซียมคาร์ไบด์) โดยศึกษาโครงสร้างทางจุลภาคด้วยกล้องจุลทรรศน์อิเล็กตรอนแบบส่องผ่านเพื่อวิเคราะห์ปัจจัยที่มีผลต่อการพัฒนากำลังของตัวอย่าง สำหรับทุกตัวอย่างที่ผสมด้วยตัวเร่งปฏิกิริยาทุกสัดส่วนที่อายุ 7 วัน มีกำลังอัดเพิ่มขึ้นตามสัดส่วนของกากแคลเซียมคาร์ไบด์ที่เพิ่มขึ้นด้วยเหตุนี้ ผลกระทบของจีโอโพลิเมอร์ก็เกิดขึ้นมากด้วยเช่นกัน สัดส่วนของกากแคลเซียมคาร์ไบด์

ที่ทำให้กำลังสูงสุดจะอยู่ที่ร้อยละ 20 หากเพิ่มสัดส่วนของกากแคลเซียมคาร์ไบด์ในระบบที่ร้อยละ 30 จะทำให้ตัวอย่างเกิดรูปพรุนคล้ายฟองน้ำและผิวเผินจะเกิดรอยแตก กำลังอัดสูงสุดที่อายุบ่ม 90 วัน คือ 18.80 เมกะปาสกาล พบที่สัดส่วนโซเดียมซิลิเกตต่อสารละลายโซเดียมไฮดรอกไซด์ 90:10 ผสมด้วยกากแคลเซียมคาร์ไบด์ ร้อยละ 20

งานวิจัยในส่วนสุดท้าย นำเสนอกำลังอัดของดินลูกรังที่ปรับปรุงแล้วโดยจีโอโพลิเมอร์กับ ตะกรันเตาหลอมบดย่อยเป็นตัวผสมเพิ่ม การพัฒนาโครงสร้างทางจุลภาคของตัวอย่าง ศึกษาโดยใช้ กล้องจุลทรรศน์อิเล็กตรอนแบบส่องผ่านและการวิเคราะห์ห้องปฏิบัติการด้วยเทคนิคการ เลี้ยวเบนของรังสีเอ็กซ์ ปัจจัยสำคัญที่ศึกษาในครั้งนี้ประกอบด้วย สัดส่วนของตะกรันเตาหลอมบด ย่อย สัดส่วนของโซเดียมซิลิเกตต่อสารละลายโซเดียมไฮดรอกไซด์ และ ระยะเวลาการบ่ม กำลังอัด ที่อายุ 7 วัน ของตัวอย่างดินลูกรังแล้วโดยจีโอโพลิเมอร์ผสมด้วยตะกรันเตาหลอมบดย่อย ผ่านเกณฑ์ มาตรฐานงานชั้นรองพื้นทางและชั้นพื้นทางของหน่วยงานด้านงานทางของประเทศไทย กำลังอัด สูงสุดที่อายุบ่ม 60 วันคือ 19.97 เมกะปาสกาล พบที่สัดส่วน โซเดียมซิลิเกตต่อสารละลายโซเดียม ไฮดรอกไซด์ 90:10 และสัดส่วนตะกรันเตาหลอมบดย่อยร้อยละ 10 ผลลัพธ์ที่เกิดขึ้นของตัวอย่าง ดินลูกรังแล้วโดยจีโอโพลิเมอร์ผสมด้วยตะกรันเตาหลอมบดย่อย ประกอบด้วย โซเดียมอลูมิโนซิลิเกตไฮดรต แคลเซียมซิลิเกตไฮดรต และแคลเซียมไฮดรต ผลการวิจัยที่ได้ในครั้งนี้จะช่วยให้มีการนำ กากแคลเซียมคาร์ไบด์และตะกรันเตาหลอมบดย่อย ซึ่งเป็นวัสดุเหลือใช้ มาใช้ประโยชน์ในงาน ปรับปรุงวัสดุสำหรับงานทางด้วยจีโอโพลิเมอร์

สาขาวิชา วิศวกรรมโยธา

ปีการศึกษา 2558

ลายมือชื่อนักศึกษา \_\_\_\_\_

ลายมือชื่ออาจารย์ที่ปรึกษา \_\_\_\_\_

ITTHIKORN PHUMMIPHAN : STABILIZATION OF MARGINAL  
LATERITIC SOIL BY HIGH CALCIUM FLY ASH BASED  
GEOPOLYMER WITH CALCIUM CARBIDE RESIDUE AND GROUND  
GRANULATED BLAST FURNACE SLAG AS ADDITIVES. THESIS  
ADVISOR : PROF. SUKSUN HORPIBULSUK, Ph.D., 177 PP.

GEOPOLYMER/FLY ASH / STRENGTH/ CALCIUM CARBIDE RESIDUE/ SLAG

Marginal soils are traditionally stabilized with Portland Cement (PC) when used as a pavement material. The production of PC is however an energy-intensive process and emits a large amount of greenhouse gas into the atmosphere. Geopolymer is an alternative environmentally friendly “green” binder, which has many advantageous properties, including high strength and durability. This research investigated the possibility of stabilization of marginal lateritic soil (LS) by Fly Ash (FA) based geopolymer with Calcium Carbide Residue (CCR) and Ground Granulated Blast Furnace Slag (GBFS) as additives. To achieve this goal, this thesis consists of three main parts. First part presents the effects of alkali activator and curing time on Unconfined Compression Strength (UCS) and microstructural characteristics of LS stabilized with high calcium fly ash (FA)-based geopolymer, which is novel in the field of pavement geotechnics. A liquid alkali activator was a mixture of sodium silicate ( $\text{Na}_2\text{SiO}_3$ : NS) solution and sodium hydroxide (NaOH: NH) solution at various NS:NH ratios. The results showed that the UCS increased with the curing time and the 7-day UCS for all NS:NH ratios tested meets the local national standard as pavement bound material. The maximum 7-day UCS were found at NS:NH of 90:10 and the maximum 90-day UCS was found at a NS:NH ratio of 50:50.

Second part presents UCS and microstructural characteristic of LS stabilized by FA geopolymer with CCR as an additive under different influential factors (curing times, NS:NH ratios and CCR replacement ratios). Scanning Electron Microscope (SEM) analysis was subsequently performed to investigate the effect of influential factors on UCS development. For all NS:NH ratios, the early 7-day UCS increases with increasing CCR replacement ratio whereby the cementitious products increase with CCR replacement ratio. The CCR replacement ratio providing the maximum 90-day strength is found at 20%. FA particles in FA-CCR geopolymer stabilized LS at excessive CCR replacement ratio of 30% are evidently spongy and cracked. The maximum 90-day UCS is found to be 18,800 kPa at NS:NH = 90:10 and CCR = 20%.

Last part presents the UCS of LS stabilized by FA geopolymer with GBFS as an additive. The microstructural development of the FA- GBFS geopolymer stabilized LS was observed through SEM and X-Ray Diffraction (XRD) analysis. The significant factors studied consisted of GBFS content, NS:NH ratio, and curing time. The soaked 7-day UCS of LS-FA- GBFS geopolymer tested meets the standard of national road authorities. The highest 60-day UCS was found to be 19.97 MPa at NS:NH = 90:10 and GBFS = 10%. The cementitious products of FA – GBFS geopolymer stabilized LS were a coexisted Sodium Alumino Silicated Hydrate (N-A-S-H), Calcium Silicate Hydrate (C-S-H) and calcite. The outcome of this research enables CCR and GBFS, which are a waste material to be used in FA geopolymer pavement applications.

School of Civil Engineering

Academic Year 2015

Student's Signature \_\_\_\_\_

Advisor's Signature \_\_\_\_\_

## ACKNOWLEDGEMENT

The thesis could not have been finished without the help of a number of persons, academic and research institutes, government services, sponsoring agencies and industrial organizations. To acknowledge all of them involved is an arduous task and I would like to apologize for any omission that might have been occurred inadvertently.

I would like to express my deep sense of gratitude and indebtedness to my supervisor, Professor Dr. Suksun Horpibulsuk, Chair of School of Civil Engineering, Chair of Center of Excellence in Innovation for Sustainable Infrastructure Development and Chair of Graduate Program in Construction and Infrastructure Management, for his invaluable help and constant encouragement throughout the course of this research. I am most grateful to his teaching and advice not only for the research methodologies but also philosophical thoughts. I would not have achieved this far and this thesis would not have been completed without all the support from him.

The examining committee members have played a significant role in the completion of my thesis. I am grateful to Professor Dr. Arul Arulrajah for serving as a chair of the Ph.D. thesis examining committee as well as Associate Professor Dr. Avirut Chinkulkijniwat, Associate Professor Dr. Panich Voottipruex and Dr. Cherdsak Suksiripattanapong for serving as Ph.D. thesis examiners.

Thanks are extended to Associate Professor Dr. Vacharapoom Benjaoran, Associate Professor Dr. Kwunkamol Donkwa, Graduate Program in Construction and Infrastructure Management, School of Civil Engineering, Suranaree University of Technology, for their excellent lectures. Appreciation is also due to all faculty staff, laboratory staff of Graduate Program in Construction and Infrastructure Management for their academic, administrative and technical support during my Ph.D. study. I acknowledge the help and encouragement from my best friends, Miss Punvalai Cheonklang and Mr. Chanyuth Kongkerd.

I would like to acknowledge a financial support from Department of Rural Roads for the Ph.D. studies at Suranaree University of Technology and Mr. Darron Saengchai, Deputy Permanent Secretary of Ministry of Transport and Dr. Chakree Bumrongwong, Department of Rural Roads for all their support.

Last but not least, profound gratitude is expressed to my family and my co-workers for their sacrifice and constant inspiration and encouragement throughout the course of this study.

Itthikorn Phummiphan

# TABLE OF CONTENTS

	<b>Page</b>
ABSTRACT (THAI).....	I
ABSTRACT (ENGLISH).....	III
TABLE OF CONTENTS.....	VI
LIST OF TABLES.....	XII
LIST OF FIGURES.....	XIII
SYMBOLS AND ABBREVIATIONS.....	XIX
<b>CHAPTER</b>	
<b>I INTRODUCTION.....</b>	<b>1</b>
1.1 Statement of the problem.....	1
1.2 Objectives of the study.....	5
1.3 Organization of the dissertation.....	6
1.4 References.....	8
<b>II LITERATURE REVIEW.....</b>	<b>18</b>
2.1 Introduction.....	18
2.2 Geopolymer.....	18
2.3 Geopolymerization.....	23
2.4 Alkaline activators.....	33
2.5 Raw materials.....	35
2.6 Role of materials in FA geopolymer.....	39

## TABLE OF CONTENTS (Continued)

	<b>Page</b>
2.6.1 Slag.....	39
2.6.2 Metakaolin.....	41
2.6.3 Silica fume .....	43
2.6.4 Portland cement.....	44
2.6.5 Lime.....	46
2.6.6 Natural pozzolan.....	46
2.6.7 Calcium carbide residue.....	46
2.7 Factors affecting compressive strength.....	49
2.8 Use of promoters.....	55
2.9 Analytical techniques.....	59
2.10 Soil stabilization with geopolimer.....	63
2.11 References.....	70
<b>III STABILIZATION OF MARGINAL LATERITIC SOIL</b>	
<b>USING HIGH CALCIUM FLY ASH – BASED</b>	
<b>GEOPOLYMER.....</b>	<b>86</b>
3.1 Statement of problem .....	86
3.2 Materials and methods.....	88
3.2.1 Soil sample.....	88
3.2.2 Fly ash.....	91

## TABLE OF CONTENTS (Continued)

	<b>Page</b>
3.2.3 Liquid alkali activator.....	92
3.2.4 LS – FA Geopolymer.....	92
3.3 Results.....	94
3.3.1 Compaction characteristics .....	94
3.3.2 Unconfined compressive Strength .....	96
3.4 Microstructural analysis .....	98
3.5 Conclusions .....	103
3.6 References.....	105
<b>IV STRENGTH AND MICROSTRUCTURE OF MARGINAL LATERITIC SOIL STABILIZED WITH CALCIUM CARBIDE RESIDUE AND FLY ASH GEOPOLYMER.....</b>	<b>112</b>
4.1 Statement of problem .....	112
4.2 Materials and methods.....	117
4.2.1 Soil sample.....	117
4.2.2 Fly ash.....	119
4.2.3 Calcium carbide residue .....	120
4.2.4 Liquid alkali activator .....	121
4.2.5 LS – FA – CCR geopolymer.....	121

## TABLE OF CONTENTS (Continued)

	<b>Page</b>
4.3 Results.....	122
4.3.1 Compaction characteristics .....	122
4.3.2 Unconfined compressive Strength .....	124
4.4 Microstructural analysis .....	126
4.5 Conclusions .....	132
4.6 References.....	133
<b>V STRENGTH AND MICROSTRUCTURE ANALYSIS OF LATERITIC SOIL STABILIZED WITH FLY ASH AND GROUND GRANULATED BLAST FURNACE SLAG PRECUSORS .....</b>	<b>142</b>
5.1 Statement of problem .....	142
5.2 Materials and methods.....	144
5.2.1 Soil sample.....	144
5.2.2 Fly ash.....	147
5.2.3 Ground granulated blast furnace slag .....	148
5.2.4 Liquid alkali activator .....	149
5.2.5 Methods .....	149
5.3 Results.....	150
5.3.1 Compaction characteristics .....	150
5.3.2 Unconfined compressive Strength .....	152

## TABLE OF CONTENTS (Continued)

	<b>Page</b>
5.4 SEM analysis .....	154
5.5 XRD analysis .....	158
5.6 Conclusions .....	160
5.7 References.....	161
<b>VI CONCLUSIONS AND RECOMMENDATIONS .....</b>	<b>169</b>
6.1 Summary and conclusions.....	169
6.1.1 Stabilization of marginal lateritic soil using high calcium fly ash – based geopolymer.....	169
6.1.2 Strength and microstructure of marginal lateritic soil stabilized with calcium carbide residue and fly ash geopolymer.....	170
6.1.3 Strength and microstructure analysis of lateritic soil stabilized with fly ash and ground granulated blast furnace slag precursors .....	171
6.2 Recommendations for future work.....	172
<b>APPENDIX</b>	
APPENDIX A. LIST OF PUBLICATIONS.....	173
BIOGRAPHY.....	177

## LIST OF TABLES

Table	Page
2.1 Applications of geopolymeric materials based on silica-to-alumina atomic ratio .....	23
3.1 Chemical compositions of FA and marginal LS .....	90
3.2 Initial molar ratios of LS-FA geopolymer .....	94
3.3 Optimum liquid alkali activator and maximum dry unit weight.....	95
4.1 The engineering properties of the soil sample and subbase specifications.....	118
4.2 The chemical compositions of the marginal LS, FA and CCR .....	119
5.1 The engineering property comparisons of the soil sample and subbase specifications.....	146
5.2 The chemical compositions of LS, FA, and GBFS.....	147

## LIST OF FIGURES

<b>Figure</b>		<b>Page</b>
2.1	Poly(sialate) structures .....	20
2.2	Computer molecular graphics of polymeric $M_n(-Si-O-Al-O)_n$ poly(sialate) and $M_n(-Si-O-Al-O-Si-O)_n$ poly(sialate-siloxo), and related frameworks .....	21
2.3	Schematic description of the alkaline activation of fly ash .....	26
2.4	Descriptive model for alkali activation of aluminosilicates .....	28
2.5	Conceptual model for geopolymerization.....	29
2.6	Schematic description of mechanical properties evolution to the reaction time. The increment of mechanical performances is related to the Si/Al ratio in the gel.....	30
2.7	Descriptive model of the alkali activation of fly ash .....	31
2.8	SEM pictures: (a) original fly ash and (b) fly ash activated with 8 M NaOH for 5 h at 85°C .....	32
2.9	SEM pictures of fly ash activated with 8 M NaOH for 20 h at 85°C; (a) reaction process of a large sphere and (b) singular details of the reaction of some small spheres .....	33
2.10	Influence of the concentration and kind of the alkaline solution on the pH value .....	52
2.11	Formation of geopolymeric gel (A) and CSH gel (B) .....	57

## LIST OF FIGURES (Continued)

Figure	Page
2.12	Development over time of the compressive mechanical strength of alkali activated mortars .....58
2.13	SEM micrographs of the M5 and M25 pastes, respectively, at: (a) and (b) 1 day; (c) and (d) 28 days; and (e) and (f) 91 days .....59
2.14	XRD spectra (a) unreacted fly ash; (b) alkali-activated fly ash 20 h at 85°C. Q=Quartz; M=Mullite; F=Hematite; C=CaO; H=Herschelite; X=Hydroxysodalite .....60
2.15	SEM micrograph of fracture surface of alkali-activated PFA geopolymer. Fe <sub>2</sub> O <sub>3</sub> is arrowed .....61
2.16	SEM micrograph of fracture surface of alkali-activated PFA geopolymer .....62
2.17	SEM micrograph of fracture surface of alkali-activated PFA geopolymer showing PFA particle with reaction shells and also unidentified spherical assemblages (arrowed).....62
2.18	SEM micrograph of fracture surface of alkali-activated PFA geopolymer showing considerably eroded PFA particle and also unidentified spherical assemblages (arrowed).....63
2.19	The UCS of MKG stabilized soils, soil, and Portland cement stabilized soil samples after 7 and 28 day curing .....65
2.20	UCS of stabilized clays at 7, 28, 90 and 180 days .....66
2.21	Poly(sialate) structures according to Davidovits (2005) .....67

## LIST OF FIGURES (Continued)

Figure	Page
2.22	Effects of heat condition on the compressive strength of the 0.7–0.6 CLAY– FA specimens heated at (a) 65°C, (b) 75°C and (c) 85°C .....68
2.23	SEM images of the 0.7–0.6 CLAY–FA specimens heated at 75°C for (a) 24 h, (b) 48 h and (c) 72 h after 28 days of curing .....69
2.24	Effect of state of liquid content on unsoaked strengths of clay-FA geopolymers .....70
3.1	Particle size distributions of the LS and FA .....90
3.2	SEM images of: (a) FA and (b) LS .....92
3.3	Compaction curves of LS – FA geopolymer at different ingredients .....95
3.4	Effect of curing time on UCS of LS – FA geopolymer. .... 97
3.5	SEM images of LS – FA geopolymer cured at 7 days of curing at ambient temperature for different NS:NH ratios of (a) 100:0, (b) 90:0, (c) 80:20 and (d) 50:50.....100
3.6	SEM images of LS-FA geopolymer cured at ambient temperature for NS:NH ratio of 90:10 and 50:50 for (a) 90:10 cured at 7 days, (b) 50:50 cured at 7 days (c) 90:10 cured at 60 days and (d) 50:50 cured at 60 days ...101
3.7	SEM images of LS – FA geopolymer cured at 90 days at ambient temperature for various ingredients of Na <sub>2</sub> SiO <sub>3</sub> : NaOH (a) 100:0, (b) 90:10, (c) 80:20 and (d) 50:50.....103

## LIST OF FIGURES (Continued)

Figure	Page
4.1 Particle size distributions of FA, CCR and LS .....	118
4.2 SEM images of: (a) LS, (b) FA and (c) CCR .....	120
4.3 XRD pattern of CCR.....	121
4.4 Compaction curves of the LS – CCR – FA geopolymer .....	123
4.5 Prediction of optimum liquid alkaline activator for each proportion .....	124
4.6 The UCS of LS – CCR – FA geopolymer at various CCR contents cured at 7 to 90 days for different NS:NH ratios (a) 100:0, (b) 90:10, (c) 80:20 and (d) 50:50 .....	125
4.7 SEM images of samples at NS:NH ratio of 90:10 cured 7 days at room temperature for different CCR contents: (a) 0%, (b) 10%, (c) 20% and (d) 30% .....	127
4.8 SEM images of samples at NS:NH ratio of 90:10 cured 7 days at room temperature for different CCR contents: (a) 10%, (b) 20% and (c) 30% .....	128
4.9 SEM images of samples at NS:NH ratio of 80:20, cured for 90 days at room temperature for different CCR replacement ratios of (a) 0%, (b) 10%, (c) 20% and (d) 30% .....	129
4.10 SEM images of LS-FA- geopolymer cured for 90 days at high NH (NS:NH ratio of 50:50) for: (a) 10% CCR, (b) 20% and (c) 30% CCR .....	131

## LIST OF FIGURES (Continued)

Figure	Page
5.1	Particle size distributions of FA, LS and GBFS .....146
5.2	SEM images of: (a) LS, (b) FA and (c) GBFS .....148
5.3	XRD pattern of GBFS and FA .....149
5.4	Compaction curves of the LS – FA – GBFS geopolymer .....151
5.5	OLC versus NS relationships for various GBFS replacement ratios .....152
5.6	The UCS of FA-GBFS geopolymer stabilized LS at various GBFS replacement ratios, cured at 7 to 60 days for different NS:NH ratios (a) 100:0, (b) 90:10, (c) 80:20 and (d) 50:50 .....154
5.7	SEM images of stabilized geopolymer samples with NS:NH ratios of 90:10 and 10% GBFS after 7, 28 and 60 days of curing .....156
5.8	SEM images of 30% GBFS content samples at NS:NH ratio of 90:10 and 50:50 .....157
5.9	XRD of 20% GBFS content samples at NS:NH ratio of 90:10 and 40:60 for different curing times at room temperature .....159

## SYMBOLS AND ABBREVIATIONS

z	=	1, 2, 3, or higher
M	=	a monovalent cation such as K <sup>+</sup> or Na <sup>+</sup>
n	=	degree of poly-condensation
°C	=	degree Celsius
XRD	=	x-ray diffraction
SEM	=	scanning electron microscopy
EDX	=	energy Dispersive X-ray Spectrometer
XRF	=	X-ray fluorescence
pH	=	potential of Hydrogen ion
M	=	molar
h	=	hours
OPC	=	Portland cement
CFA	=	classified fly ash
OFA	=	original fly ash
$\gamma_{d,max}$	=	maximum dry unit weight
OMC	=	optimum moisture content
CCR	=	calcium carbide residue
NS	=	sodium silicate
NH	=	sodium hydroxide
NASH	=	sodium aluminosilicate hydrate
CSH	=	sodium silicate hydrate

# **CHAPTER I**

## **INTRODUCTION**

### **1.1 Statement of the problem**

Highway pavement generally consists of base and subbase, which are constructed from suitable materials. When no suitable materials are available and it is expensive to bring the materials from distant sources. An alternative way which is widely practiced around the world is to compact the in-situ marginal soil mixed with Portland Cement (PC). The production of PC is however an energy-intensive process and emits a very large amount of greenhouse gas – carbon dioxide (CO<sub>2</sub>) into the atmosphere (Davidovits, 1991, 1994a, 1994b, 1994c, 2002). Among greenhouse gases, CO<sub>2</sub> contributes about 65% of global warming (McCaffrey, 2002). The production of 1 ton of PC clinker directly generates 0.55 tons of CO<sub>2</sub> and requires the combustion of carbon-fuel to yield an additional 0.40 tons of carbon dioxide. Generally speaking, the production of 1 ton of PC releases about 1 ton of CO<sub>2</sub> (Davidovits, 2002).

A utilization of various kinds of waste materials in a range of civil engineering applications including pavement materials has been researched continuously. The sustainable alternative materials that have been researched including recycled concrete aggregates (RCA), reclaimed asphalt pavement (RAP) (Arulrajah et al., 2011; Arulrajah et al., 2014; Arulrajah et al., 2013; Azam and Cameron, 2013; Cetin

et al., 2010; Ebrahim et al., 2013; Galvín et al., 2013; Poon and Chan, 2006; Rahman et al., 2014; Sata et al., 2013; Schoenberger et al., 1999; Soleimanbeigi et al., 2013), recycled glass (Arulrajah et al., 2014; Arulrajah et al., 2013; Puertas and Torres-Carrasco, 2014) , industrial and manufacturing waste and other forms of municipal wastes (Krammart and Tangtermsirikul, 2004; Galiano et al., 2011; Maria et al., 2001; Muñoz et al., 2014; Zekkos et al., 2006; Zheng et al., 2010). Moreover, the research has been increasingly undertaken and investigated the replacement usage of alternative binders, which create low greenhouse gas – CO<sub>2</sub>, to the Portland cement (Phetchuay et al., 2014).

Geopolymer is an inorganic aluminosilicate material synthesized by alkaline activation of materials rich in alumina (Al<sub>2</sub>O<sub>3</sub>) and silica (SiO<sub>2</sub>). It is formed through polycondensation of tetrahedral silica (SiO<sub>4</sub>) and alumina (AlO<sub>4</sub>), which are linked with other by sharing all the oxygen atoms (Davidovits, 1991; Gambrell et al., 2010).

It is also described that geopolymer is a commercial and industrial utilization of alkali-activated aluminosilicate cements (i.e. fly ash, slag, burned clay or kaolin, rice hush ash bottom ash and other aluminosilicate materials) (Palomo et al., 1999; Rashad, 2013, 2014) with low CO<sub>2</sub> emission and energy consumption. Since Fly Ash (FA) as the greatest opportunity and plentiful worldwide raw material supply (Van Jaarsveld et al., 1998), essentially contains a large amount of silica (SiO<sub>2</sub>) and alumina (AlO<sub>3</sub>), it is frequently a suitable precursor for producing geopolymers. FA is also a by-product as a waste material of thermal power plants following combustion of pulverized coal in the furnaces. The amounts of FA are annually produced about one billion tons worldwide in coal-fired power plants (Alvarez-Ayuso et al., 2008; Chindapasirt et al., 2011; Chindapasirt et al., 2009; Nath and Kumar, 2013).

Approximately 1.8 million tons of FA is used as a pozzolanic material in the concrete industry in Thailand (Chindaprasirt et al., 2009). FA can regularly replace cement content up to 30% and 50-70% in the high volume fly ash concrete (Rashad, 2014). It is clear that geopolymer materials, exhibiting the following performance properties from not only laboratory scale but also real world - scale, can be made with both technological and commercial confidence (Duxson et al., 2007): high compressive strength gain, (Amnadnua et al., 2013; Bagheri and Nazari, 2014; Chen and Chang, 2007; Chindaprasirt et al., 2011; Davidovits, 1994a; Komljenovic et al., 2010; Lee and Van Deventer, 2002; Nugteren et al., 2009) rapid controllable setting and hardening (Lee and Van Deventer, 2002), fire resistance (Cheng and Chiu, 2003; Lyon et al., 1997; Sakkas et al., 2014; Sarker et al., 2014), high level of resistance to a range of different acids and salt solutions (Palomo et al., 1999), not subject to deleterious alkali–aggregate reactions (García-Lodeiro et al., 2007), low shrinkage (Zhang et al., 2013), and high surface definition that replicates mold patterns (Davidovits, 1991). Sukmak et al. (2013) used locally available soil as an aggregate and FA as a precursor to develop green masonry units. Furthermore, the factors controlling the strength development and sulfate resistance of soil stabilized with high - calcium FA geopolymer were also investigated in the same year (Sukmak et al., 2014). Zhang et al. (2013) illustrated the feasibility of using geopolymer as an effective soil stabilizer for clayey soils based on an experimental study. The engineering properties of FA geopolymer can be improved by calcium-rich additives such as Calcium Carbide Residue (CCR) and steel slag.

Many studies have used Calcium Carbide Residue (CCR), a by-product of acetylene production process, for replacement of PC in concrete application.

Makaratat et al. (2010) used CCR and FA for full replacement of PC as a concrete binder which generated the high UCS of 28.4 and 33.5 MPa after 28 and 90 days, respectively. Amnadnua et al. (2013) produced a high strength concrete by using the mixture of CCR, FA and 20% PC which generated the UCS of 67 MPa or 95% of PC concrete at 28 days. Some authors used CCR with pozzolanic materials as a new cementitious material for building material applications such as CCR and Rice Husk Ash (RHA) (Rattanashotinunt et al., 2013), CCR and bagasse ash (Rattanashotinunt et al., 2013). Furthermore, some authors used CCR to enhance engineering properties of problematic soil (Du et al., 2011; Horpibulsuk et al., 2012; Horpibulsuk et al., 2013; Kampala and Horpibulsuk, 2013; Kampala et al., 2013; Vichan and Rachan, 2013). Recently, Phetchuay et al. (2014) used sodium silicate ( $\text{Na}_2\text{SiO}_3$ ) solution and CCR as an alkali activator and FA as a precursor for geopolymer binder to stabilize problematic silty clay as a pavement subgrade material.

Ground granulated blast furnace slag (GBFS) is a byproduct obtained from the manufacturing of iron in a blast furnace (Rashad, 2013b). GBFS is usually utilized as a binder in the cement industry for preparation of blended cement due to its high content of CaO,  $\text{SiO}_2$  and  $\text{Al}_2\text{O}_3$  in an amorphous state (Phoo-ngernkham et al., 2015). Consequently, GBFS is commonly used as cementing material by alkali activation (Rashad, 2013b). Many studies found that the addition of GBFS system can improve the mechanical properties and microstructure of FA geopolymer (Kumar et al., 2010; Puertas et al., 2000; Rashad, 2013a). The main reaction products of GBFS geopolymer are calcium silicate hydrate (CSH) and/or calcium aluminosilicate hydrate (CASH) gels similar to those of PC (Ismail et al., 2014) while the main reaction products of FA geopolymer is sodium aluminosilicate hydrate (NASH) gel

(Garcia-Lodeiro et al., 2013). Moreover, some authors confirmed that the incorporation of GBFS and FA in geopolymer system results in the strength improvement (Ismail et al., 2013; Phoo-ngernkham et al., 2015). In Thailand GBFS is also a by-product obtained from the steel industrial factory. The vast majority of this slag is widely disposed in landfills. To solve this disposal, the GBFS can be used as an additive in FA based geopolymer stabilized problematic soil to develop a pavement material.

In this study, FA is used as a main precursor because of the plentiful worldwide raw material supply. The industrial waste, CCR and GBFS, are used as additives in geopolymer system to stabilize marginal soil to be a sustainable bound pavement material. This study attempts to investigate the visibility of using FA-based geopolymer to stabilize a marginal soil to be a sustainable bound pavement material. The microstructural development of FA-based geopolymer stabilized soil at various geopolymer ingredients and curing is also investigated via Scanning Electron Microscope (SEM) and X-Ray Diffraction (XRD) to understand the growth of geopolymerization products.

## **1.2 Objectives of the study**

This research has been undertaken with the following objectives:

- (i) To investigate the visibility of using FA-based geopolymer to stabilize a marginal soil to be a sustainable bound pavement material.
- (ii) To study the effect of Calcium Carbide Residue (CCR) as an additive on strength and microstructure development of FA geopolymer stabilized marginal lateritic soil.

- (iii) To study the effect of ground granulated blast furnace slag (GBFS) as an additive on strength and microstructure development of FA geopolymer stabilized marginal lateritic soil.

### 1.3 Organization of the dissertation

This thesis consists of six chapters and outlines of each chapter are presented as follows:

**Chapter I** presents the introduction part, describing the statement of the problems, the objectives of the study and the organization of the dissertation.

**Chapter II** presents the literature review of the geopolymerization, alkaline activator, precursor for producing geopolymer, factors affecting compressive strength, analytical techniques, geopolymer binder and geopolymer applications.

**Chapter III** presents the possibility of using high calcium FA based geopolymer to stabilize a marginal lateritic soil to be a sustainable bound pavement material. Unconfined Compressive Strength (UCS) is used as an indicator for this investigation. The microstructural development of FA geopolymer stabilized marginal lateritic soil is observed through Scanning Electron Microscope (SEM) analysis for understanding the role of influential factors controlling the strength development. The influential factors studied in this study include  $\text{Na}_2\text{SiO}_3:\text{NaOH}$  ratio and curing time at ambient room temperature. The marginal lateritic soil to FA ratio is 70:30 and the liquid alkali activator of  $\text{Na}_2\text{SiO}_3:\text{NaOH}$  ratio are 100:0, 90:10, 80:20, and 50:50. The mixtures with different ingredients are compacted under modified Proctor energy in a standard mold of 101.6 mm in diameter and 116.4 mm in height. The compacted samples are then dismantled and wrapped with vinyl sheet

at room temperature. UCS tests and SEM analysis on the soaked samples are undertaken after 7, 28, 60 and 90 days of curing time.

**Chapter IV** presents the role of CCR replacement on UCS and microstructure development of FA geopolymer stabilized marginal lateritic soil. The strength and microstructure of the geopolymer will be investigated at different curing times. The FA content is fixed at 30% while the soil and CCR contents are varied. The soil: FA: CCR ratios are 60:30:10, 50:30:20, and 40:30:30. The  $\text{Na}_2\text{SiO}_3$ :NaOH ratio are 100:0, 90:10, 80:20 and 50:50. The mixtures are mixed with liquid alkaline activators and compacted under modified Proctor energy. The samples are demolded, wrapped with plastic sheet and cured at room temperature of 7, 28, 60 and 90 days. Next, UCS of the soaked geopolymer samples is measured after curing periods. The small fragments from the center of geopolymer samples tested are analyzed the microstructural characterizations by using SEM.

**Chapter V** presents the role of GBFS replacement on UCS and microstructure development of FA geopolymer stabilized marginal lateritic soil. The strength and microstructure of the geopolymer will be investigated at different curing times. The FA content is fixed at 30% of the total mix while the soil and GBFS contents are varied. The soil: FA: GBFS ratios are 60:30:10, 50:30:20, and 40:30:30 and the  $\text{Na}_2\text{SiO}_3$ :NaOH ratio are 100:0, 90:10, 80:20, 50:50 and 40:60. The mixtures are mixed together and then compacted under modified Proctor energy. The compacted samples are next demolded and wrapped with plastic sheet before curing at room temperature. UCS of soaked geopolymer samples are measured after 7, 28, and 60 days of curing periods. The small fragments from the center of geopolymer samples tested are demonstrated the development of the geopolymer products by

using SEM. Additionally, the microstructural characterizations are also confirmed the amorphous and crystalline phases of materials by X-ray Diffraction (XRD).

**Chapter VI** presents the conclusion of each chapter and overall conclusion.

The suggestion for further study is also presented in this chapter.

## 1.4 References

- Alvarez-Ayuso, E., Querol, X., Plana, F., Alastuey, A., Moreno, N., Izquierdo, M., . . . Barra, M. (2008). **Environmental, physical and structural characterisation of geopolymer matrixes synthesised from coal (co-) combustion fly ashes.** *Journal of Hazardous materials*, 154(1-3), 175-183.
- Amnadnua, K., Tangchirapat, W., and Jaturapitakkul, C. (2013). **Strength, water permeability, and heat evolution of high strength concrete made from the mixture of calcium carbide residue and fly ash.** *Materials and Design*, 51, 894-901. doi: 10.1016/j.matdes.2013.04.099
- Arulrajah, A., Ali, M. M. Y., Disfani, M. M., and Horpibulsuk, S. (2014). **Recycled-Glass Blends in Pavement Base/Subbase Applications: Laboratory and Field Evaluation.** *Journal of Materials in Civil Engineering*, 26(7), 04014025. doi: 10.1061/(asce)mt.1943-5533.0000966
- Arulrajah, A., Ali, M. M. Y., Disfani, M. M., Pirathepan, J., and Bo, M. W. (2013). **Geotechnical Performance of Recycled Glass-Waste Rock Blends in Footpath Bases.** *Journal of Materials in Civil Engineering*, 25(5), 653-661. doi: 10.1061/(asce)mt.1943-5533.0000617

- Arulrajah, A., Piratheepan, J., Aatheesan, T., and Bo, M. W. (2011). **Geotechnical Properties of Recycled Crushed Brick in Pavement Applications**. *Journal of Materials in Civil Engineering*, 23(10), 1444-1452.
- Arulrajah, A., Piratheepan, J., and Disfani, M. M. (2014). **Reclaimed Asphalt Pavement and Recycled Concrete Aggregate Blends in Pavement Subbases: Laboratory and Field Evaluation**. *Journal of Materials in Civil Engineering*, 26(2), 349-357. doi: 10.1061/(asce)mt.1943-5533.0000850
- Arulrajah, A., Piratheepan, J., Disfani, M. M., and Bo, M. W. (2013). **Geotechnical and Geoenvironmental Properties of Recycled Construction and Demolition Materials in Pavement Subbase Applications**. *Journal of Materials in Civil Engineering*, 25(8), 1077-1088. doi: 10.1061/(asce)mt.1943-5533.0000652
- Azam, A. M., and Cameron, D. A. (2013). **Geotechnical Properties of Blends of Recycled Clay Masonry and Recycled Concrete Aggregates in Unbound Pavement Construction**. *Journal of Materials in Civil Engineering*, 25(6), 788-798. doi: 10.1061/(asce)mt.1943-5533.0000634
- Bagheri, A., and Nazari, A. (2014). **Compressive strength of high strength class C fly ash-based geopolymers with reactive granulated blast furnace slag aggregates designed by Taguchi method**. *Materials and Design*, 54, 483-490. doi: 10.1016/j.matdes.2013.07.035
- Cetin, B., Aydilek, A. H., and Guney, Y. (2010). **Stabilization of recycled base materials with high carbon fly ash**. *Resources, Conservation and Recycling* 54(11), 878-892. doi: 10.1016/j.resconrec.2010.01.007

- Chen, J.-W., and Chang, C.-F. (2007). **High-Strength Ecological Soil Materials**. *Journal of Materials in Civil Engineering*, 19, 149-154.
- Cheng, T. W., and Chiu, J. P. (2003). **Fire-resistant geopolymer produced by granulated blast furnace slag**. *Minerals Engineering*, 16(3), 205-210. doi: 10.1016/s0892-6875(03)00008-6
- Chindaprasirt, P., Chareerat, T., Hatanaka, S., and Cao, T. (2011). **High-Strength Geopolymer Using Fine High-Calcium Fly Ash**. *Journal of Materials in Civil Engineering*, 23(3), 264-270. doi: 10.1061/(asce)mt.1943-5533.0000161
- Chindaprasirt, P., Jaturapitakkul, C., Chalee, W., and Rattanasak, U. (2009). **Comparative study on the characteristics of fly ash and bottom ash geopolymers**. *Waste Management*, 29(2), 539-543.
- Davidovits, J. (1991). **Geopolymer: inorganic polymeric new materials**. *Journal of Thermal Analysis*, 37, 1633-1656.
- Davidovits, J. (1994a). **Geopolymers: Man-Made Rock Geosynthesis And The Resulting Development Of Very Early High Strength Cement**. *Journal of Materials Education*, 16(2&3), 91-139.
- Davidovits, J. (1994b). **Global Warming Impact on the Cement and Aggregates Industries**. *World Resource Review*, 6(2), 263-278.
- Davidovits, J. (1994c). **Properties Of Geopolymer Cements**. *Alkaline Cements and Concretes, KIEV Ukraine*.
- Davidovits, J. (2002). *Environmentally Driven Geopolymer Cement Applications*. Paper presented at the Geopolymer 2002 Conference, Melbourne, Australia.
- Du, Y., Zhang, Y., and Liu, S. (2011). *Investigation of Strength and California Bearing Ratio Properties of Natural Soils Treated by Calcium Carbide*

*Residue*. Paper presented at the Proceedings of Geo-Frontiers 2011: Advances in Geotechnical Engineering, March 13-16, Dallas, Texas, USA.

Duxson, P., Provis, J. L., Lukey, G. C., and van Deventer, J. S. J. (2007). **The role of inorganic polymer technology in the development of 'green concrete'**. *Cement and Concrete Research*, 37(12), 1590-1597.

Ebrahim Abu El-Maaty Behiry, A. (2013). **Utilization of cement treated recycled concrete aggregates as base or subbase layer in Egypt**. *Ain Shams Engineering Journal*, 4(4), 661-673. doi: 10.1016/j.asej.2013.02.005

Galvín, A. P., Ayuso, J., Agrelá, F., Barbudo, A., and Jiménez, J. R. (2013). **Analysis of leaching procedures for environmental risk assessment of recycled aggregate use in unpaved roads**. *Construction and Building Materials*, 40, 1207-1214. doi: 10.1016/j.conbuildmat.2011.12.091

Gambrell, R. P., He, J., and Zhang, G. (2010). **Synthesis, Characterization, and Mechanical Properties of Red Mud-Based Geopolymers**. *Transportation Research Record: Journal of the Transportation Research Board*, 2167(-1), 1-9. doi: 10.3141/2167-01

García-Lodeiro, I., Fernández-Jiménez, A., and Palomo, A. (2013). **Hydration kinetics in hybrid binders: Early reaction stages**. *Cement and Concrete Composites*, 39, 82-92. doi: 10.1016/j.cemconcomp.2013.03.025

García-Lodeiro, I., Palomo, A., and Fernández-Jiménez, A. (2007). **Alkali-aggregate reaction in activated fly ash systems**. *Cement and Concrete Research*, 37(2), 175-183. doi: 10.1016/j.cemconres.2006.11.002

- Horpibulsuk, S., Phetchuay, C., and Chinkulkijniwat, A. (2012). **Soil Stabilization by Calcium Carbide Residue and Fly Ash**. *Journal of Materials in Civil Engineering*, 24(2), 184-193. doi: 10.1061/(asce)mt.1943-5533.0000370
- Horpibulsuk, S., Phetchuay, C., Chinkulkijniwat, A., and Cholaphatsorn, A. (2013). **Strength development in silty clay stabilized with calcium carbide residue and fly ash**. *Soils and Foundations*, 53(4), 477-486.
- Ismail, I., Bernal, S. A., Provis, J. L., San Nicolas, R., Brice, D. G., Kilcullen, A. R., . . . Van Deventer, J. S. J. (2013). **Influence of fly ash on the water and chloride permeability of alkali-activated slag mortars and concretes**. *Construction and Building Materials*, 48, 1187-1201.
- Ismail, I., Bernal, S. A., Provis, J. L., San Nicolas, R., Hamdan, S., and Van Deventer, J. S. J. (2014). **Modification of phase evolution in alkali-activated blast furnace slag by the incorporation of fly ash**. *Cement and Concrete Composites*, 45, 125-135. doi: 10.1016/j.cemconcomp.2013.09.006
- Kampala, A., and Horpibulsuk, S. (2013). **Engineering Properties of Silty Clay Stabilized with Calcium Carbide Residue**. *Journal of Materials in Civil Engineering*, 25(5), 632-644. doi: 10.1061/(asce)mt.1943-5533.0000618
- Kampala, A., Horpibulsuk, S., Chinkullijniwat, A., and Shen, S.-L. (2013). **Engineering properties of recycled Calcium Carbide Residue stabilized clay as fill and pavement materials**. *Construction and Building Materials*, 46, 203-210. doi: 10.1016/j.conbuildmat.2013.04.037
- Komljenovic, M., Bascarevic, Z., and Bradic, V. (2010). **Mechanical and microstructural properties of alkali-activated fly ash geopolymers**.

*Journal of Hazardous Materials*, 181(1-3), 35-42. doi: 10.1016/j.jhazmat.2010.04.064

Krammart, P., and Tangtermsirikul, S. (2004). **Properties of cement made by partially replacing cement raw materials with municipal solid waste ashes and calcium carbide waste.** *Construction and Building Materials*, 18(8), 579-583. doi: 10.1016/j.conbuildmat.2004.04.014

Kumar, S., Kumar, R., and Mehrotra, S. P. (2010). **Influence of granulated blast furnace slag on the reaction, structure and properties of fly ash based geopolymer.** *Journal of Materials Science*, 45(3), 607-615.

Lee, W. K. W., and Van Deventer, J. S. J. (2002). **The effect of ionic contaminants on the early-age properties of alkali-activated fly ash-based cements.** *Cement and Concrete Research*, 32, 577–584.

Luna Galiano, Y., Fernandez Pereira, C., and Vale, J. (2011). **Stabilization/solidification of a municipal solid waste incineration residue using fly ash-based geopolymers.** *Journal of Hazardous Materials*, 185(1), 373-381. doi: 10.1016/j.jhazmat.2010.08.127

Lyon, R. E., Balaguru, P. N., Foden, A., Sorathia, U., Davidovits, J., and Davidovics, M. (1997). **Fire Resistant Aluminosilicate Composites.** *Fire and Materials* 21, 67-73.

Makaratat, N., Jaturapitakkul, C., and Laosamathikul, T. (2010). **Effects of Calcium Carbide Residue–Fly Ash Binder on Mechanical Properties of Concrete.** *Journal of Materials in Civil Engineering*, 22, 1164-1170.

Maria, I., Enric, V., Xavier, Q., Marilda, B., Ángel, L., and Felicià, P. (2001). **Use of bottom ash from municipal solid waste incineration as a road material.**

*2001 International Ash Utilization Symposium, Center for Applied Energy Research, University of Kentucky, USA.*

McCaffrey, R. (2002). **Climate change and the Cement Industry**. *Cement and Lime Magazine (Environmental Special Issue)*, 15-19.

Muñoz Velasco, P., Morales Ortíz, M. P., Mendivil Giró, M. A., and Muñoz Velasco, L. (2014). **Fired clay bricks manufactured by adding wastes as sustainable construction material – A review**. *Construction and Building Materials*, 63, 97-107. doi: 10.1016/j.conbuildmat.2014.03.045

Nath, S. K., and Kumar, S. (2013). **Influence of iron making slags on strength and microstructure of fly ash geopolymer**. *Construction and Building Materials*, 38, 924-930. doi: 10.1016/j.conbuildmat.2012.09.070

Nugteren, H. W., Butselaar-Orthlieb, V. C. L., Izquierdo, M., Witkamp, G.-J., and Kreutzer, M. T. (2009). *High Strength Geopolymers from Fractionated and Pulverized Fly Ash*. Paper presented at the 2009 World of Coal Ash (WOCA) Conference, Lexington, KY, USA.

Palomo, A., Grutzeck, M. W., and Blanco, M. T. (1999). **Alkali-activated fly ashes A cement for the future**. *Cement and Concrete Research*, 29, 1323–1329.

Phetchuay, C., Horpibulsuk, S., Suksiripattanapong, C., Chinkulkijniwat, A., Arulrajah, A., and Disfani, M. M. (2014). **Calcium carbide residue: Alkaline activator for clay–fly ash geopolymer**. *Construction and Building Materials*, 69, 285-294. doi: 10.1016/j.conbuildmat.2014.07.018

Phoo-ngernkham, T., Maegawa, A., Mishima, N., Hatanaka, S., and Chindaprasirt, P. (2015). **Effects of sodium hydroxide and sodium silicate solutions on**

**compressive and shear bond strengths of FA–GBFS geopolymer.**

*Construction and Building Materials*, 91, 1-8.

Poon, C. S., and Chan, D. (2006). **Feasible use of recycled concrete aggregates and crushed clay brick as unbound road sub-base.** *Construction and Building*

*Materials*, 20(8), 578-585. doi: 10.1016/j.conbuildmat.2005.01.045

Puertas, F., Martóñez-Ramírez, S., Alonso, S., and Vaázquez, T. (2000). **Alkali-activated fly ash/slag cement Strength behaviour and hydration products.**

*Cement and Concrete Research*, 30, 1625 - 1632.

Puertas, F., and Torres-Carrasco, M. (2014). **Use of glass waste as an activator in the preparation of alkali-activated slag. Mechanical strength and paste**

**characterisation.** *Cement and Concrete Research*, 57, 95-104. doi:

10.1016/j.cemconres.2013.12.005

Rahman, M. A., Imteaz, M., Arulrajah, A., and Disfani, M. M. (2014). **Suitability of recycled construction and demolition aggregates as alternative pipe**

**backfilling materials.** *Journal of Cleaner Production*, 66, 75-84. doi:

10.1016/j.jclepro.2013.11.005

Rashad, A. M. (2013a). **Alkali-activated metakaolin: A short guide for civil**

**Engineer – An overview.** *Construction and Building Materials*, 41, 751-765.

doi: 10.1016/j.conbuildmat.2012.12.030

Rashad, A. M. (2013b). **A comprehensive overview about the influence of**

**different additives on the properties of alkali-activated slag – A guide for**

**Civil Engineer.** *Construction and Building Materials*, 47, 29-55. doi:

10.1016/j.conbuildmat.2013.04.011

- Rashad, A. M. (2014). **A comprehensive overview about the influence of different admixtures and additives on the properties of alkali-activated fly ash.** *Materials and Design*, 53, 1005-1025. doi: 10.1016/j.matdes.2013.07.074
- Rattanashotinunt, C., Thairit, P., Tangchirapat, W., and Jaturapitakkul, C. (2013). **Use of calcium carbide residue and bagasse ash mixtures as a new cementitious material in concrete.** *Materials and Design*, 46, 106-111. doi: 10.1016/j.matdes.2012.10.028
- Sakkas, K., Panias, D., Nomikos, P. P., and Sofianos, A. I. (2014). **Potassium based geopolymer for passive fire protection of concrete tunnels linings.** *Tunnelling and Underground Space Technology*, 43, 148-156. doi: 10.1016/j.tust.2014.05.003
- Sarker, P. K., Kelly, S., and Yao, Z. (2014). **Effect of fire exposure on cracking, spalling and residual strength of fly ash geopolymer concrete.** *Materials and Design*, 63, 584-592. doi: 10.1016/j.matdes.2014.06.059
- Sata, V., Wongsas, A., and Chindaprasirt, P. (2013). **Properties of pervious geopolymer concrete using recycled aggregates.** *Construction and Building Materials*, 42, 33-39. doi: 10.1016/j.conbuildmat.2012.12.046
- Schoenberger, y. J. E., Hardy, D. L., and Pekar, J. W. (1999). **Use of diesel-contaminated soil in recycled cold-mix pavement.** *Practice periodical of hazardous, toxic, and radioactive waste management*, 3(118-123).
- Soleimanbeigi, A., Edil, T., and Benson, C. (2013). **Evaluation of Fly Ash Stabilization of Recycled Asphalt Shingles for Use in Structural Fills.** *Journal of Materials in Civil Engineering*, 25, 94-104.

- Sukmak, P., De Silva, P., Horpibulsuk, S., and Chindaprasirt, P. (2014). **Sulfate Resistance of Clay-Portland Cement and Clay High-Calcium Fly Ash Geopolymer.** *Journal of Materials in Civil Engineering*, 04014158. doi: 10.1061/(asce)mt.1943-5533.0001112
- Van Jaarsveld, J. G. S., Van Deventer, J. S. J., and Lorenzen, L. (1998). **Factors Affecting the Immobilization of Metals in Geopolymerized Flyash.** *Metallurgical and Materials Transactions B*, 29, 283-291.
- Vichan, S., and Rachan, R. (2013). **Chemical stabilization of soft Bangkok clay using the blend of calcium carbide residue and biomass ash.** *Soils and Foundations*, 53(2), 272-281. doi: 10.1016/j.sandf.2013.02.007
- Zekkos, D., Bray, J. D., Jr., E. K., Matasovic, N., Rathje, E. M., Riemer, M. F., and Stokoe, K. H. (2006). **Unit Weight of Municipal Solid Waste.** *Journal of Geotechnical and Geoenvironmental Engineering*, 132(10), 1250-1261. doi: 10.1061//asce/1090-0241/2006/132:10/1250
- Zhang, M., Guo, H., El-Korchi, T., Zhang, G., and Tao, M. (2013). **Experimental feasibility study of geopolymer as the next-generation soil stabilizer.** *Construction and Building Materials*, 47, 1468-1478. doi: 10.1016/j.conbuildmat.2013.06.017
- Zheng, L., Wang, W., and Shi, Y. (2010). **The effects of alkaline dosage and Si/Al ratio on the immobilization of heavy metals in municipal solid waste incineration fly ash-based geopolymer.** *Chemosphere*, 79(6), 665-671. doi: 10.1016/j.chemosphere.2010.02.018

## **CHAPTER II**

### **LITERATURE REVIEW**

#### **2.1 Introduction**

In recent year, green materials mostly considered are used for various constructions such as building, road, and other infrastructure. Geopolymer, a new green material, is extremely environmentally attractive for various reasons. Its performance as construction materials can replaced to Portland cement in lots of ways. Moreover, geopolymer needs no heat in its manufacturing process while Portland cement needs an energy-intensive process in its production. This implies a considerable benefit with regards to reducing greenhouse gas – CO<sub>2</sub> emissions. In addition, the utilization of industrial by-products runs into the increasing trend towards waste re-utilization. Geopolymer is categorically as an alumino-silicate material including outstanding physical and chemical properties of numerous applications (Komnitsas and Zaharaki, 2007).

#### **2.2 Geopolymer**

Pacheco-Torgal et al. (2008a) quoted Glukhovsky in 1959 that the first author who had investigated the binders used in ancient Roman and Egyptian constructions. He summarized that they were comprised of aluminosilicate calcium hydrates similar to the ones of Portland cement and also of crystalline phases of a natural rock (analcite) that would explain the durability of those binders. Glukhovsky

firstly developed a new type of binders named “soil–cement”. The word soil and cement are used because it seemed like a ground rock and its capacity like a cementitious material, respectively. The “soil–cement” was obtained from aluminosilicate materials mixed with rich alkalis industrial wastes. Glukhovsky also divided binders into two groups, depending on the composition of the starting materials: alkaline binding systems  $\text{Me}_2\text{O–Al}_2\text{O}_3\text{–SiO}_2\text{–H}_2\text{O}$  and “alkali–alkaline–earth” binding systems  $\text{Me}_2\text{O–MO–Al}_2\text{O}_3\text{–SiO}_2\text{–H}_2\text{O}$  (where  $\text{Me}=\text{Na, K, ...}$  and  $\text{M}=\text{Ca, Mg, ...}$ ) (Shi et al., 2011) .

In 1978, French researcher, Davidovits (1979) developed and patented binders came from the alkali-activation of metakaolin, having named it after the term “geopolymer”. After this research results, the investigations in the field of alkali activation had an exponential increase.

The chemical structure of geopolymer can generally be expressed as (Gambrell et al., 2010)  $\text{M}_n\text{-(Si-O)}_z\text{[-Al-O]}_n \cdot w\text{H}_2\text{O}$  where M is the alkaline element, - indicates the presence of a bond, z is 1, 2, or 3, and n is the degree of polymerization (Davidovits, 1991). Three typical structures of geopolymer are: Poly (sialate) Si:Al = 1 (-Si-O-Al-O-), Poly (sialate-siloxo) Si:Al = 2 (-Si-O-Al-O-Si-O-), Poly (sialate-disiloxo) Si:Al = 3 (-Si-O-Al-O-Si-O-Si-O-).

Juenger et al. (2011) studied in advances in alternative cementitious binders, reporting that alkali-activated binders are receiving increasing attention as an alternative to Portland cement as a result of their high strength and durability and friendly environment. Alkali-activated binders are made by mixing solid aluminosilicate materials such as fly ash, blast furnace slag, or metakaolin with an alkaline activator. The reaction product, or gel, can have a network structure similar to

those of organic thermoset polymers, and thus the binders are sometimes called “inorganic polymers” or “geopolymers”.

Davidovits (2005) advised the name “polysialates”, in which Sialate is an abbreviation for aluminosilicate oxide for the chemical designation of the geopolymer. The sialate network is constitute of tetrahedral anions  $[\text{SiO}_4]^{4-}$  and  $[\text{AlO}_4]^{5-}$  sharing the oxygen, which need positively charged ions such as ( $\text{Na}^+$ ,  $\text{K}^+$ ,  $\text{Li}^+$ ,  $\text{Ca}^{2+}$ ,  $\text{Na}^+$ ,  $\text{Ba}^{2+}$ ,  $\text{NH}_4^+$ ,  $\text{H}_3\text{O}^+$ ) to compensate the electric charge of  $\text{Al}^{3+}$  in tetrahedral coordination. **Figure 2.1** shows the diferent types of poly (sialates) structures. Davidovits also explained the computer molecular graphics of polymeric  $\text{M}_n(-\text{Si}-\text{O}-\text{Al}-\text{O})_n$  poly(sialate) and  $\text{M}_n(-\text{Si}-\text{O}-\text{Al}-\text{O}-\text{Si}-\text{O})_n$  poly(sialate-siloxo), and related frameworks as shows in **Figure 2.2**.

It is mentioned that geopolymers are polymers because of their transforming, polymerizing and hardening at low temperature. Nevertheless they are also geopolymers, because they are inorganic, hard and stable at high temperature and also noncombustible (Davidovits, 2005; Pacheco-Torgal et al., 2008a).

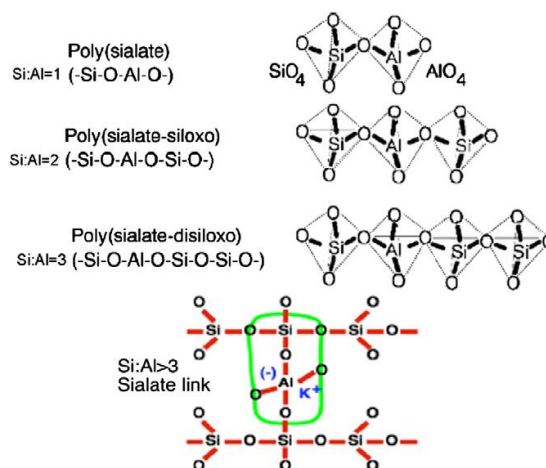


**Figure 2.1** Poly(sialate) structures according to Davidovits (2005)

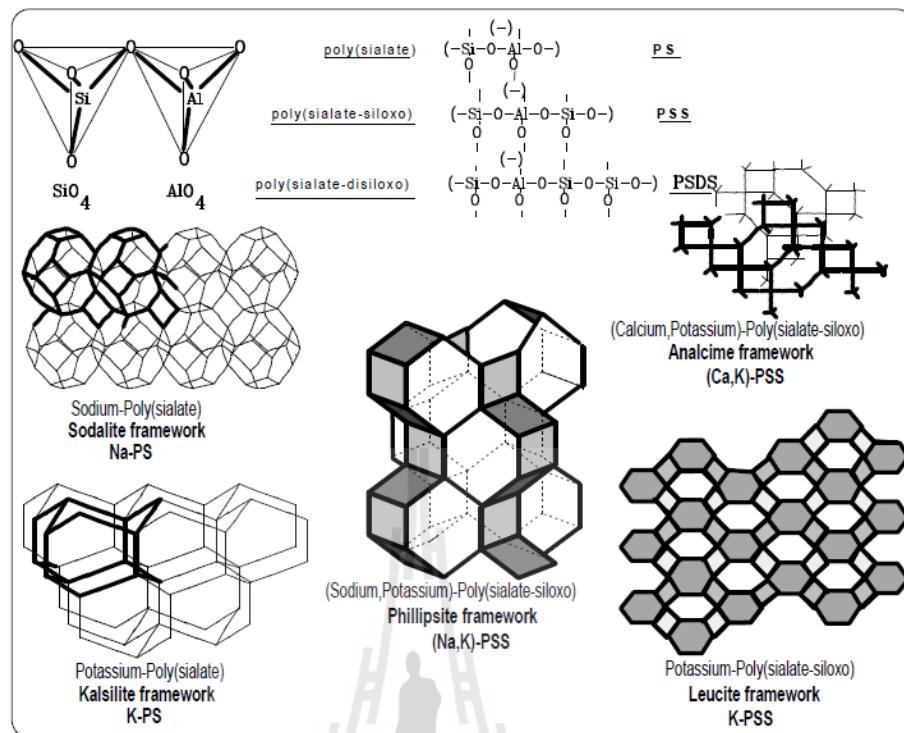


**Figure 2.2** Computer molecular graphics of polymeric  $M_n(-\text{Si}-\text{O}-\text{Al}-\text{O}-)_n$  poly(sialate) and  $M_n(-\text{Si}-\text{O}-\text{Al}-\text{O}-\text{Si}-\text{O}-)_n$  poly(sialate-siloxo), and related frameworks (Davidovits, 1991).

Some authors (Davidovits, 1991; Rangan, 2014) suggested that an alkaline activator could be used to react with the silicon (Si) and the aluminum (Al) in a raw material of natural materials or in by-product materials such as fly ash, blast furnace slag, and rice husk ash to produce binders. Because the chemical reaction that takes place in this case is a polymerization process, the term ‘Geopolymer’ to represent these binders has created.

Rangan (2014) stated that water excluded from the geopolymer matrix during the curing and further drying periods, leaves behind nano-pores in the matrix,

providing benefits to the performance of geopolymers. The water in a low-calcium FA-based geopolymer mixture plays no direct role in the chemical reaction taking place. It only provides the workability. The geopolymer system is in contrast to the chemical reaction of water in a Portland cement concrete mixture during the hydration process. However, the proportion of high calcium materials such as slag, class C FA, and so on may be included in the source material in order to accelerate the setting time and to alter the curing regime adopted for the geopolymer mixture. In that situation, the water released during the geopolymerisation reacts with the calcium present to produce hydration products such as calcium silicate hydrate (CSH).

Geopolymeric materials have a wide range of applications in the field of industries such as in the automobile and aerospace, non-ferrous foundries and metallurgy, civil engineering and plastic industries (Davidovits, 1991, 1994a, 1994c; Lyon et al., 1997; Zhang et al., 2013). The type of application of geopolymeric materials is determined by the chemical structure in terms of the atomic ratio Si: Al in the polysialate. Davidovits (1994b) categorized the type of application according to the Si:Al ratio as presented in Table 1. A low ratio of Si: Al of 1, 2, or 3 initiates a 3D-Network that is very rigid, while Si: Al ratio higher than 15 provides a polymeric character to the geopolymeric material. For many applications in the civil engineering field, a low Si: Al ratio is suitable (**Table 2.1**) (Davidovits, 1994b; Rangan, 2014).

**Table 2.1** Applications of geopolymeric materials based on silica-to-alumina atomic ratio (Rangan, 2014)

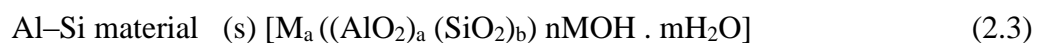
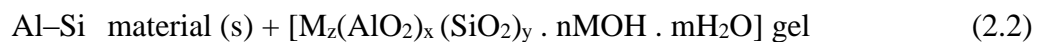
<b>Si:Al ratio</b>	<b>Applications</b>
1	<ul style="list-style-type: none"> <li>- Bricks</li> <li>- Ceramics</li> <li>- Fire protection</li> </ul>
2	<ul style="list-style-type: none"> <li>- Low CO<sub>2</sub> cements and concretes</li> <li>- Radioactive and toxic waste encapsulation</li> </ul>
3	<ul style="list-style-type: none"> <li>- Fire protection fibre glass composite</li> <li>- Foundry equipments</li> <li>- Heat resistant composites, 200°C to 1000°C</li> <li>- Tooling for aeronautics titanium process</li> </ul>
>3	<ul style="list-style-type: none"> <li>- Sealants for industry, 200°C to 600°C</li> <li>- Tooling for aeronautics SPF aluminium</li> </ul>
20 - 35	<ul style="list-style-type: none"> <li>- Fire resistant and heat resistant fibre composites</li> </ul>

### 2.3 Geopolymerization

Khale and Chaudhary (2007) explained clearly that geopolymerization is a geosynthesis that involves naturally occurring silico-aluminates. Any pozzolanic compound or source of silica and alumina, which is readily dissolved in the alkaline solution or activator, acts as a source of geopolymer precursor species and thus lends itself to geopolymerization. The alkali component as an activator is also called as alkali activated aluminosilicate binders or alkali activated cementitious material.

Geopolymerisation is an exothermic procedure that is completed through oligomers (dimer, trimer) which provide the definite unit structures for the three dimensional macromolecular edifice. Among several hardening mechanisms could be the chemical reaction of alumino-silicate oxides with alkalis and alkali-polysilicates, leading to polymeric Si–O–Al bonds with a  $(\text{Si}_2\text{O}_5, \text{Al}_2\text{O}_2)_n$  formula, which may be accomplished by calcining alumino-silicate hydroxides  $(\text{Si}_2\text{O}_5, \text{Al}_2(\text{OH})_4)$  through the reaction (Davidovits, 1988).

Generally, the primary steps of geopolymerization comprise of (I) dissolution of solid alumino-silicate oxides in MOH solution (M: alkali metal), (II) diffusion or transportation of dissolved Al and Si complexes from the particle surface to the inter-particle space, (III) formation of a gel phase resulting from the polymerization between added silicate solution and Al and Si complexes and (IV) finally hardening of the gel phase (Xu, 2001). Xu and Van Deventer (2000) proposed the following reaction scheme for the polycondensation taking place during geopolymerization of minerals:



In reactions (2.1) and (2.2), the amount of Al–Si material used in solid phase depends on the particle size, the extent of dissolution of Al–Si materials and the concentration of the alkaline solution. The formation of  $[M_z(\text{AlO}_2)_x (\text{SiO}_2)_y \cdot n\text{MOH} \cdot m\text{H}_2\text{O}]$  gel fundamentally relies on the extent of dissolution of alumino-silicate materials, while geopolymers with amorphous structure are formed during reaction (2.3). The alumino-silicate solution requires the enough time to form a continuous gel, depending on raw material processing conditions (Komnitsas & Zaharaki, 2007) .

Duxson et al. (2007) stated that the dissolution of the starting materials is the major step having a twofold role. Firstly, polysialate forming species are liberated from the starting materials in a similar way as in the formation of zeolite precursors. Secondly, dissolution activates the surface and binding reactions take place contributing significantly to the final strength of the geopolymer structure.

commented about alkaline conditions, alumino-silicates are transformed into extremely reactive materials. It is commonly believed that the dissolution process is initiated by the presence of hydroxyl ions ( $\text{OH}^-$ ). Higher amounts of hydroxyl ions simplify the dissociation of different silicate and aluminate species, promoting thus further polymerisation. However, if an excess high alkaline environment ( $>30$  mol% overall  $\text{Na}_2\text{O}$  content) is used, the connectivity of silicate anions may be decreased resulting thus in poor polymerization (Singh et al., 2005).

Panagiotopoulou et al., (2007) studied the dissolution of aluminosilicate minerals and by-products in alkaline media and described that the level of dissolution is higher when NaOH instead of KOH is used. This is due to the smaller size of  $\text{Na}^+$  which can better stabilize the silicate monomers and dimers present in the solution, enhancing thus the minerals dissolution rate (Xu and Van Deventer, 2003). It was

also reported that Si and Al seem to have a synchronized leaching behavior in both alkaline activator.

The fundamentals of alkaline activation of aluminosilicates simply started by way of mixing a solid with the suitable proportions of highly reactive silicate and aluminate raw materials and a liquid alkaline activator with a high alkali concentration. The solid and liquid can be mixed in various liquid: solid ratios proportions, depending on the fineness of the solid material (the finer the material, the higher the water demand). The resulting sample can set and harden as a Portland cement (**Figure 2.3**) (Shi et al., 2011).

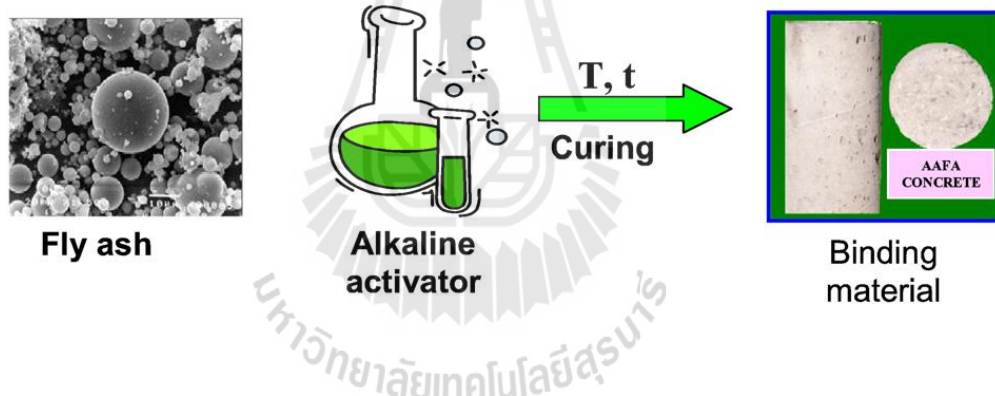


**Figure 2.3** Schematic description of the alkaline activation of fly ash

(Shi et al., 2011).

Shi et al. (2011) additionally explained that the three stages of Glukhovskiy model comprising the alkaline activation reaction are as described below (**Figure 2.4**).

First stage called “destruction–coagulation” is the disaggregation process entailing the separation of the Me–O, Si–O–Si, Al–O–Al and Al–O–Si bonds in the

raw material. The presence of alkaline metal cations counterbalances these anions, generating Si–O–Na<sup>+</sup> bonds, by way of hindering reaction reversibility. Additionally, the conditions created by the Si–O–Na<sup>+</sup> complexes, which are stable in alkaline media, are appropriate for the transport of the reacting structural units and the development of the coagulated structure. In this step, the vitreous/amorphous component of the solid particles dissolves when it comes into contact with the alkaline solution (pH>10). This is the mechanism that rules the early stage solid particle dissolution, in which aluminates and silicates are released. The dissolution rate is dependent on the pH of the medium and the other system components.

Second stage called coagulation – condensation, accumulation enhances contact among the disaggregated products which form a coagulated structure where polycondensation takes place. The polycondensation rate is imposed by the state of the dissolved ions and the existence or otherwise of the conditions necessary for gel precipitation.

For the third stage called condensation–crystallization, the presence of particles from the initial solid phase and the micro-particles resulting from condensation supports product precipitation. The mineralogical composition of the initial phase, the nature of the alkaline component and the hardening conditions determine the qualitative and quantitative composition of the crystallized products.

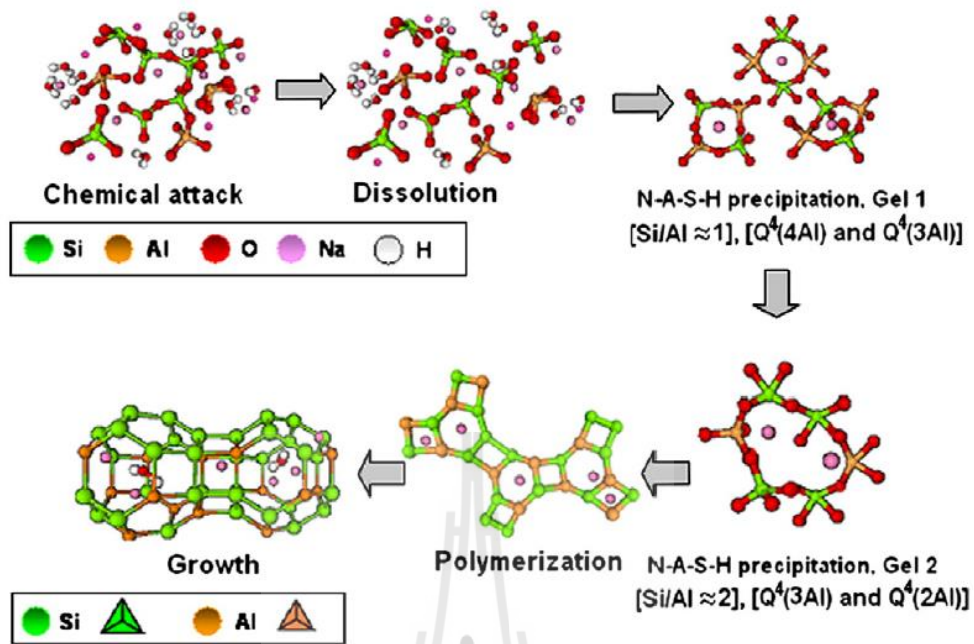


**Figure 2.4** Descriptive model for alkali activation of aluminosilicates  
 (Shi et al., 2011).

Duxson et al. (2007) confirmed the geopolymerization model of Glukhovskiy. They presented a highly simplified reaction mechanism for geopolymerization as shown in **Figure 2.5**. The reaction mechanism shown summarizes the key processes occurring in the transformation of a solid aluminosilicate material into a synthetic alkali aluminosilicate.

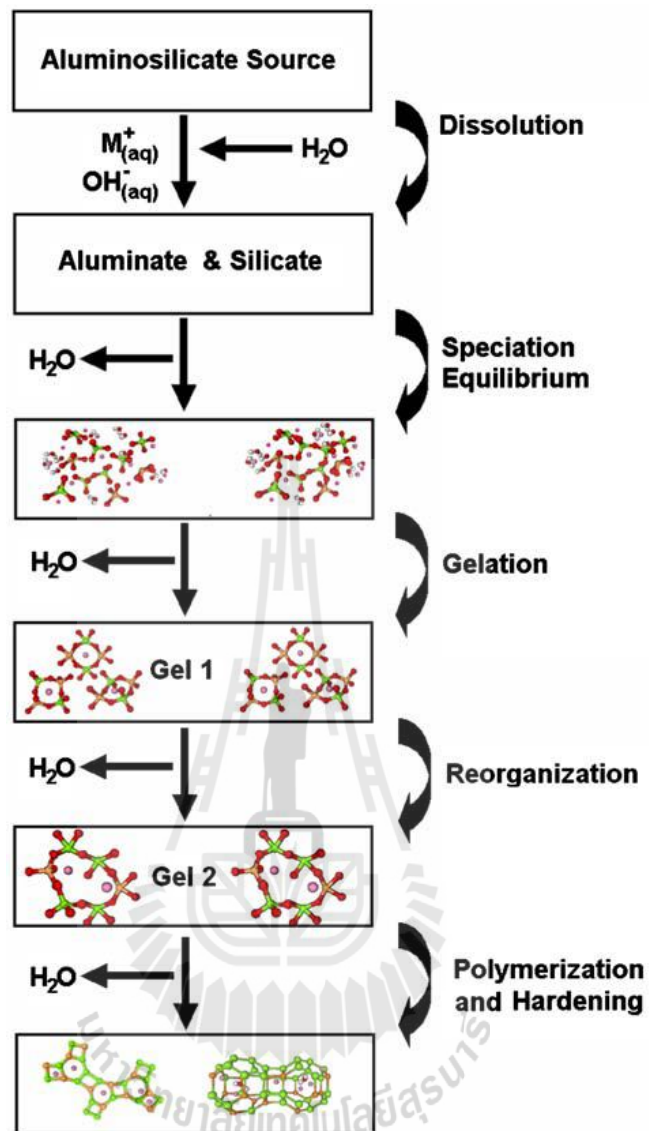


**Figure 2.5** Conceptual model for geopolymerization (Duxson et al., 2007).

Fernández-Jiménez et al. (2006) studied the role of reactive alumina content playing in the alkaline activation of fly ashes. They explored the relationship between the chemical composition of FA and the microstructural characteristics and mechanical properties of the cementitious materials resulting from the alkali activation of fly ashes.

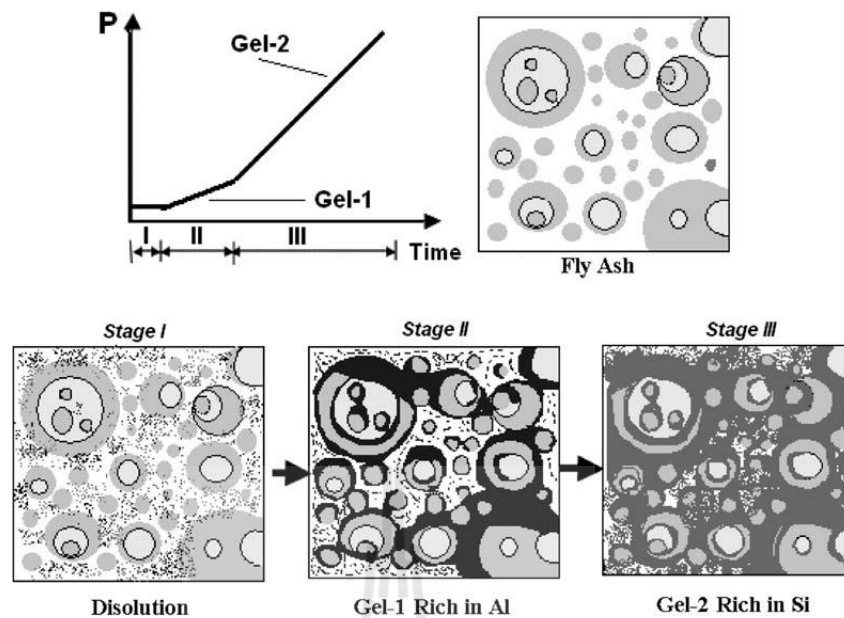


**Figure 2.6** Schematic description of mechanical properties evolution to the reaction time. The increment of mechanical performances is related to the Si/Al ratio in the gel (Fernández-Jiménez et al., 2006).

From this study, the results have clearly exhibited that the advantages of dissolved Al and Si at a given moment highly influences the kinetics of the alkaline activation of fly ashes. Apart from which other factors such as concentration of the activator, curing temperature and curing time, play also a significant role in kinetics of gels formation. From a thermodynamic point of view, the process of activation of fly ashes can be divided up to three main stages (see **Figure 2.6**) (Fernández-Jiménez et al., 2006). The first Stage (Dissolution stage) starting when most of the glassy component of the fly ash is dissolved. Mechanical strength development is not detected during the dissolution process. The second Stage (Induction period), occurring during the induction period a massive precipitation of a Gel 1 takes place,

that produces the coating of unreacted fly ash particles. This gel displays the singular characteristic of incorporate a big part of the reactive aluminium. This stage is helped to the initial setting of the paste. The latest stage (Silicon incorporation stage) corresponds to a period in which Gel 1 is transformed into Gel 2 being a Si-rich material because it accommodates into the structural framework. The reaction degree runs advancing till reaching values  $> 90\%$  and the strength increases considerably (Fernández-Jiménez et al., 2006).

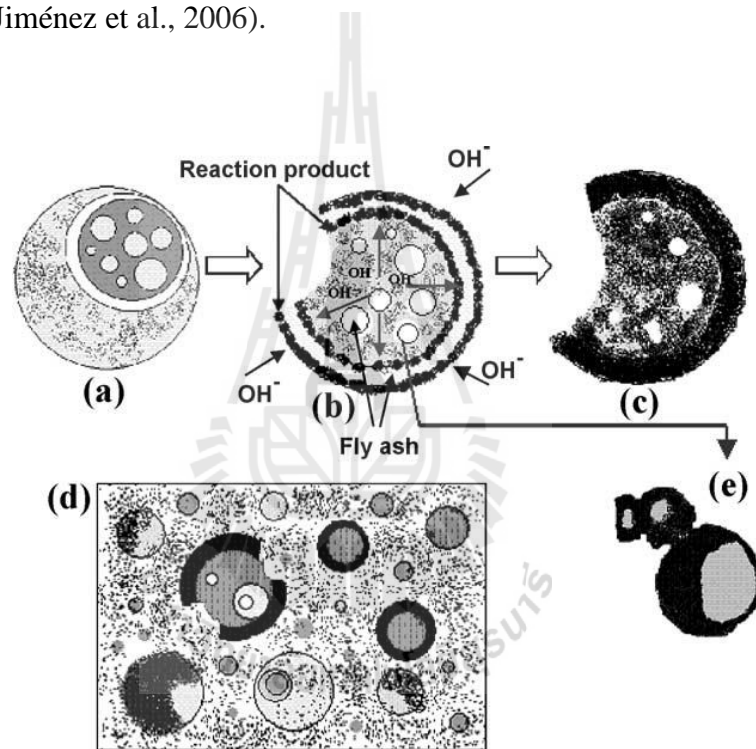


**Figure 2.7** Descriptive model of the alkali activation of fly ash

(Fernández-Jiménez et al., 2005).

Fernández-Jiménez et al. (2005) explained the descriptive model of the alkali activation of fly ash as **Figure 2.7**. **Figure 2.7a** exhibits the initial chemical attack at one point on the surface of a FA particle, which then amplifies into a larger hole (see

**Figure 2.8b**), exposing smaller particles. Either hollow or partially large FA is filled with other smaller ashes to bi-directional alkaline attack such as both of from the outside in and from the inside out (see **Figure 2.7b** and **2.9a**). In the same line with this, the reaction product is generated both inside and outside the shell of the sphere, until the FA particle is completely or nearly completely consumed (see **Figure 2.7c**). The mechanism involved at this phase is dissolution. At the same time, whilst the alkaline solution infiltrates and contacts the smaller particles located within a larger spheres, the interior space of the latter starts to fill up with reaction product, forming a dense matrix. **Figure 2.7e** presents one of the consequences of the massive precipitation of reaction products that a layer of these products covers certain parts of the smaller spheres. This coating prevents their contact with the alkaline medium (see **Figure 2.9b**). Furthermore, the geopolymerization processes are not uniform throughout the gel but vary locally from one point in the matrix to another. They depend on many factors such as the distribution of particle size and the local chemistry (e.g. pH). **Figure 2.7d** shows several morphologies comprised of unreacted particles, particles attacked by the alkaline solution but which maintain their spherical shape, reaction product and so on.

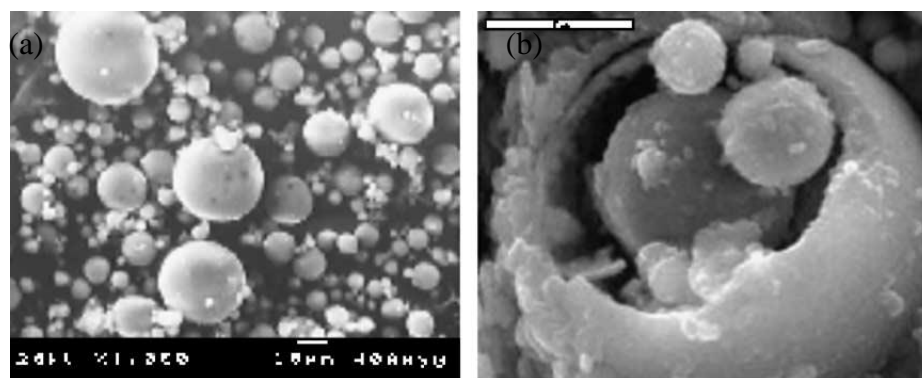


**Figure 2.8** SEM pictures: (a) original fly ash and (b) fly ash activated with 8 M NaOH for 5 h at 85°C (Fernández-Jiménez et al., 2005).

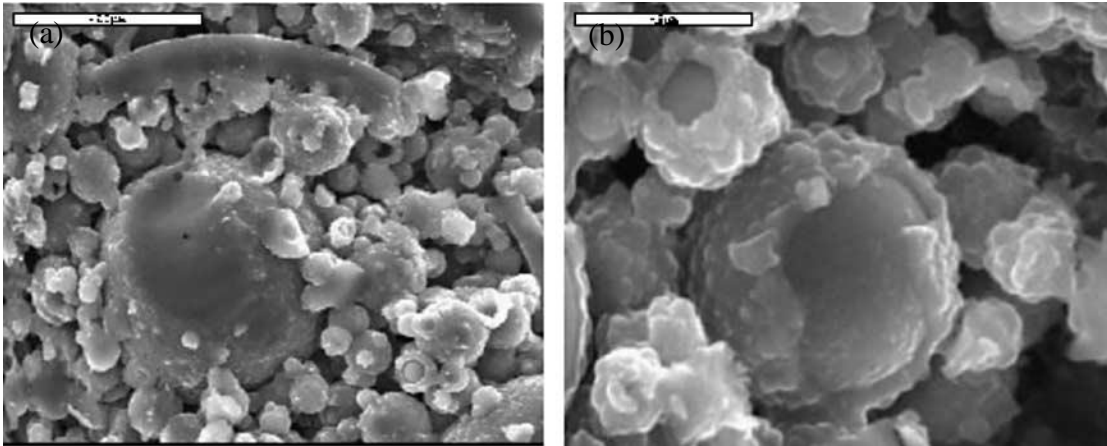


**Figure 2.9** SEM pictures of fly ash activated with 8 M NaOH for 20 h at 85°C; (a) reaction process of a large sphere and (b) singular details of the reaction of some small spheres (Fernández-Jiménez et al., 2005).

## 2.4 Alkaline Activators

Rangan (2014) proposed that the liquid alkaline activators are from soluble alkali metals that are generally Sodium or Potassium based. The most common alkaline activators used in geopolymerisation is a mixture of sodium hydroxide (NaOH) or potassium hydroxide (KOH) and sodium silicate or potassium silicate. Additionally, Many authors the most used alkaline activators are a mixture of sodium or potassium hydroxide (NaOH, KOH) with sodium waterglass ( $n\text{SiO}_2\text{Na}_2\text{O}$ ) or potassium waterglass ( $n\text{SiO}_2\text{K}_2\text{O}$ ) .

Palomo et al. (1999) studied the alkali-activation of fly ashes reporting an activator with a 12 M concentration leads to better results than a 18 M concentration. They also used free waterglass alkaline activators, having noticed lower mechanical performances (Palomo et al., 1999) . They mentioned that the alkaline activator plays

a crucial role in the polymerization reaction, behaving more swiftly when the soluble silica is present. Additionally, is also shared the same statement, according to whom waterglass supports the polymerization process leading to a reaction product with more Si and more mechanical strength.

Fernández-Jiménez and Palomo (2003, 2005) reported an increase from 40 to 90 MPa just after one day curing, when an alkaline activator with NaOH and waterglass are used together instead of just NaOH.

Xu and Van Deventer (2000) confirmed that the use of waterglass increase the dissolution of the prime materials. They studied the alkali-activation of different natural alumino-silicate minerals, having noticed that most of them could not provide enough Si to start the geopolymerization, thus needing additional soluble silica. studied pastes of fly ashes/slag and claim that compressive strength is influenced by the concentration of sodium hydroxide. They also reported compressive strength increase with slag content increase, explaining that with higher reactivity of the blast furnace slag. Lee and Van Deventer (2002a) reported on increasing dissolution due to an excess of alkali, but it also leads to a formation of a alumino-silicate gel in the first curing ages, leading to mechanical strength decrease. Krizan and Zivanovic (2002) investigated the alkali-activation of blast furnace slag with waterglass and metasilicate noticing that the highest strength was obtained for Ms (1.2–1.5). Other authors (Xie & Xi, 2001) used fly ash based mixtures activated with waterglass and sodium hydroxide. They reported that when the NaOH amount increase lowering the silica modulus ( $M_s = 1.64$ ), the silicate excess crystallized and was responsible for higher strength.

Fernández-Jiménez and Palomo (2005) studied the activation of fly ash. They investigated with several activators in which the  $\text{Na}_2\text{O}$  content changes from 5% to 15%. They summarized that the  $\text{SiO}_2/\text{Na}_2\text{O}$  molar ratio and the W/B ratio influence mechanical strength. They also noticed that using a  $\text{Na}_2\text{O}$  content of 5.5% by fly ash mass leads to a very low pH, which affects the reaction development in a negative way and also that the  $\text{Na}_2\text{O}$  content increase leads mechanical strength increase, and that the use of 14% of  $\text{Na}_2\text{O}$  by fly ash mass leads to optimum mechanical performance. Another time, different alkali concentrations are used for different raw materials, and that calcium free materials use higher alkali concentrations.

Phetchuay et al. (2014) studied the liquid alkaline activator which is a mixture of sodium silicate solution ( $\text{Na}_2\text{SiO}_3$ ), water and CCR. Their observation can explain the role and contribution of influential factors on strength development. CCR dissolves the silicon and aluminum in amorphous phase of FA and the  $\text{Na}_2\text{SiO}_3$  acts as a binder. The maximum soaked strength of the clay-FA geopolymer is found at  $\text{Na}_2\text{SiO}_3/\text{water}$  ratio of 0.6 and FA replacement ratio of 15%. The optimal  $\text{Na}_2\text{SiO}_3/\text{water}$  ratio is approximated from index test, which is a very practical approach. CCR is found to be a sustainable alkaline activator for geopolymer stabilized subgrade.

## **2.5 Raw Materials**

Rangan (2014) indicated that the source materials for geopolymers based on alumina-silicate should be rich in silicon (Si) and aluminium (Al). There are from either natural materials or by-product materials. These could be natural minerals such as kaolinite, clays, etc. The by-product materials could be mostly used fly ash, silica

fume, slag, rice husk ash, red mud and so on. The factors that choose what source materials for producing geopolymer depends on availability, cost, type of application, and specific demand of the end users.

Shi et al. (2011) described that alkali-activated cements usually comprise of two components: alkaline activators and a cementitious component. Caustic alkalis or alkaline salts are normally used as alkaline activators in alkali activated cements and concretes. Various industrial by-products and waste materials and a number of aluminosilicate raw materials have been used as the cementitious components. These materials include granulated blast furnace slag, granulated phosphorus slag, steel slag, coal fly ash, volcanic glass, zeolite, metakaolin, silica fume and non-ferrous slag and so on. Additionally, the same authors also mentioned that alkali-activated cements can be classified into five groups:

(1) alkali-activated slag-based cements: blast furnace slag, phosphorus slag, blast furnace slag-fly ash, blast furnace slag-steel slag, blast furnace slag-MGO, and blast furnace slag-based multiple component cement

(2) alkali-activated pozzolan cements: fly ash, natural pozzolan, metakaolin and soda lime glass

(3) alkali-activated lime-pozzolan/slag cements: lime–natural pozzolan, lime–fly ash, lime–metakaolin and lime–blast furnace slag

(4) alkali-activated calcium aluminate blended cements: metakaolin/ calcium aluminate, pozzolan/ calcium aluminate and alkali-activated fly ash/ calcium aluminate

(5) alkali-activated Portland blended cements (hybrid cements): Portland blast furnace slag, Portland phosphorus slag, Portland Fly ash, Portland blast furnace slag–steel slag, Portland blast furnace slag–fly and multiple components blended

Pacheco-Torgal et al. (2008b) mentioned theoretically that any materials comprised of silicon and aluminium can be alkali activated. Up to now the investigations performed have used the following raw materials: kaolinitic clays, metakaolin, fly ash, slag, mixtures of fly ash and slag, mixtures of fly ash and metakaolin, mixtures of slag and metakaolin, mixtures of slag and red mud, mixtures of fly ash and non-calcined materials like kaolin, mixtures of fly ash and silica fume, and mixtures of rice husk ash and other materials

In 1974 and 1975, Kaolinite and other clays were originally used as fillers for the encapsulation of radioactive wastes into a monolithic solid (Komnitsas and Zaharaki, 2007). Davidovits (1984))Davidovits (1984)) primarily used kaolinite and calcined kaolinite (metakaolin) as source of alumino-silicate oxides for geopolymer. Xu and Van Deventer (2000) indicated that the addition of kaolinite is necessary because of the insufficient rate of Al dissolution from the raw materials to produce a desired composition gel. Moreover, the low reactivity of kaolinite also requires adequate time for forming of the source materials and gel phase. They have also concentrated on the manufacture of geopolymeric products using either kaolinite or metakaolinite as the main reactant (Xu and Deventer, 2002b). However, Van Jaarsveld et al. (2002) stated that a large amount of kaolinite added may not participate in the synthesis reaction at all. Many other researchers are to determine the most convenient calcination temperature of kaolinite clays in view of producing

geopolymer cements and to determine new approach for the production of kaolinite-based geopolymers (Hamaideh et al., 2014; Zhang et al., 2009) .

Xu and Van Deventer (2000) examined sixteen different alumino-silicate minerals with the addition of kaolinite in order to synthesize geopolymer and observed that for the majority of the alumino- silicate minerals. They discovered that the addition of kaolinite is required for the forming of gel. If only kaolinite used in the system have no the presence of other alumino-silicates, a fragile structure is formed, which means synergy between different aluminosilicates is seemingly quite important.

Palomo et al. (1999) studied the usage of natural minerals and wastes (in particular fly ash) in geopolymerization and immobilization of toxic metals was also investigated extensively in recent years. Also, Van Jaarsveld et al. (1998) have used black coal fly ash and construction wastes as the beginning for geopolymerization.

Xu and Deventer (2002a) used fly ash, kaolinite and albite (Na-rich end member of the Albite-Anorthite Series.) in various proportions for the synthesis of geopolymer. It is supposed that the larger reactivity of fly ash and albite, the interaction between the source materials and the gel phase along with the reinforcing effect induced by the large unreacted albite particles are accountable for a required mechanical behavior (high compressive strength and low cracking probability).

Davidovits (2005) studied the 15 types of combustion fly ashes tested for suitability in geopolymer cements. The samples were cured at room temperature and the compressive strength was measured after 28 days. A sizable variation in the behavior of the fly ashes was detected ranging from unworkable situations to strength of 95 MPa.

Some authors (Xu and Van Deventer, 2000) evidenced that calcined materials for example slag, fly ash and metakaolinite which are generally amorphous, usually display a greater reactivity during geopolymerization in comparison to non-calcined materials. This is described by the truth that calcination activates materials by changing their crystalline into amorphous structure with subsequent storage of the additional energy (Xu and Deventer, 2002a).

Furthermore, the production of consistent geopolymer from heterogeneous industrial waste sources is a certainly challenging issue for the minerals industry, since raw material suitability cannot be completely guaranteed by elemental composition analysis (Fernández-Jiménez and Palomo, 2003). Thus far as fly ash based geopolymers are concerned, the mechanical strength increases as a result of the formation of an Al-rich aluminosilicate gel during the early stage of alkaline activation of ash particles, and may further increase as a result of the Si enrichment of the material. Duxson et al., (2007) summarized that it is, therefore, important to operate Al and Si dissolution from the raw materials, through pre-processing and/or utilization of combinations of raw materials with diverse reactivity.

After study about the microstructure development of alkali-activated fly ash cement: a descriptive model, Fernández-Jiménez et al. (2005) concluded that it is important that the activation reaction rate is dependent upon several factors such as the particle size distribution and the mineral composition of the starting material as well as the type and concentration of the activator.

## **2.6 Role of materials in FA geopolymer**

### **2.6.1. Slag**

Goretta et al. (2004) examined the compressive strength of Class C - FA, slag and sodium silicate alkali-activated concrete. The aggregate constituted 52% and an alkali activator 11.2% of the total mass; the mass ratio of silicate to (FA + slag) was 0.29. The result described that compressive strength of 35 MPa at 14 days curing time. Smith and Osborne (1977) and Bijen and Waltje (1989) found that waterglass-activated FA/slag blends gave very low strength, but NaOH activation contributed higher strengths.

Weiguo et al. (2011) studied that replaced FA with slag at levels of 0% to 100% by weight, in FA/slag cements. Waterglass and NaOH which was used as alkaline activator. The results showed that the compressive and flexural strengths increased as the slag content increased. Garía et al. (2006) studied the compressive strength of the alkali activated FA/slag composites. The FA/slag ratios were 100/0, 75/25, 50/50, 25/75 and 0/100, by weight. Sodium silicate with modulus ( $\text{SiO}_2/\text{Na}_2\text{O}$ ) of 0, 0.75, 1, 1.5 and 2 was used as alkaline activator. The % $\text{Na}_2\text{O}$  was added at 4%, 6% and 8%, related to the binder weight. The pastes were cured at 75°C for 24 h and then at 20°C up to 28 days. The results indicated that for 0/100 pastes, the highest strengths were for 4%  $\text{Na}_2\text{O}$  (80–85 MPa).

Chi and Huang (2013) presented the compressive strength and flexural strength, at ages of 7, 14 and 28 days, of geopolymer mortars made of different combinations of FA/slag ratios of 100/0, 70/30, 50/50, 30/70, 0/100, by weight. Sodium silicate with modulus ratio of 1 was used as alkaline activator. Two concentrations of  $\text{Na}_2\text{O}$  of 4% and 6% were employed. The results showed that the composition of 50/50 achieved the highest compressive strength and flexural strength followed by 30/70, 0/100, 70/30 and 100/0, respectively, at both 4% and 6%  $\text{Na}_2\text{O}$ .

Yang et al. (2012) studied the activation of FA/slag pastes with alkaline activator with modulus of 1.2, 1.4 and 2.0. The ratios of FA/slag were 100/0, 80/20, 60/40, 40/60, 20/80 and 0/100, by weight. The compressive strength of the pastes measured at ages of 3, 7 and 28 days were showed that the composition of 20/80 gave the highest compressive strength followed by 40/60, 0/100, 60/40, 80/20 and 100/0, respectively.

Kumar et al. (2010) partially substituted FA with slag at levels of 0%, 5%, 15%, 25%, 35% and 50%, by weight, in FA/slag-based geopolymers. An increase in the compressive strength was detected with the inclusion of slag. As slag content increased as the compressive strength increased.

Wang et al. (2012) investigated the compressive strength and porosity of alkali- activated FA–slag–MK cementitious materials arranged by hydrothermal method. Waterglass was used as alkaline activator with the modulus adjusted to 1.0 by dissolving NaOH. The ratio of water to solid was about 0.35. Different mixtures with different contents of slag, MK and FA were employed. The slag contents ranging from 16.2% to 31.33%, the FA contents ranging from 20.46% to 73.52%, and MK contents ranging from 7.22% to 49.39%. The compressive strength results indicated that this type of material had higher mechanical strength. The highest compressive strength value reached nearly 80 MPa. They suggested that the higher compressive strength was attributed to the addition of slag. The more contents of slag in the system, the more hydration products of CSH and hydrated aluminates calcium were obtained.

### **2.6.2 Metakaolin**

Zhang et al. (2009) mixed FA with MK to produce FA/MK-based geopolymers. The FA/MK ratios were 66.7/33.3, 50/50, 33.3/66.7 and 0/100, by weight. NaOH and water were mixed into sodium silicate to adjust the mole ratio of 1.2. Curing conditions were either in steam at 80°C or in air at 20°C for 1, 3 and 6 days. They concluded that proper addition of MK (66.7%) increased the fluidity of fresh paste, prolonged its setting time and improved the compressive strength of hardened geopolymer. The compressive strength of the geopolymer containing 66.7% MK, by steam curing for 6 days, was improved by 35.5%.

Wu and Sun (2010) partially replaced FA with MK at levels of 0%, 10%, 20% and 30%, by weight, in FA/MK-based geopolymers. The investigational results presented an increased in the workability as well as an increase in the 1, 7 and 28 days compressive strength with increasing MK content.

Yunsheng et al. (2009) examined some properties of FA/MK mortars. The ratios of FA/MK were 70/30, 50/50, 30/70, 10/90 and 0/100, by weight. NaOH and sodium silicate solution with the molar ratio of 3.2 was used as alkaline activator. There were different curing conditions. They summarized that geopolymer containing 30% FA and 70% MK that was synthesized at steam curing (80 °C for 8 h), exhibited higher mechanical strength. The compressive strength was 32.2 MPa.

Zhang et al. (2009) studied some properties of alkali-activated FA/MK. The proportions of FA/MK were 70/30, 50/50, 30/70, 10/90 and 0/100, by weight. NaOH and sodium silicate solution were used as alkaline activator. The compressive and flexural strengths at 2 days presented that the composite 0/100 gave the highest compressive strength and flexural strength followed by 30/70, 10/90 and 50/50, respectively, whilst the composite of 70/30 came in the last place. The incorporation

of FA increased the electrical resistivity of geopolymeric pastes, whereas FA content had a little impact on the electrical resistivity.

### 2.6.3 Silica fume

Nuruddin et al. (2010) studied the partial replacement of FA, in geopolymer concretes, with silica fume (SF) at levels of 0%, 3%, 5% and 7%, by weight. Sodium silicate and NaOH solution was used as alkaline activator. Sugar based material was incorporated, 3% of total binder, to increase the setting time. There were three different curing conditions named hot gunny, ambient and external exposure curing. The compressive strength results showed that the optimal replacement level with SF that gave the highest compressive strength depended on curing condition. In hot gunny curing, 3% SF was the optimal. In ambient temperature curing, 7% SF was the optimal, whilst 100% FA was the optimal at the external exposure curing.

Dutta et al. (2010) and Thokchom et al. (2011) studied the partial replacement of FA with SF, in pastes and mortars, at levels of 0%, 2.5% and 5%, by weight. Sodium silicate and NaOH solution was used as activator. The activator concentration was 8% Na<sub>2</sub>O, while molar ratio was 1. The specimens were cured at 85°C for 48 h then allowed to cool inside the oven. The compressive strength results indicated that as the SF content increased in the pastes as the compressive strength slightly decreased. In contrast, as the SF content increased in the mortars as the compressive strength increased.

Songpiriyakij et al. (2011) also studied the partial replacement of FA with SF, in pastes at levels of 0%, 10%, 20%, 30% and 40%, by weight. Mixture of Na<sub>2</sub>OSiO<sub>2</sub> and NaOH was used as activator. The NaOH concentration was 10 M or

18 M. The  $\text{Na}_2\text{OSiO}_2/\text{NaOH}$  ratio was 2.5. The compressive strength and bonding strength, at ages of 1, 3, 7, and 28 days, increased with increasing SF content and NaOH concentration.

#### **2.6.4 Portland cement**

Lohani et al. (2012) studied the replacement of FA in concretes with PC at levels of 0%, 10%, 25%, 40%, 60% and 100%, by weight. NaOH was used as alkaline activator. The slump results indicated higher workability with decreasing PC content. On the other hand, compressive strength increased with increasing PC content.

Palomo et al. (2007) studied partially substituted FA with PC clinker at level of 30%, by weight. The composite was activated with either NaOH solution or waterglass + NaOH solution. Mixture hydrated with deionized water was employed for comparison. The compressive strength results showed that the highest compressive strength was obtained when waterglass + NaOH was used as activator. Mixture mixed with deionized water came in the second place, while mixture activated with NaOH came in the last place.

Guo et al. (2009) studied the compressive strength at ages of 3, 7 and 28 days of FA/PC-based geopolymers activated with alkaline activator as NaOH solution and sodium silicate solution. FA was partly replaced with PC at levels of 0%, 10%, 20%, 30%, 40% and 50%, by weight. The specimens were cured at 23°C. They reported that the 40% PC provided better mechanical performance compared to the binders using other mixture ratios. They also partially replaced Class C FA with PC at levels of 0%, 10%, 20%, 30%, 40% and 50%, by weight. NaOH solution and sodium silicate solution were used to activate the composites in which the amount of  $\text{Na}_2\text{O}$

was fixed at 10 wt%. The pastes were cured at 75°C for 4, 8 and 24 h or at 23°C for 3, 7 and 28 days. They concluded that specimens made of 60/40 had better mechanical performance compared to binders using other mixture ratios.

Pangdaeng et. al.(2014) studied the influence of curing conditions on properties of high calcium FA geopolymer containing OPC as additive with different curing conditions. OPC was replaced at dosages of 0%, 5%, 10%, and 15% by weight. Three curing methods comprised of vapour-proof membrane curing, wet curing and temperature curing were used. The results showed that the use of OPC as additive improved the properties of high calcium fly ash geopolymer. The strength increased due to the formation of additional C–S–H and C–A–S–H gel.

### **2.6.5 Lime**

Shi (1996) studied the strength of FA/lime paste preparing FA/lime at ratio of 80/20 without activation or with activation by 4% Na<sub>2</sub>SO<sub>4</sub>. The water to solid ratio of 0.35 was used to produce a paste with normal consistency. Paste specimens were cured in fog room at temperature of 23°C, up to testing date. The results indicated that the addition of Na<sub>2</sub>SO<sub>4</sub> raised the alkalinity of pore solutions, accelerated initial pozzolanic reaction which gave the high early strength of the FA/lime paste.

Shi and Day (1999) investigated the effect of addition of lime on the strength development and hydration of FA/slag mixtures activated with NaOH and sodium silicate. They concluded that the addition of a small amount of hydrated lime significantly increased the early-age strength, but slightly decreased the later-age strength of the cements.

Fan et al. (1999) offered new method of FA activation with addition of lime and a small quantity of Na<sub>2</sub>SiO<sub>3</sub>. FA/lime pastes without or with small quantity

of  $\text{Na}_2\text{SiO}_3$  were tested in compression at ages of 3, 14, 28, 56, 90 and 120 days. The results indicated that the inclusion of  $\text{Na}_2\text{SiO}_3$  increased the compressive strength at ages of 3, 14 and 28 days, whilst no effect on the compressive strength at age of 56 days. On the other hand, the inclusion of  $\text{Na}_2\text{SiO}_3$  decreased the compressive strength at ages of 90 and 120 days, in comparison with FA/lime without  $\text{Na}_2\text{SiO}_3$ .

### **2.6.6 Natural pozzolan**

Nazari et al. (2011) studied the partial replacement FA with rice husk-bark ash (RHBA) at levels of 20%, 30% and 40%, by weight, in geopolymers activated with waterglass + NaOH. The compressive strength results showed that 30% RHBA combined with 70% FA gave the highest compressive strength at 7 and 28 days. The composition of 20% RHBA coupled with 80% FA came in the second place, while the composite of 40% RHBA coupled with 60% FA came in the last place.

Nuruddin et al. (2011) showed the compressive strength development (from 3 days up to 56 days in curing) through polymerization process of alkaline solution and FA blended with microwave incinerated rice husk ash (MIRHA). FA was blended with MIRHA at levels of 3%, 5% and 7%. A solution of NaOH and  $\text{Na}_2\text{SiO}_3$  was used as alkaline activator. Concrete specimens were cured at three different conditions named hot gunny curing (33–38°C), ambient curing (27–32°C) and external exposure curing (39–44°C). At hot gunny and ambient curing, the results indicated that the addition of 5% MIRHA gave the highest compressive strength, followed by 0%, followed by 3% and 7%. At external exposure curing, the results indicated that the addition of MIRHA at level of 0% provided the highest compressive strength, followed by 7%, followed by 3% and 5%.

### **2.6.7 Calcium carbide residue**

Jaturapitakkul and Roongreung (2003) proposed a new cementitious material from a mixture of CCR and rice husk ash which consist mainly of  $\text{Ca(OH)}_2$  and  $\text{SiO}_2$ , respectively. The CCR to rice husk ash ratio was 50:50. The UCS of mortar was 15.6 MPa at 28 days and increased to 19.1 MPa at 180 days of curing time. According to the UCS of mortar, this mixture has a high potential to be used as a cementing material.

Krammart and Tangtermsirikul (2004) investigated on using municipal solid waste incinerator bottom ash (MSWI) and calcium carbide waste (CCW) as a part of the cement raw materials. The mixture were replaced by 5% and 10% of MSWI and CCW, respectively to study the compressive strength and compare with these made of cement.. It was found that the compressive strength of CCW cement mortars was close to that of the control cement. However, compressive strength of MSWI cements was smaller than that of the control cement mortar.

Makaratat et al. (2010) investigated the use of CCR and FA as a low  $\text{CO}_2$  emission concrete binder. The CCR and FA was mixed at ratio of 30:70 by weight and was used as a binder to cast concrete without portland cement. Without the use of portland cement, the compressive strengths of samples were 28.4 and 33.5 MPa at 28 and 90 days, respectively. The hardened concretes produced from the mixtures had mechanical properties similar to those of control cement concrete. In addition, the addition of 3%  $\text{CaCl}_2$  by weight of binder produced CCR-FA concrete that demonstrated high workability and accelerated the compressive strength at early ages (Makaratat et al., 2011). Somna et al. (2011) studied the microstructures of CCR and CCR-ground fly ash (GFA) pastes by using SEM and XRD. A ratio of CCR to GFA of 30 to 70 by weight was used as a binder without PC. The three different water-to-

binder (W/B) ratios were 0.3, 0.4, and 0.5 were prepared. This chemical reaction was possibly similar to the pozzolanic reaction. The compressive strengths of all samples increased with curing time and remained constant after 42 days. Amnadhua et al. (2013) evaluated the mixture of CCR and ground fly ash (GFA) for use as a new cementing material with PC for use as an activator to promote the reaction to produce high strength concrete. The compressive strength of mixture containing 20% PC could be as high as 67 MPa or 95% of OPC concrete at 28 days and increased up to 73 MPa at 90 days or 90% of OPC concrete. The samples with and without PC had moduli of elasticity similar to OPC concrete.

Horpibulsuk et al. (2012) and Horpibulsuk et al. (2013) investigated the possibility of using this cementitious material (a mixture of CCR and FA) to improve the strength of problematic silty clay in northeast Thailand. The significant factors involved in this study were water content, binder content, CCR:FA ratio, and curing time. Strength development is investigated using the UCS test and a microstructural study using SEM. The result shown that the input of CCR reduces specific gravity and soil plasticity. The maximum strength of the stabilized soil occurred at approximately the optimum water content for different binder contents, CCR:FA ratios, and curing times. The improvement in strength for a particular curing time was classified into three zones: active, inert, and deterioration. The strength increases remarkably with the CCR content for all CCR:FA ratios in the active zone.

Kampala and Horpibulsuk (2013) studied the engineering properties of CCR-stabilized silty clay to ascertain its performance in pavement base and subbase applications. The result presented that the soaked engineering properties were thus dependent upon the state of water content. The optimal mix proportion is the CCR

fixation point at optimum water content (OWC). CCR stabilization was more effective than lime stabilization in terms of engineering, economic, and environmental viewpoints. Kampala et al. (2013) studied the engineering properties of recycled CCR stabilized clay as fill and pavement materials. The research outcome supported the possibility of using the recycled CCR stabilized clay as fill and pavement materials. The strength and resistance to compressibility were slightly lower than those of the original CCR stabilized clay for the same CCR content while the unit weight of recycled CCR stabilized clay was much lower.

## **2.7 Factors affecting compressive strength**

Provis et al. (2005) mentioned that measurements of compressive strength are employed by many researchers as an instrument to measure the success of geopolymerization due to the low cost and simplicity of compressive strength testing, along with of the truth that strength development is really a primary way of measuring the utility of the materials found in different applications of the construction industry.

Van Jaarsveld et al. (2003) and Xu (2001) described that the compressive strength of geopolymer is dependent upon many factors such as the gel phase strength, the ratio of the gel phase/undissolved Al–Si particles, the distribution and the hardness of the undissolved Al–Si particle sizes, the amorphous nature of geopolymer or the amount of crystallinity, and the surface reaction between the gel phase and the undissolved Al–Si particles.

Furthermore, factors such as %CaO, %K<sub>2</sub>O and the kinds of alkali have an important correlation with compressive strength. The significance of the molar Si/Al

ratio during the alkaline dissolution of the individual minerals suggests that compressive strength is obtained by complex reactions between the mineral surface, kaolinite and the concentrated sodium silicate solution (Komnitsas and Zaharaki, 2007).

After geopolymerization, the undissolved particles remain bonded in the matrix, so the hardness of the minerals correlates positively with the last compressive strength (Xu and Van Deventer, 1999, 2000). During geopolymerization of natural minerals, it is known that after adding aggregate for instance granular sand to the geopolymer mixture, the compressive strength increases (Xu and Deventer, 2002a).

The quantity of metakaolinite added to the geopolymer matrix, along with the KOH concentration and the addition of sodium silicate, also play an important role on the last compressive strength. Swanepoel et al. (1999) proved that the strength increases with increasing addition of metakaolinite. The main reason might be that the more metakaolinite added, the more Al gel forms in the system, causing a higher level of polymerization.

Wang et al. (2005) proved experimentally that the compressive strength, along with the apparent density and the content of the amorphous phase of metakaolinite-based geopolymer, increase with the increase of NaOH concentration within the range 4–12 mol/L. This is caused by the enhanced dissolution of the metakaolinite particulates and therefore the accelerated condensation of the monomer in the clear presence of higher NaOH concentration.

It is supposed that the quantity of unreacted materials in specimens with higher silica content acts as defect site and includes a negative impact on strength. Higher strength was recorded once the ratios  $\text{SiO}_2/\text{Al}_2\text{O}_3$  and  $\text{Na}_2\text{O}/\text{Al}_2\text{O}_3$  were 3.0–

3.8 and approximately 1, respectively (Duxson et al., 2005; Stevenson & Sagoe-Crentsil, 2005) . However, De Silva et al. (2007) mentioned that these initial ratios might be changed based on the total amount of the raw materials used as  $\text{Al}_2\text{O}_3$  and  $\text{SiO}_2$  source.

Based on Phair and Van Deventer (2001), the most significant factor that controls the compressive strength of fly ash-based geopolymer may be the pH of the original alkali metal silicate precursor. When working with cement as a setting additive in the geopolymer matrix, the compressive strength increases almost exponentially with increasing pH.

Khale and Chaudhary (2007) explained that the most significant factor controlling the compressive strength is pH. The setting time of cement decreased as the pH of the activating solution increased. At lower pH values the geopolymeric mix remained viscous and behaves like cement while at higher pH, the mix attained a more fluid gel composition, which was less viscous and is more workable. Higher solubility of monomers was expected by KOH than NaOH because of higher alkalinity (**Figure 2.10**). From the above observations it is clear that pH range 13–14 is most suitable for the formation of the geopolymers with better mechanical strength.

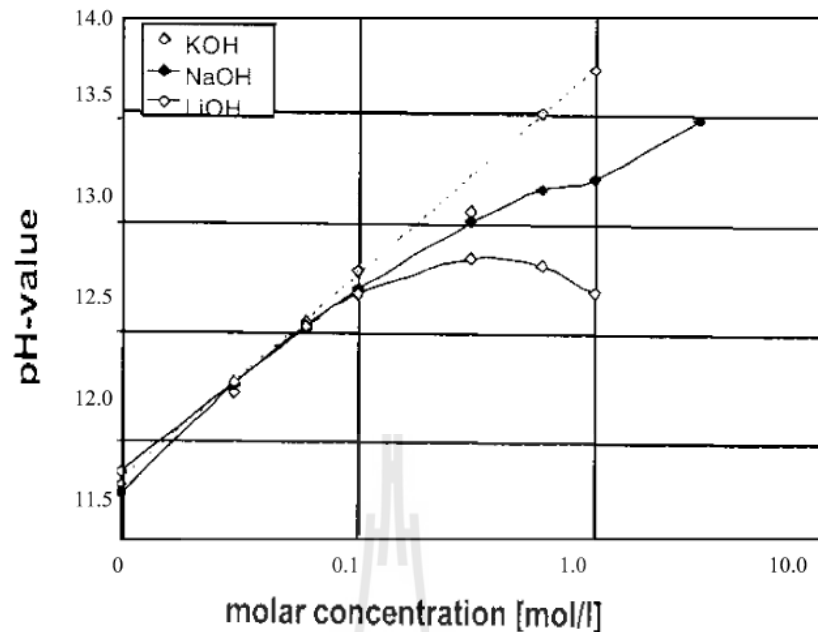


**Figure 2.10** Influence of the concentration and kind of the alkaline solution on the pH value (Khale and Chaudhary, 2007).

The influence of curing temperature and time on the flexural properties of geopolymer centered on class C fly ash has been investigated by Miller et al. (2005). Duxson et al. (2007) discovered that the curing regime includes a very significant effect on the physical and chemical properties of fly ash-based geopolymer. Indeed, the mere escalation in synthesis temperature is sufficient to boost the degree of long-range ordering in geopolymer binders.

Chindaprasirt et al. (2007) stated that moisture evaporation results in deterioration of the geopolymer product which cannot develop satisfactory strength. Furthermore, the addition of water improves the workability of the mortar. Perera et al. (2007) studied that the water within geopolymer and its subsequent removal by evaporation plays a significant role in obtaining a crack-free geopolymer, which

means that rapid drying during curing should be avoided, while curing at less relative humidity (e.g. 30%) is advised. Also, it had been found that when the curing temperature is high (approximately 90°C), the geopolymer will substantially lose the moisture (Bakharev, 2005).

Pangdaeng et al. (2014) studied the influence of curing conditions on properties of class C FA geopolymer containing OPC as additive with different curing conditions. OPC was replaced at dosages of 0%, 5%, 10%, and 15% by weight. Three curing methods comprised of vapour-proof membrane curing, wet curing and temperature curing were used. The results showed that the curing methods also significantly affected the properties of geopolymers with OPC. The temperature curing resulted in a high early compressive strength development.

Bakria et al., (2011) studied the effect of curing temperature on physical and chemical properties of geopolymers. The geopolymer samples were prepared using different curing temperatures (room temperature, 50°C, 60°C, 70°C, 80°C), in which sodium silicate and NaOH were used as alkaline activators. The samples were cured for 24 hours in the oven and tested on the seventh day. The result revealed that the maximum compressive strength (67.04 MPa) was obtained at a temperature of 60°C. However when the geopolymers sample cured at temperature more than 60°C, the compressive strength decreased. From the FTIR spectra, the higher content of Si on sample cured at 60°C also contributed to higher compressive strength. Moreover, SEM analysis showed a denser matrix as well as less unreacted fly ash of the sample cured at 60°C compared to other temperatures.

Xie and Kayali (2014) studied the effect of initial water content and curing moisture conditions on the development of fly ash-based geopolymers in heat and

ambient temperature The research presented in this paper was conducted in the aim of improving the ambient-cured (20°C) geopolymer. This has been achieved by controlling the moisture condition of the specimens after hardening. This paper also examines whether there are mechanical effects as a result of variation in the initial water content. It further explores whether a combination of such variation together with controlling the curing regime may lead to desired improvement in the mechanical properties. The role of water was studied by monitoring the microstructural and mineralogical developments and relating them to the gain in strength. It has been found that reducing water content in the initial state and controlling the moisture condition during a curing period after hardening are beneficial and lead to extra strength gain in the ambient-cured fly ash-based geopolymer.

Bakharev (2005) studied the influence of elevated temperature curing on phase composition, microstructure and strength development in geopolymer materials prepared using Class F fly ash and sodium silicate and sodium hydroxide solutions. In particular, the effect of storage at room temperature before the application of heat on strength development and phase composition was studied. X-ray diffraction (XRD), Fourier transform infrared spectroscopy (FTIR) and SEM were utilised in this study. Long precuring at room temperature before application of heat was beneficial for strength development in all studied materials, as strength comparable to 1 month of curing at elevated temperature can develop in this case only after 24 h of heat curing. The main product of reaction in the geopolymeric materials was amorphous alkali aluminosilicate gel.

Hou Yunfen et al. (2009) studied the influences of concentration and modulus of sodium silicate solution and curing mode on the phase composition, microstructure and strength development in the geopolymers prepared using Class F fly ash. The result show that the compressive strength increases as sodium silicate solution modulus increases, but when modulus exceeds 1.4, the compressive strength decreases, and it decreases markedly while the modulus is greater than 2.0. The compressive strength was improved by the increase of sodium silicate solution concentration. When the concentration is 32%, the compressive strength reaches the maximum, and then it reduces as concentration increasing. Elevated temperature can increase the strength of samples that synthesized from sodium silicate solution with 32% concentration and modulus 1.2. Compared to the strength of the sample cured at 50°C, the strength of the samples cured at 65°C and 80 °C are higher at 1 d and 3 d, but the same at 7 d. The main product of reaction in the geopolymeric material is amorphous alkali aluminosilicate gel.

## 2.8 Use of Promoters

Douglas et al. (1991) remarked that the replacement of blast furnace slag by silica fume and fly ash in alkali-activated mixtures led to mechanical strength increase. However, the strength reduces noticeably when high replacement amounts are used. Cheng et al. (1992) studied alkali-activated slag. They have reported a considerable increase in mechanical strength when 1.9–3.4% of  $\text{Ca(OH)}_2$  was used. In another investigation,

Alonso and Palomo (2001) studied the influence of the sodium hydroxide concentration on the nature of the formed reaction products which conclude that parameter has a crucial role on them:

- When the alkaline activator concentration is 10 M or higher, dissolution of  $\text{Ca}(\text{OH})_2$  is very difficult because of the presence of hydroxides ( $\text{OH}^-$ ), meaning there will not be enough to the formation of CSH gel. As a replacement for sodium based alumino-silicate is formed. When that occurs, it attracts  $\text{OH}^-$  to its structure, lowering the amount of them and allowing the formation of CSH gel as a secondary reaction product.
- When the alkaline activator concentration is lower than 5 M, the amount of hydroxides ( $\text{OH}^-$ ) is very low, so the dissolution of calcium hydroxide takes place, meaning enough  $\text{Ca}^{2+}$  will be present to form CSH gel. Moreover, low alkaline concentration media prevents the metakaolin dissolution, so there is not enough dissolved aluminium to the formation of alkaline alumino-silicates, meaning that silica will be free to form CSH.

Lee and Van Deventer (2002b) investigated the influence of inorganic salt in alkali-activated mixtures of fly ash and kaolin. They have reported that strength and durability are undesirably affected by chloride salts, because they formed crystals inside the structure lowering its strength. They also found that carbonate salts are beneficial because they weaken the amount of dissolved water preventing the hydrolytic attack. Yip and Van Deventer (2003) informed that calcium increased strength because of the formation of Ca–Al–Si amorphous structures. They also found the coexistence of geopolymeric gel and CSH (**Figure 2.11**) and recommended that the formation of those two phases would explain the durability of ancient binders.

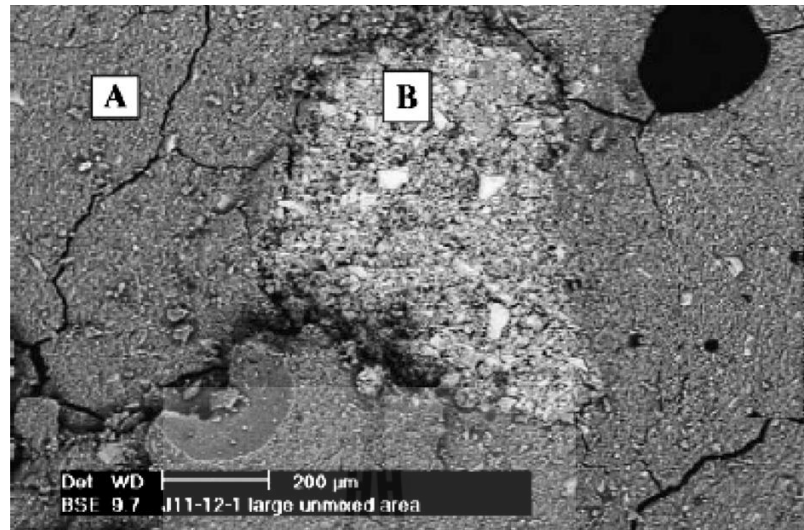


**Figure 2.11** Formation of geopolymeric gel (A) and CSH gel (B) (Cheng et al., 1992) .

De Vargas et al. (2014) studied the compressive strength development of fly ash-based mortars alkali-activated with activating solutions containing varying proportions of a mixture of NaOH and  $\text{Ca}(\text{OH})_2$ . M5 matrices ( $C/S = 0.05$  and  $C/N = 0.033$ ) containing small amounts of  $\text{Ca}(\text{OH})_2$  exhibited increasing compressive strength as age increased. However, M15 ( $C/S = 0.15$  and  $C/N = 0.37$ ) and M25 ( $C/S = 0.25$  and  $C/N = 0.70$ ) matrices, containing higher proportions of  $\text{Ca}(\text{OH})_2$ , exhibited a decrease in compressive strength over time, from 28 days of age. There, the  $C/S$  and  $C/N$  ratios are important variables for the mechanical stability of alkali-activated fly ash matrices using combined NaOH and  $\text{Ca}(\text{OH})_2$  activators. Additionally, the SEM of the M5 and M25 matrices also investigated and showed the presence of two different aluminosilicate gels, the M5 and M25 sample. The first one developed a massive aluminosilicate gel over time, while the second one exhibited a spongy gel

from 28 days onwards, resulting in a weaker material. **Figure 2.12** and **Figure 2.13** show the development of compressive strength of alkali-activated mortars and SEM images of the M5 and M25 pastes, respectively.

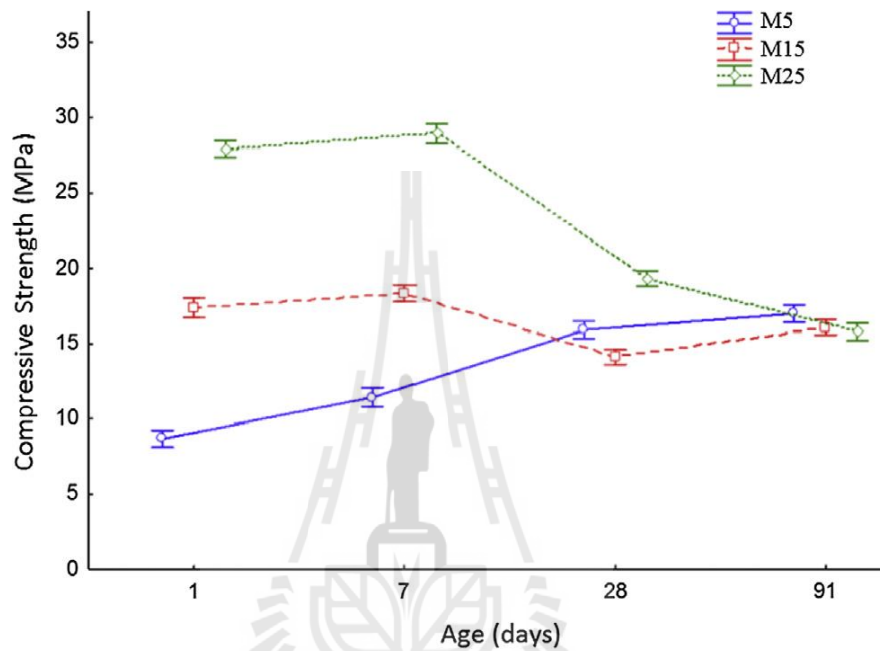


**Figure 2.12** Development over time of the compressive mechanical strength of alkali activated mortars (De Vargas et al., 2014).

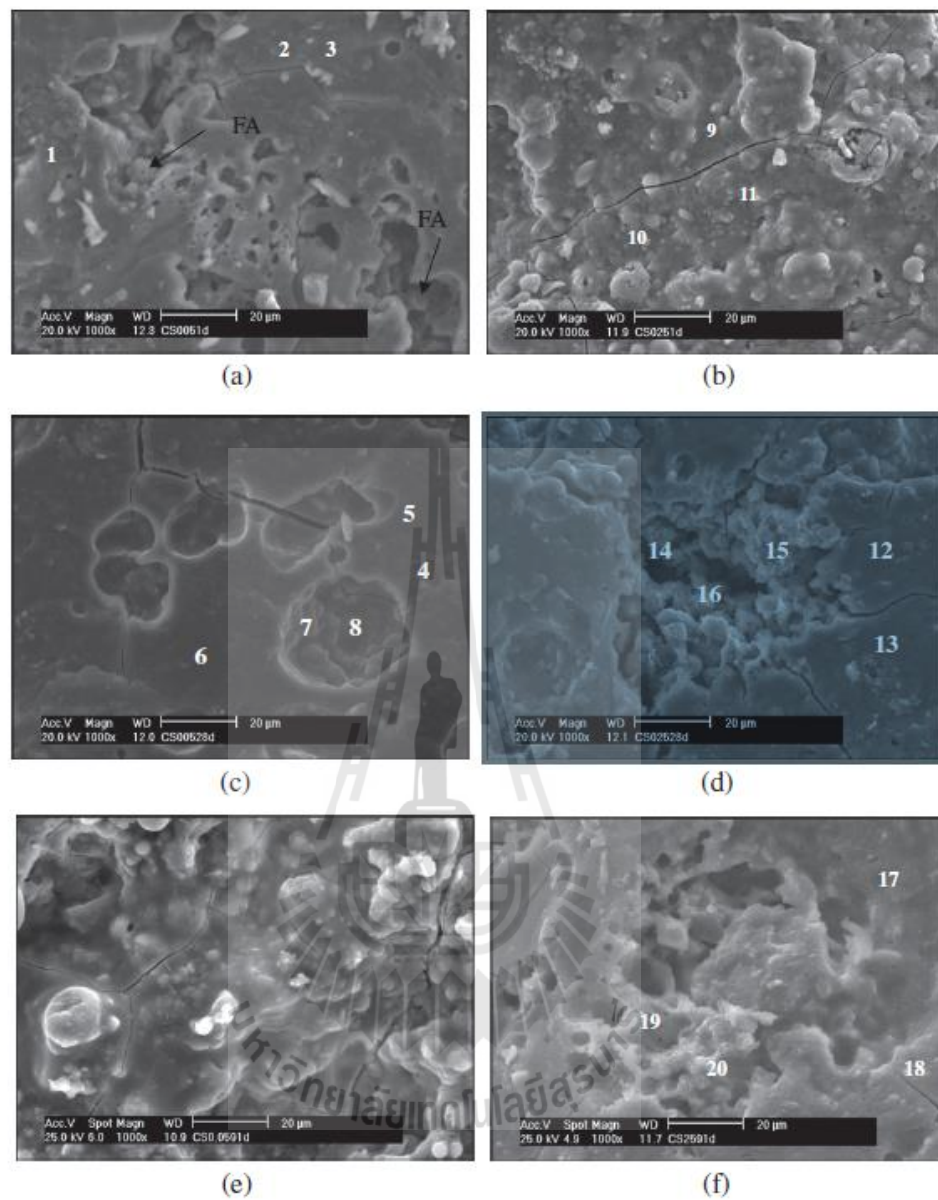


**Figure 2.13** SEM micrographs of the M5 and M25 pastes, respectively, at: (a) and (b) 1 day; (c) and (d) 28 days; and (e) and (f) 91 days (De Vargas et al., 2014).

## 2.9 Analytical techniques

Several easy or advanced techniques can be utilized to acquire maximum information and elucidate geopolymerization mechanisms. The capability of Al–Si

minerals to undergo geopolymerization might be predicted by specific surface area measurements, which offer an indication of how much surface area participates in heterogeneous reactions inside a solid–fluid system (Van Jaarsveld et al., 2002). Optical microscopy provides a visible description of the microstructure because it is shown in scale the physical size and model of the different aspects of geopolymer. X-ray fluorescence (XRF) spectrometry works extremely well for elemental analysis of Al–Si minerals. X-ray diffraction (XRD) might be also a helpful tool although the quantity of information which may be obtained is restricted as a result of substantial amorphous nature of geopolymer. However it will provide information concerning the extent to which crystalline starting materials have reacted (Van Jaarsveld et al., 2002). **Figure 2.14** presents the XRD pattern of geopolymer when fly ash is employed as raw materials and activated employing a NaOH (8M) solution and cured at 85°C (20 h) (Fernandez Jiminez et al., 2004) .

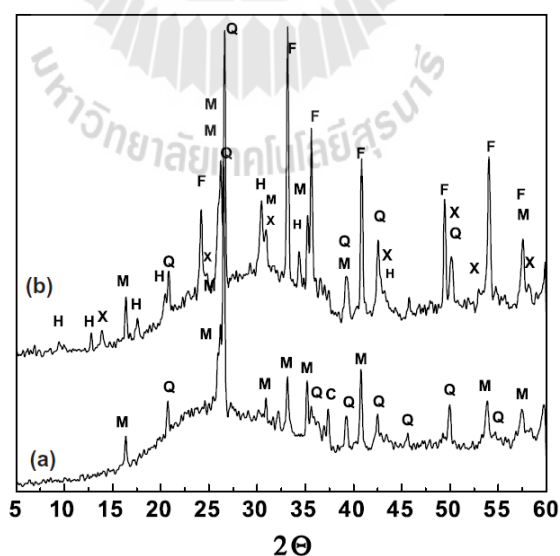


**Figure 2.14** XRD spectra (a) unreacted fly ash; (b) alkali-activated fly ash 20 h at 85°C. Q=Quartz; M=Mullite; F=Hematite; C=CaO; H=Herschelite; X=Hydroxysodalite (Fernandez Jiminez et al., 2004).

Duxson et al. (2006) and Lee mentioned that Scanning electron microscopy (SEM) allows visual examination of a product from millimeters to micrometers to yield definitive topographical information along with good physical and mechanical description of the microstructure of crystalline and amorphous materials, which may not be detected by other techniques. Fernandez Jiminez et al. (2004) provided the geopolymer microstructures (**Figure 2.15-2.18**) are characterized by way of a dispersion of distinctive morphologies in a large of predominantly featureless hydration product (alumino-silicate gel). Occasionally, cracking in the item is observed. This might be because of the thermal treatment carried out within the activation process, mechanical damage during sample preparation or to drying shrinkage in the vacuum of the electron microscope. The relatively low magnification images (**Figure 2.15 and 2.16**) offer a summary of the distribution of numerous constituent phases with an increase of local detail being provided in **Figure. 2.17 and 2.18** (Fernandez Jiminez et al., 2004).

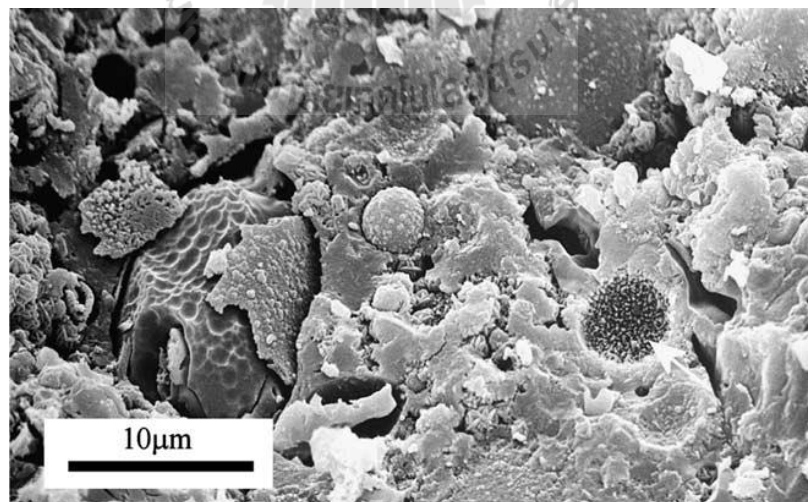


**Figure 2.15** SEM micrograph of fracture surface of alkali-activated PFA geopolymer  $\text{Fe}_2\text{O}_3$  is arrowed (Fernandez Jiminez et al., 2004).

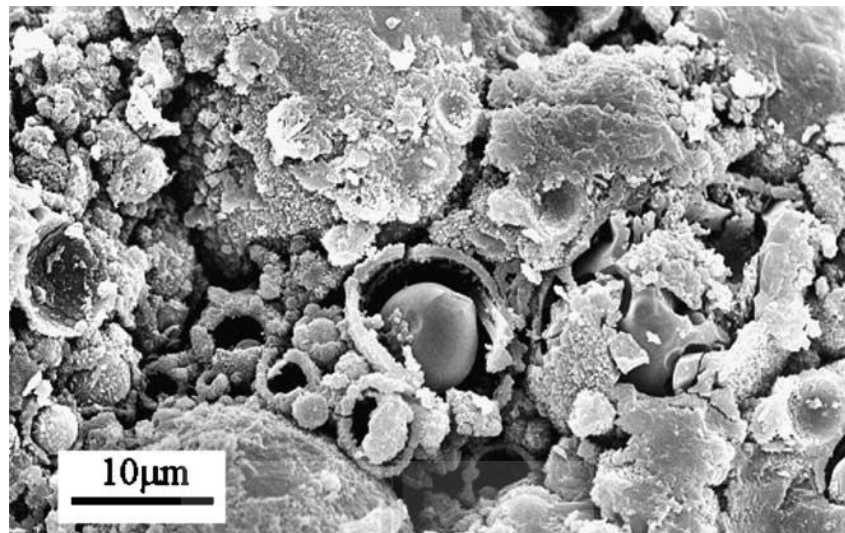


**Figure 2.16** SEM micrograph of fracture surface of alkali-activated PFA Geopolymer (Fernandez Jiminez et al., 2004).

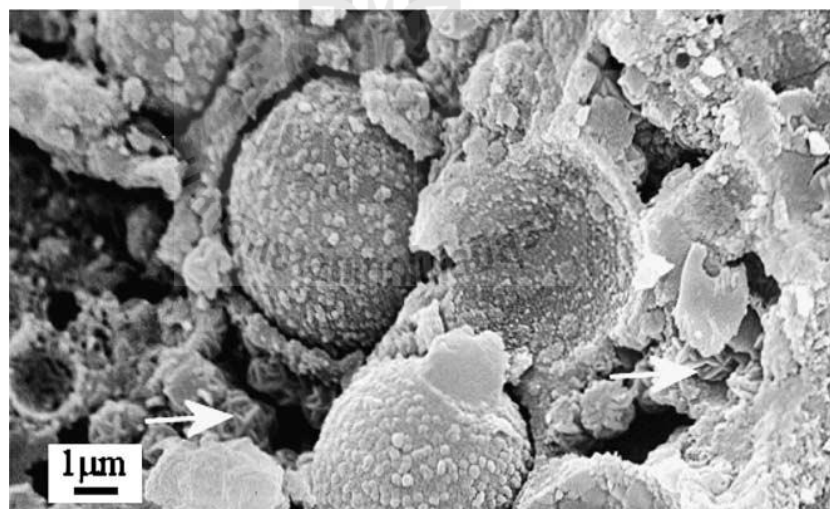


**Figure 2.17** SEM micrograph of fracture surface of alkali-activated PFA geopolymer showing PFA particle with reaction shells and also unidentified spherical assemblages (arrowed) (Fernandez Jiminez et al., 2004).

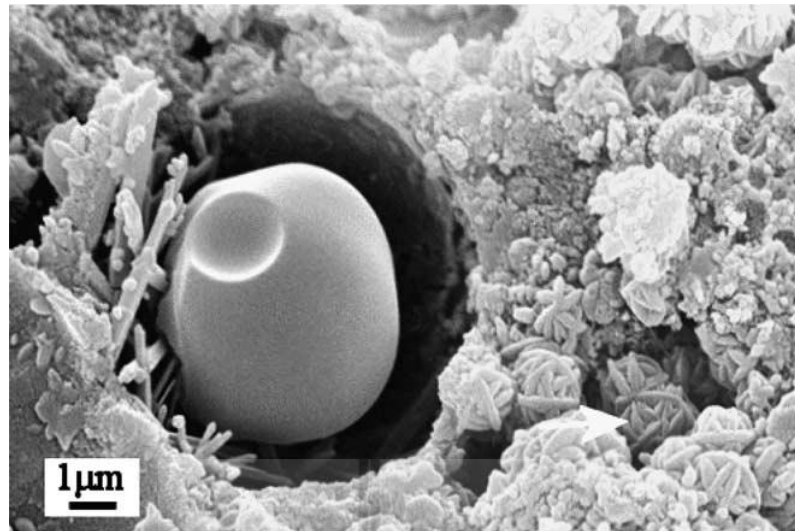


**Figure 2.18** SEM micrograph of fracture surface of alkali-activated PFA geopolymer showing considerably eroded PFA particle and also unidentified spherical assemblages (arrowed) (Fernandez Jiminez et al., 2004).

## 2.10 Soil stabilization with geopolymer

Many previous research reviewed in this work is geopolymer applications for replacement of concrete applications. However, present work studies geopolymer application for soil stabilizer which Portland cement plays significantly important role in soil improvement such as in those of clay for subgrade in low volume road (Phetchuay et al., 2014), marginal lateritic soil and crushed rock for subbase and base, respectively. Especially, pavement recycling for modified crushed rock base in road authority of Thailand has been using Portland cement as stabilizer.

Some author applied geopolymer form many raw materials for soil stabilizer replacing ordinary Portland cement, due to its mechanical properties, durability, friendly environments and so on.

Zhang et al. (2013) studied the experimental feasibility of geopolymer as the next-generation soil stabilizer. In present study, a lean clay was stabilized with metakaolin based geopolymer at different concentration (ranging from 3 to 15 wt.% of unstabilized soil at its optimum water content) to examine the feasibility of geopolymer in stabilizing soils. The UCS values of MKG stabilized soils are much higher than the soil and higher than 5% PC stabilized soil when MKG concentration is higher than 11% (see **Figure 2.19**). However, the strength increase from 7-day curing to 28-day curing is not appreciable, which might be due to quick reactions of MK-based geopolymer precursor. The testing results indicated that with geopolymer concentrations, compressive strength, failure strain and Young's modulus of the stabilized soil specimens increased, and shrinkage strains during curing decreased. The microstructural analyses confirmed the formation of geopolymer gels in the stabilized soil, and showed the soil tended to form more homogeneous and compact microstructures after stabilization. This study illustrated that metakaolin based geopolymer can be an effective soil stabilizer for clayey soils.

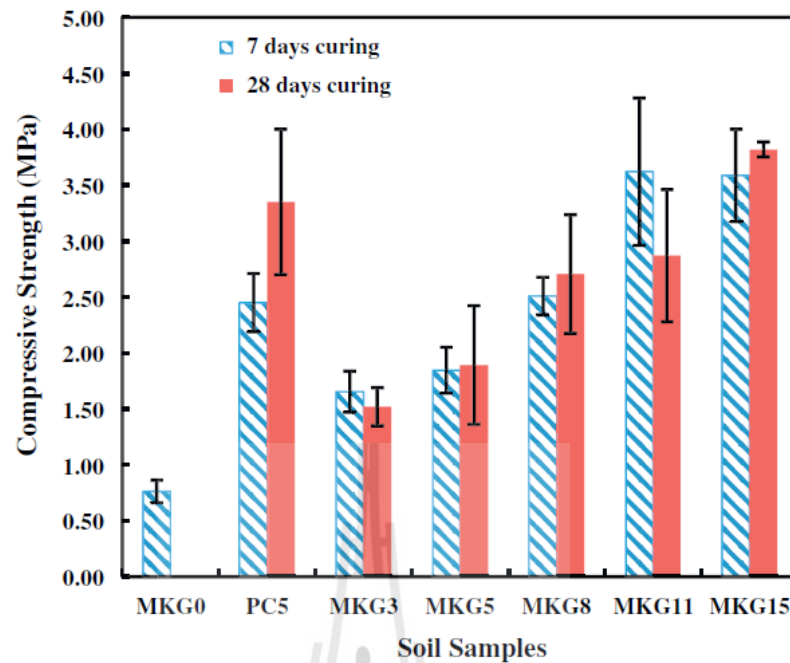


**Figure 2.19** The UCS of MKG stabilized soils, soil, and Portland cement stabilized soil samples after 7 and 28 day curing (Zhang et al., 2013).

Yi (2014) investigated the stabilization effectiveness of alkali-activated ground-granulated blast furnace slag (GGBS) for a marine soft clay, compared with that of Portland cement (PC). The influence of activators, including NaOH, Na<sub>2</sub>CO<sub>3</sub>, carbide slag (CS), NaOH-CS, Na<sub>2</sub>CO<sub>3</sub>-CS, and Na<sub>2</sub>SO<sub>4</sub>-CS, on the stabilization efficacy was investigated. The results indicated that Na<sub>2</sub>CO<sub>3</sub>-GGBS had no stabilization efficacy for this marine soft clay. NaOH-GGBS-stabilized clay yielded the highest UCS at 7, 28, and 90 days; however, the UCS decreased from 90 to 180 days because of the micro-cracking. CS-GGBS-stabilized clay had higher 90-day and 180-day UCS than that of PC-stabilized clay, but significantly lower 7-day and 28-day UCS. NaOH, Na<sub>2</sub>CO<sub>3</sub>, and Na<sub>2</sub>SO<sub>4</sub> could improve the strength development rate

of CS-GGBS-stabilized clay. However, the UCS of NaOH-CS-GGBS and Na<sub>2</sub>CO<sub>3</sub>-CS-GGBS-stabilized clays decreased from 90 to 180 days as well. Na<sub>2</sub>SO<sub>4</sub>-CS-GGBS was found to be the optimum binder for this marine soft clay, yielding at least twice higher UCS than that of PC stabilized clay at any age studied (via **Figure 2.20**).

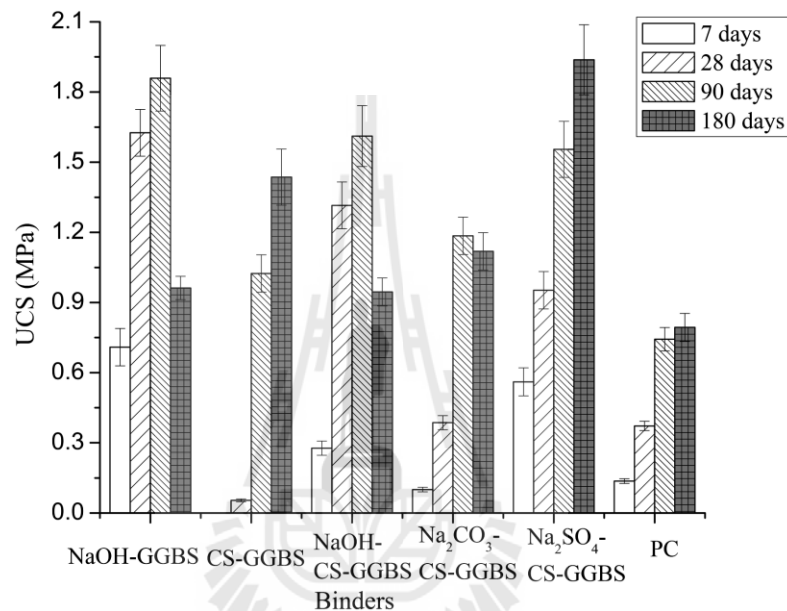


**Figure 2.20** UCS of stabilized clays at 7, 28, 90 and 180 days (Yi et al., 2014).

Sukmak et al. (2013) used locally available silty clay as an aggregate and high calcium FA as a precursor to develop masonry geopolymer units. The factors controlling the strength development (sukmak et al., 2013) and sulfate resistance of soil stabilized with high calcium FA based geopolymer were also investigated (sukmak et al., 2014). It is summarized that the strength increases with increasing the liquid alkaline activator. The excess input alkaline activator causes the precipitation at very early stage before the condensation process in geopolymerization

and results in the cracks on the FA particles. The overheating (very high temperature) and excess heat duration cause the micro-cracks on the specimens. The relationship between the strength and heat energy is proposed to integrate the role of heat temperature and duration on the geopolymerization (see **Figure 2.21 and 2.22**).

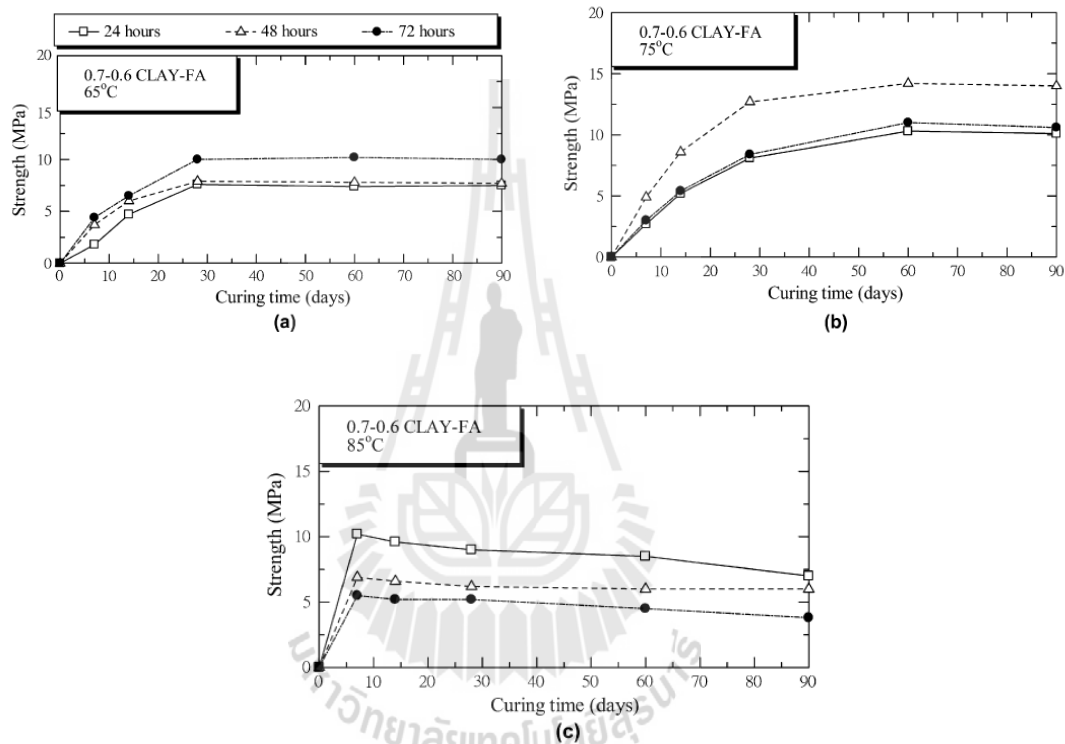


**Figure 2.21** Effects of heat condition on the compressive strength of the 0.7–0.6 CLAY– FA specimens heated at (a) 65°C, (b) 75°C and (c) 85°C (Sukmak et al., 2013).

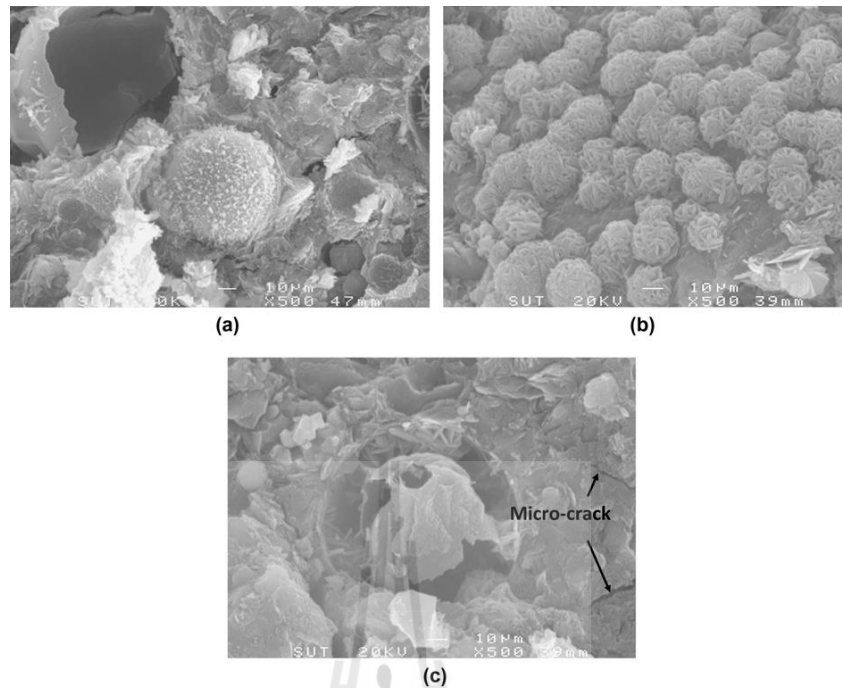


**Figure 2.22** SEM images of the 0.7–0.6 CLAY–FA specimens heated at 75°C for (a) 24 h, (b) 48 h and (c) 72 h after 28 days of curing.

Phetchuay et al. (2014) recently studied the viability of using calcium carbide residue (CCR) as an alkaline activator and FA as a precursor to stabilize problematic silty clay as a bound pavement material whose compressive strength meets the strength requirement, specified by the local national road authority of Thailand. The influential factors studied are  $\text{Na}_2\text{SiO}_3/\text{water}$  ratio, FA replacement ratio, curing time, curing temperature and soaking condition for a fixed CCR content of 7%. The maximum soaked strength of the clay-FA geopolymer is occurred at  $\text{Na}_2\text{SiO}_3/\text{water}$  ratio of 0.6 and FA replacement ratio of 15%. The samples with 40°C curing present higher strength than those with room temperature curing, CCR is found to be a

sustainable alkaline activator for geopolymer stabilized subgrade materials (see

Figure 2.23 and 2.24).

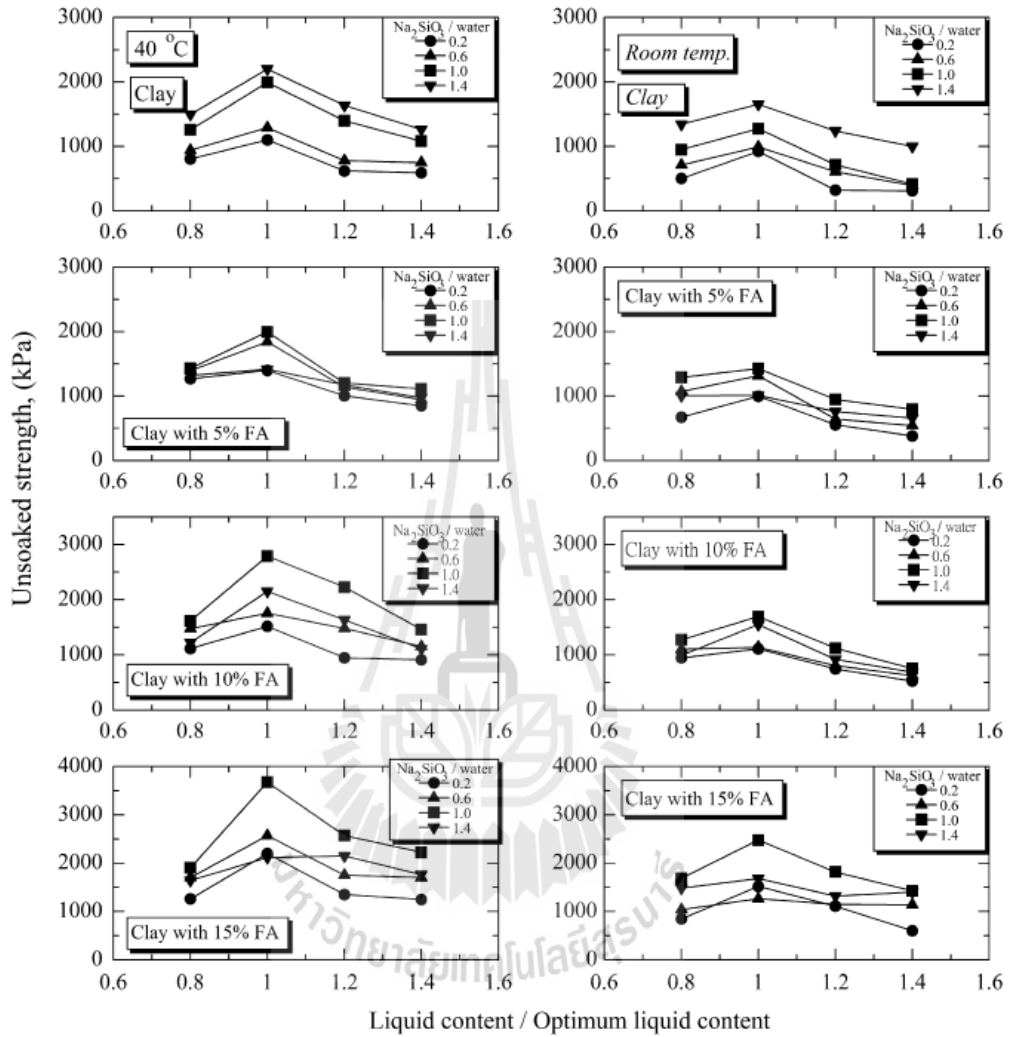
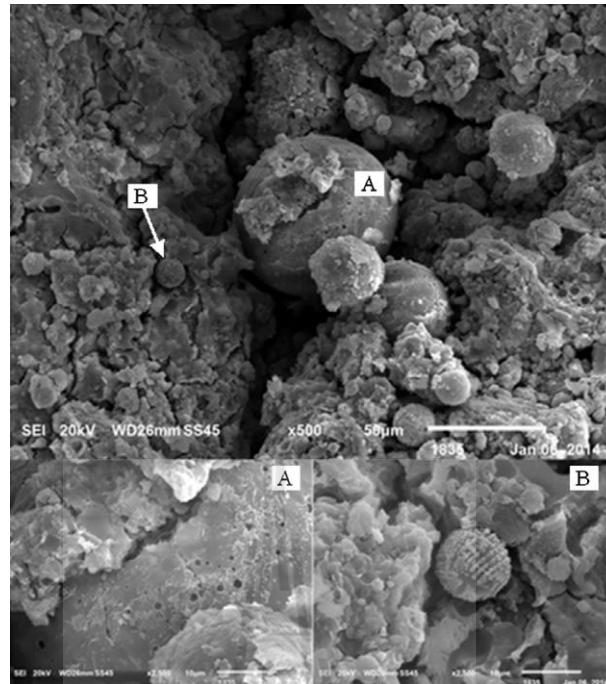


Figure 2.23 Effect of state of liquid content on unsoaked strengths of clay-FA geopolymers (Phetchuay et al., 2014).



**Figure 2.24** SEM images of clay-FA geopolymer at  $\text{Na}_2\text{SiO}_3/\text{water}$  ratio = 0.6, FA = 15%, 40°C curing after 60 days of curing (Phetchuay et al., 2014).

## 2.11 References

- Alonso, S., and Palomo, A. (2001). **Alkaline Activation of metakaolin and calcium hydroxide mixtures: influence of temperature, activator concentration and solids ratio.** *Materials Letters*, 47, 55-62.
- Amnadnua, K., Tangchirapat, W., and Jaturapitakkul, C. (2013). **Strength, water permeability, and heat evolution of high strength concrete made from the mixture of calcium carbide residue and fly ash.** *Materials and Design*, 51, 894-901. doi: 10.1016/j.matdes.2013.04.099

- Bakharev, T. (2005). **Geopolymeric materials prepared using Class F fly ash and elevated temperature curing**. *Cement and Concrete Research*, 35(6), 1224-1232. doi: 10.1016/j.cemconres.2004.06.031
- Bakria, A. M. M. A., Kamarudin, H., BinHussain, M., Nizar, I. K., Zarina, Y., and Rafiza, A. R. (2011). **The Effect of Curing Temperature on Physical and Chemical Properties of Geopolymers**. *Physics Procedia*, 22, 286-291. doi: 10.1016/j.phpro.2011.11.045
- Bijen, J., and Waltje, H. (1989, 1565-78). *Alkali activated slag-fly ash cements*. Paper presented at the Proceedings of the 3rd international conference on the use of fly ash, silica fume, slag & natural pozzolans in, concrete, SP-114.
- Brough, A. R., and Atkinson, A. (2002). **Sodium silicate-based, alkali-activated slag mortars Part I. Strength, hydration and microstructure**. *Cement and Concrete Research*, 32, 865–879.
- Cheng, Q. H., Tagnit-Hamou, A., and Sarkar, S. (1992). **Strength and microstructural properties of waterglass activated slag**. *Materials Research Society Symposium Proceedings*, 245, 49-54.
- Chi, M., and Huang, R. (2013). **Binding mechanism and properties of alkali-activated fly ash/slag mortars**. *Construction and Building Materials*, 40, 291-298. doi: 10.1016/j.conbuildmat.2012.11.003
- Chindaprasirt, P., Chareerat, T., and Sirivivatnanon, V. (2007). **Workability and strength of coarse high calcium fly ash geopolymer**. *Cement and Concrete Composites*, 29(3), 224-229. doi: 10.1016/j.cemconcomp.2006.11.002

- Criado, M., Palomo, A., and Fernandezjimenez, A. (2005). **Alkali activation of fly ashes. Part 1: Effect of curing conditions on the carbonation of the reaction products.** *Fuel*, 84(16), 2048-2054. doi: 10.1016/j.fuel.2005.03.030
- Davidovits, J. (1979). **Synthesis of new high temperature geo-polymers for reinforced plastics/composites. SPE PACTEC 79 Society of Plastic Engineers, Brookfield Center.** 151-154.
- Davidovits, J. (1984). **Synthetic mineral polymer compound of the silicoaluminates family and preparation process.** *US Patent 4, 472, 199.*
- Davidovits, J. (1988). *Long term durability of hazardous toxic and nuclear waste disposals.* Paper presented at the Proceedings of the 1st International Conference on Geopolymer '88, vol. 1, Compiègne, France, 1-3 June.
- Davidovits, J. (1991). **Geopolymer: inorganic polymeric new materials.** *Journal of Thermal Analysis*, 37, 1633-1656.
- Davidovits, J. (1994a). **Geopolymers: Man-Made Rock Geosynthesis And The Resulting Development Of Very Early High Strength Cement.** *Journal of Materials Education*, 16(2&3), 91-139.
- Davidovits, J. (1994b). *High-Alkali Cements for 21st Century Concretes in Concrete Technology, Past, Present and Future.* Paper presented at the ACI SP- 144.
- Davidovits, J. (1994c). **Properties of geopolymer cements.** *Alkaline Cements and Concretes, KIEV Ukraine.*
- Davidovits, J. (2005). *Geopolymer chemistry and sustainable Development. The Poly(sialate) terminology : a very useful and simple model for the promotion and understanding of green-chemistry.* Paper presented at the Proceedings of the World Congress Geopolymer Saint Quentin, France, 28 June–1 July.

- De Silva, P., Sagoe-Crenstil, K., and Sirivivatnanon, V. (2007). **Kinetics of geopolymerization: Role of Al<sub>2</sub>O<sub>3</sub> and SiO<sub>2</sub>**. *Cement and Concrete*, 37(4), 512–518.
- De Vargas, A. S., Dal Molin, D. C. C., Masuero, Â. B., Vilela, A. C. F., Castro-Gomes, J., and de Gutierrez, R. M. (2014). **Strength development of alkali-activated fly ash produced with combined NaOH and Ca(OH)<sub>2</sub> activators**. *Cement and Concrete Composites*, 53, 341-349.
- Douglas, E., Bilodeau, A., Brandstetr, J., and Malhotra, V. (1991). **Alkali activated ground granulated blast furnace slag concrete: preliminary investigations**. *Cement and Concrete Research*, 21, 101-108.
- Dutta, D., Thokchom, S., Ghosh, P., and Ghosh, S. (2010). **Effect of silica fume additions on porosity of fly ash geopolymers**. *ARPJ Journal of Engineering and Applied Sciences*, 5(10), 74-79.
- Duxson, P., Fernández-Jiménez, A., Provis, J. L., Lukey, G. C., Palomo, A., and Deventer, J. S. J. (2007). **Geopolymer technology: the current state of the art**. *Journal of materials science*, 42(9), 2917-2933. doi: 10.1007/s10853-006-0637-z
- Duxson, P., Lukey, G. C., and Van Deventer, J. S. J. (2006). **Nanostructural design of multifunctional geopolymeric materials**. *Ceramic Transactions*, 175, 203–214.
- Duxson, P., Lukey, G. C., and Van Deventer, J. S. J. (2007). **Physical evolution of Na-geopolymer derived from metakaolin up to 1000 °C**. *Journal of Materials Science*, 42, 3044–3054.

- Duxson, P., Provis, J. L., Lukey, G. C., Mallicoat, S. W., Kriven, W. M., and Van Deventer, J. S. J. (2005). **Understanding the relationship between geopolymer composition, microstructure and mechanical properties.** *Colloids and Surfaces A: Physicochemical and Engineering Aspects* 269(1-3), 47-58. doi: 10.1016/j.colsurfa.2005.06.060
- Elimbi, A., Tchakoute, H. K., and Njopwouo, D. (2011). **Effects of calcination temperature of kaolinite clays on the properties of geopolymer cements.** *Construction and Building Materials*, 25(6), 2805-2812.
- Fan, Y., Yin, S., Wen, Z., and Zhong, J. (1999). **Activation of fly ash and its effects on cement properties.** *Cement and Concrete Research*, 467–472.
- Fernandez-Jimenez, A., García-Lodeiro, I., and Palomo, A. (2006). **Durability of alkali-activated fly ash cementitious materials.** *Journal of materials science*, 42(9), 3055-3065. doi: 10.1007/s10853-006-0584-8
- Fernández-Jiménez, A., and Palomo, A. (2003). **Characterisation of fly ashes. Potential reactivity as alkaline cements☆.** *Fuel*, 82(18), 2259-2265. doi: 10.1016/s0016-2361(03)00194-7
- Fernández-Jiménez, A., and Palomo, A. (2005). **Composition and microstructure of alkali activated fly ash binder: Effect of the activator.** *Cement and Concrete Research*, 35(10), 1984-1992. doi: 10.1016/j.cemconres.2005.03.003
- Fernández-Jiménez, A., Palomo, A., and Criado, M. (2005). **Microstructure development of alkali-activated fly ash cement: a descriptive model.** *Cement and Concrete Research*, 35(6), 1204-1209.
- Fernández-Jiménez, A., Palomo, A., Sobrados, I., and Sanz, J. (2006). **The role played by the reactive alumina content in the alkaline activation of fly**

- ashes.** *Microporous and Mesoporous Materials*, 91(1-3), 111-119. doi: 10.1016/j.micromeso.2005.11.015
- Fernandez Jimenez, A. M., Lachowski, E. E., Palomo, A., and Macphee, D. E. (2004). **Microstructural characterisation of alkali-activated PFA matrices for waste immobilisation.** *Cement and Concrete Composites*, 26(8), 1001-1006. doi: 10.1016/j.cemconcomp.2004.02.034
- Gambrell, R. P., He, J., and Zhang, G. (2010). **Synthesis, Characterization, and Mechanical Properties of Red Mud-Based Geopolymers.** *Transportation Research Record: Journal of the Transportation Research Board*, 2167(-1), 1-9. doi: 10.3141/2167-01
- Garía, J. I. E., Campos-Venegas, K., Gorokhovskiy, A., and Fernández, A. (2006). **Cementitious composites of pulverized fuel ash and blast furnace slag activated by sodium silicate: effect of Na<sub>2</sub>O concentration and modulus.** *Advances in Applied Ceramics*, 4, 201-208.
- Goretta, K. C., Chen, N., Gutierrez-Mora, F., Routbort, J. L., Lukey, G. C., and van Deventer, J. S. J. (2004). **Solid-particle erosion of a geopolymer containing fly ash and blast-furnace slag.** *Wear*, 256(7-8), 714-719. doi: 10.1016/s0043-1648(03)00463-0
- Guo, X., Shi, H., Chen, L., and Dick, W. A. (2009). **Performance and Mechanism of Alkali-Activated Complex Binders of High-Ca Fly Ash and Other Ca-Bearing Materials.** *2009 World of Coal Ash (WOCA) Conference - May 4-7, 2009 in Lexington, KY, USA.*
- Hamaideh, A., Komnitsas, K., Esaifan, M., Al-Kafawein, J. a. K., Rahier, H., and Alshaaer, M. (2014). **Advantages of Applying a Steam Curing Cycle for the**

- Production of Kaolinite-Based Geopolymers.** *Arabian Journal for Science and Engineering*, 39(11), 7591-7597. doi: 10.1007/s13369-014-1314-1
- Horpibulsuk, S., Phetchuay, C., and Chinkulkijniwat, A. (2012). **Soil Stabilization by Calcium Carbide Residue and Fly Ash.** *Journal of Materials in Civil Engineering*, 24(2), 184-193. doi: 10.1061/(asce)mt.1943-5533.0000370
- Horpibulsuk, S., Phetchuay, C., Chinkulkijniwat, A., and Cholaphatsorn, A. (2013). **Strength development in silty clay stabilized with calcium carbide residue and fly ash.** *Soils and Foundations*, 53(4), 477-486.
- Hou, Y., Wang, D., Zhou, W., Lu, H., and Wang, L. (2009). **Effect of activator and curing mode on fly ash-based geopolymers.** *Journal of Wuhan University of Technology-Materials Science Edition*, 24(5), 711-715. doi: 10.1007/s11595-009-5711-3
- Jaturapitakkul, C., and Roongreung, B. (2003). **Cementing Material from Calcium Carbide Residue-Rice Husk Ash.** *Journal of Materials in Civil Engineering*, 15, 470-475. doi: 10.1061//ASCE/0899-1561/2003/15:5/470
- Juenger, M. C. G., Winnefeld, F., Provis, J. L., and Ideker, J. H. (2011). **Advances in alternative cementitious binders.** *Cement and Concrete Research*, 41(12), 1232-1243. doi: 10.1016/j.cemconres.2010.11.012
- Kampala, A., and Horpibulsuk, S. (2013). **Engineering Properties of Silty Clay Stabilized with Calcium Carbide Residue.** *Journal of Materials in Civil Engineering*, 25(5), 632-644. doi: 10.1061/(asce)mt.1943-5533.0000618
- Kampala, A., Horpibulsuk, S., Chinkullijniwat, A., and Shen, S.-L. (2013). **Engineering properties of recycled Calcium Carbide Residue stabilized**

- clay as fill and pavement materials.** *Construction and Building Materials*, 46, 203-210. doi: 10.1016/j.conbuildmat.2013.04.037
- Khale, D., and Chaudhary, R. (2007). **Mechanism of geopolymerization and factors influencing its development: a review.** *Journal of materials science*, 42(3), 729-746. doi: 10.1007/s10853-006-0401-4
- Komnitsas, K., and Zaharaki, D. (2007). **Geopolymerisation: A review and prospects for the minerals industry.** *Minerals Engineering*, 20(14), 1261-1277. doi: 10.1016/j.mineng.2007.07.011
- Krammart, P., and Tangtermsirikul, S. (2004). **Properties of cement made by partially replacing cement raw materials with municipal solid waste ashes and calcium carbide waste.** *Construction and Building Materials*, 18(8), 579-583. doi: 10.1016/j.conbuildmat.2004.04.014
- Krizan, D., and Zivanovic, B. (2002). **Effects of dosage and modulus of water glass on early hydration of alkali-slag cements.** *Cement and Concrete Research*, 32, 1181-1188.
- Kumar, S., Kumar, R., and Mehrotra, S. P. (2010). **Influence of granulated blast furnace slag on the reaction, structure and properties of fly ash based geopolymer.** *Journal of materials science*, 45(3), 607-615.
- Lee, W. K. W., and Van Deventer, J. S. J. (2002a). **The effect of ionic contaminants on the early-age properties of alkali-activated fly ash-based cements.** *Cement and Concrete Research*, 32, 577-584.
- Lee, W. K. W., and Van Deventer, J. S. J. (2002b). **The effects of inorganic salt contamination on the strength and durability of geopolymers.** *Colloids and Surfaces A: Physicochemical and Engineering Aspects* 211, 115-126.

- Lohani, T., Jena, S., Dash, K., and Padhy, M. (2012). **An experimental approach on geopolymeric recycled concrete using partial replacement of industrial byproduct.** *International Journal of Civil and Structural Engineering*, 3(1), 141–149.
- Lyon, R. E., Balaguru, P. N., Foden, A., Sorathia, U., Davidovits, J., and Davidovics, M. (1997). **Fire Resistant Aluminosilicate Composites.** *Fire and Materials* 21, 67-73.
- Makaratat, N., Jaturapitakkul, C., and Laosamathikul, T. (2010). **Effects of Calcium Carbide Residue–Fly Ash Binder on Mechanical Properties of Concrete.** *Journal of Materials in Civil Engineering*, 22, 1164-1170. doi: 10.1061//ASCE/MT.1943-5533.0000127
- Makaratat, N., Jaturapitakkul, C., Namarak, C., and Sata, V. (2011). **Effects of binder and CaCl<sub>2</sub> contents on the strength of calcium carbide residue-fly ash concrete.** *Cement and Concrete Composites*, 33(3), 436-443. doi: 10.1016/j.cemconcomp.2010.12.004
- Miller, N. A., Stirling, C. D., and Nicholson, C. L. (2005). *The relationship between cure conditions and flexural properties in flyash-based geopolymers.* Paper presented at the Proceedings of the World Congress Geopolymer, Saint Quentin, France, 28 June–1 July.
- Nazari, A., Bagheri, A., and Riahi, S. (2011). **Properties of geopolymer with seeded fly ash and rice husk bark ash.** *Materials Science and Engineering: A*, 528(24), 7395-7401. doi: 10.1016/j.msea.2011.06.027

- Nuruddin, M., Qazi, S., and Kusbiantoro, A. (2010). **Compressive strength & microstructure of polymeric concrete incorporating fly ash & silica fume.** *Canadian Journal of Civil Engineering*, 1(1), 15-18.
- Nuruddin, M. F., Kusbiantoro, A., Qazi, S., and Shafiq, N. (2011). **Compressive strength and interfacial transition zone characteristic of geopolymer concrete with different cast in-situ curing conditions.** *World Academy of Science, Engineering and Technology*, 49, 431–434.
- Pacheco-Torgal, F., Castro-Gomes, J., and Jalali, S. (2008a). **Alkali-activated binders: A review Part 1. Historical background, terminology, reaction mechanisms and hydration products.** *Construction and Building Materials*, 22(7), 1305-1314. doi: 10.1016/j.conbuildmat.2007.10.015
- Pacheco-Torgal, F., Castro-Gomes, J., and Jalali, S. (2008b). **Alkali-activated binders: A review. Part 2. About materials and binders manufacture.** *Construction and Building Materials*, 22(7), 1315-1322.
- Palomo, A., Fernández-Jiménez, A., Kovalchuk, G., Ordoñez, L. M., and Naranjo, M. C. (2007). **Opc-fly ash cementitious systems: study of gel binders produced during alkaline hydration.** *Journal of materials science*, 42(9), 2958-2966. doi: 10.1007/s10853-006-0585-7
- Palomo, A., Grutzeck, M., and Blanco, M. (1999). **Alkali-activated fly ashes A cement for the future.** *Cement and Concrete Research*, 29, 1323–1329.
- Panagiotopoulou, C., Kontori, E., Perraki, T., and Kakali, G. (2007). **Dissolution of aluminosilicate minerals and by-products in alkaline media.** *Journal of materials science*, 42(9), 2967-2973. doi: 10.1007/s10853-006-0531-8

- Pangdaeng, S., Phoo-ngernkham, T., Sata, V., and Chindaprasirt, P. (2014). **Influence of curing conditions on properties of high calcium fly ash geopolymer containing Portland cement as additive.** *Materials and Design*, 53, 269-274. doi: 10.1016/j.matdes.2013.07.018
- Perera, D. S., Uchida, O., Vance, E. R., and Finnie, K. S. (2007). **Influence of curing schedule on the integrity of geopolymers.** *Journal of materials science*, 42(9), 3099-3106. doi: 10.1007/s10853-006-0533-6
- Phair, J. W., and Van Deventer, J. S. J. (2001). **Effect of silicate activator ph on the leaching and material characteristics of waste-based inorganic polymers.** *Mineral Engineering*, 14(3), 289-304.
- Phetchuay, C., Horpibulsuk, S., Suksiripattanapong, C., Chinkulkijniwat, A., Arulrajah, A., and Disfani, M. M. (2014). **Calcium carbide residue: Alkaline activator for clay-fly ash geopolymer.** *Construction and Building Materials*, 69, 285-294. doi: 10.1016/j.conbuildmat.2014.07.018
- Provis, J. L., Lukey, G. C., and Van Deventer, J. S. J. (2005). **Do geopolymers actually contain nanocrystalline zeolites? A reexamination of existing results.** *Chemistry of Materials* 17, 3075–3085.
- Puertas, F., MartõÁnez-RamõÁrez, S., Alonso, S., and VaÁzquez, T. (2000). **Alkali-activated fly ash/slag cement Strength behaviour and hydration products.** *Cement and Concrete Research*, 30, 1625 - 1632.
- Rangan, B. V. (2014). **Geopolymer concrete for environmental protection.** *The Indian Concrete Journal*, 88(4), 41-59.
- Shi, C. (1996). **Early microstructure development of activated lime-fly ash pastes.** *Cement and Concrete Research*, 26(9), 1351–1359.

- Shi, C., and Day, R. (1999). **Early strength development and hydration of alkali-activated blast furnace slag/fly ash blends.** *Advances in Cement Research*, 11(4), 189–196.
- Shi, C., Fernández Jiménez, A., and Palomo, A. (2011). **New cements for the 21st century: The pursuit of an alternative to Portland cement.** *Cement and Concrete Research*, 41, 750-763. doi: 10.1016/j.cemconres.2011.03.016
- Singh, P. S., Bastow, T., and Trigg, M. (2005). **Structural studies of geopolymers by  $^{29}\text{Si}$  and  $^{27}\text{Al}$  MAS-NMR.** *Journal of Materials Science*, 40, 3951– 3961.
- Smith, M., and Osborne, G. (1977). **BFS/fly ash cements.** *World Cement Technology*, 8, 223-233.
- Somna, K., Jaturapitakkul, C., and Kajitvichyanukul, P. (2011). **Microstructure of Calcium Carbide Residue–Ground Fly Ash Paste.** *Journal of Materials in Civil Engineering*, 23, 298-304. doi: 10.1061/
- Songpiriyakij, S., Pulngern, T., Pungpremtrakul, P., and Jaturapitakkul, C. (2011). **Anchorage of steel bars in concrete by geopolymer paste.** *Materials and Design*, 32, 3021-3028.
- Stevenson, M., and Sagoe-Crentsil, K. (2005). **Relationship between composition, structure and strength of inorganic polymers: part 1 - metakaolinderived inorganic polymers.** *Journal of materials science*, 40, 2023–2036.
- Sukmak, P., De Silva, P., Horpibulsuk, S., and Chindaprasirt, P. (2014). **Sulfate Resistance of Clay-Portland Cement and Clay High-Calcium Fly Ash Geopolymer.** *Journal of Materials in Civil Engineering*, 04014158. doi: 10.1061/(asce)mt.1943-5533.0001112

- Sukmak, P., Horpibulsuk, S., and Shen, S.-L. (2013). **Strength development in clay–fly ash geopolymer**. *Construction and Building Materials*, 40, 566-574. doi: 10.1016/j.conbuildmat.2012.11.015
- Sukmak, P., Horpibulsuk, S., Shen, S.-L., Chindaprasirt, P., and Suksiripattanapong, C. (2013). **Factors influencing strength development in clay–fly ash geopolymer**. *Construction and Building Materials*, 47, 1125-1136. doi: 10.1016/j.conbuildmat.2013.05.104
- Swanepoel, J. C., Strydom, C. A., and Smit, J. P. (1999). *Safe disposal of brine water in fly-ash geopolymeric material*. Paper presented at the Proceedings of the 2nd International Conference on Geopolymer '99, Saint Quentin, France, June 30–July 2.
- Thokchom, S., Dutta, D., and Ghosh, S. (2011). **Effect of incorporating silica fume in fly ash geopolymers**. *World Academy of Science, Engineering and Technology*, 60, 243-247.
- Van Jaarsveld, J. G. S., Van Deventer, J. S. J., and Lorenzen, L. (1998). **Factors Affecting the Immobilization of Metals in Geopolymerized Flyash**. *Metallurgical and Materials Transactions B*, 29, 283-291.
- Van Jaarsveld, J. G. S., Van Deventer, J. S. J., and Lukey, G. C. (2002). **The effect of composition and temperature on the properties of fly ash- and kaolinite-based geopolymers**. *Chemical Engineering Journal*, 89, 63–73.
- Van Jaarsveld, J. G. S., Van Deventer, J. S. J., and Lukey, G. C. (2003). **The characterisation of source materials in fly ash-based geopolymers**. *Materials Letters*, 57, 1272–1280.

- Wang, H., Li, H., and Yan, F. (2005). **Synthesis and mechanical properties of metakaolinite-based geopolymer**. *Colloids and Surfaces A: Physicochemical and Engineering Aspects* 268(1-3), 1-6. doi: 10.1016/j.colsurfa.2005.01.016
- Wang, J., Wu, X.-l., Wang, J.-x., Liu, C.-z., Lai, Y.-m., and Hong, z.-k. (2012). **Hydrothermal synthesis and characterization of alkali-activated slagfly ash-metakaolin cementitious materials**. *Microporous and Mesoporous Materials*, 155, 186-191.
- Weiguo, S., Yiheng, W., Tao, Z., Mingkai, Z., Jiasheng, L., and Xiaoyu, C. (2011). **Magnesia modification of alkali-activated slag fly ash cement**. *Journal of Wuhan University of Technology-Materials Science Edition* 2011(February), 121-125.
- Wu, H.-C., and Sun, P. (2010). **Effect of mixture compositions on workability and strength of fly ash-based inorganic polymer mortar**. *ACI Materials Journal*, 11-12, 554-561.
- Xie, J., and Kayali, O. (2014). **Effect of initial water content and curing moisture conditions on the development of fly ash-based geopolymers in heat and ambient temperature**. *Construction and Building Materials*, 67, 20-28. doi: 10.1016/j.conbuildmat.2013.10.047
- Xie, Z., and Xi, Y. (2001). **Hardening mechanisms of an alkaline-activated class F fly ash**. *Cement and Concrete Research*, 31, 1245–1249.
- Xu, H. (2001). *Geopolymerisation of aluminosilicate minerals*. (PhD Thesis), University of Melbourne, Australia.
- Xu, H., and Deventer, J. S. J. V. (2002a). **Geopolymerisation of multiple minerals**. *Minerals Engineering*, 15, 1131–1139.

- Xu, H., and Deventer, J. S. J. V. (2002b). **Microstructural characterisation of geopolymers synthesized from kaolinite/stilbite mixtures using XRD, MAS-NMR, SEM/EDX, TEM/EDX and HREM.** *Cement and Concrete Research*, 32, 1705–1716.
- Xu, H., and Van Deventer, J. S. J. (1999). *The geopolymerisation of natural aluminosilicates*. Paper presented at the Proceedings of the 2nd International Conference on Geopolymer '99, Saint Quentin, France, June 30–July 2
- Xu, H., and Van Deventer, J. S. J. (2000). **The geopolymerisation of aluminosilicate minerals.** *International of mineral processing*, 59, 247-266.
- Xu, H., and Van Deventer, J. S. J. (2003). **The effect of alkali metals on the formation of geopolymeric gels from alkali-feldspars.** *Colloids and Surfaces A: Physicochemical and Engineering Aspects* 216(1-3), 27-44. doi: 10.1016/s0927-7757(02)00499-5
- Yang, T., Yao, X., Zhang, Z., and Wang, H. (2012). **Mechanical property and structure of alkali-activated fly ash and slag blends.** *Journal of Sustainable Cement/Based Materials*, 1(4), 167-178.
- Yi, Y., Li, C., and Liu, S. (2014). **Alkali-Activated Ground-Granulated Blast Furnace Slag for Stabilization of Marine Soft Clay.** doi: 10.1061/
- Yip, C. K., Lukey, G. C., and Van Deventer, J. S. J. (2005). **The coexistence of geopolymeric gel and calcium silicate hydrate at the early stage of alkaline activation.** *Cement and Concrete Research*, 35(9), 1688-1697. doi: 10.1016/j.cemconres.2004.10.042

- Yip, C. K., and Van Deventer, S. (2003). **Microanalysis of calcium silicate hydrate gel formed within a geopolymeric binder**. *Journal of materials science*, 38, 3851–3860.
- Yunsheng, Z., Wei, S., Wei, S., and Guoei, S. (2009). **Synthesis and heavy metal immobilization behaviors of fly ash based gepolymer**. *Journal of Wuhan University of Technology-Materials Science Edition*, 10, 819-825.
- Zhang, M., Guo, H., El-Korchi, T., Zhang, G., and Tao, M. (2013). **Experimental feasibility study of geopolymer as the next-generation soil stabilizer**. *Construction and Building Materials*, 47, 1468-1478. doi: 10.1016/j.conbuildmat.2013.06.017
- Zhang, Y., Li, Z., Sun, W., and Li, W. (2009). **Setting and hardening of geopolymeric cement pastes incorporated with fly ash**. *ACI Materials Journal*, 405-412.
- Zhang, Z., Yao, X., Zhu, H., Hua, S., and Chen, Y. (2009). **Activating process of geopolymer source material: Kaolinite**. *Journal of Wuhan University of Technology-Materials Science Edition*, 24(1), 132-136. doi: 10.1007/s11595-009-1132-6
- Zhang Zu-hua, Yao Xiao, Zhu Hua-jun, Hua Su-dong, and Yue, C. (2009). **Preparation and mechanical properties of polypropylene fiber reinforced calcined kaolinfly ash based geopolymer**. *Journal of Central South University of Technology*, 16, 0049–0052.

# **CHAPTER III**

## **STABILIZED SATURATION OF MARGINAL LATERITIC SOIL USING HIGH CALCIUM FLY ASH – BASED GEOPOLYMER**

### **3.1 Statement of problem**

Generally, highway pavement generally consists of base and subbase layers, which are constructed from suitable materials such as crushed rock and lateritic soil (LS). Due to high rainfall, temperature and humidity with alternative wet and dry period, nearly 60% of the soils in Thailand are LS with colours ranging from red to yellowish red. The LS in East and Central of Thailand, which are the largest industrial zone of the country, does not typically meet the standard requirement as subbase/base materials. The LS in North, South and Northeast region of Thailand is classified suitable subbase materials. But some of these areas are located far away from quarry sources. When no such suitable materials are available and it is expensive to bring the materials from distant sources, an alternative way, widely practiced around the world, is to compact the *in situ* marginal soil mixed with Portland Cement (PC) (Chinkulkijniwat and Horpibulsuk, 2002; Jamsawang et al., 2015). However, the production process of PC is an energy-intensive and releases a very large amount of carbon dioxide (CO<sub>2</sub>) in to the atmosphere (Davidovits, 1991, 1994a, 1994b, 1994c, 2002, 2013). It can be said that the production of 1 tons of PC clinker directly

generates 0.55 tons of CO<sub>2</sub> and 0.4 tons of CO<sub>2</sub> for the combustion (Davidovits, 2013).

In the light of these problems, the utilisation of low energy-intensive cementing agents in civil engineering applications has been increasingly researched in recent years. Low energy-intensive cementing agents include cement kiln dust (Ebrahimi et al., 2012), calcium carbide residue (Horpibulsuk et al., 2013; Kampala and Horpibulsuk, 2013; Kampala et al., 2013; Kampala et al., 2014), granulated blast furnace slag (Puppala et al., 2003) and geopolymer binder (Sukmak et al., 2014; Sukmak, Horpibulsuk, and Shen, 2013; Sukmak, Horpibulsuk, Shen, et al., 2013).

The mechanism of geopolymerization involves the dissolution of Al and Si in the alkaline, then transportation of dissolved species, followed by a polycondensation forming a 3D network of aluminosilicate structures (Silva and Sagoe-Crenstil, 2008, 2009). Three typical structures of geopolymer are

Poly (sialate) Si:Al = 1 (-Si-O-Al-O-),

Poly (sialate-siloxo) Si:Al = 2 (-Si-O-Al-O-Si-O-),

Poly (sialate-disiloxo) Si:Al = 3 (-Si-O-Al-O-Si-O-Si-O-).

Since fly ash (FA) offers the greatest opportunity given the plentiful worldwide stockpiles (Van Jaarsveld et al., 1998), it is frequently used as a precursor for producing geopolymers. One billion tons of FA is produced annually worldwide in coal-fired power plants (Alvarez-Ayuso et al., 2008; Chindaprasirt et al., 2011; Chindaprasirt et al., 2009; Nath and Kumar, 2013). Regularly, FA can replace cement content up to 50–70% in the high volume FA concrete (Rashad, 2014). For concrete industry in Thailand, FA is used as a pozzolanic material about 1.8 million tons (Chindaprasirt et al., 2009).

Though there is readily available literature on the application of FA-based geopolymer, they have been predominantly used as building materials while the studies on the application of FA-based geopolymer to pavement materials are limited to date. Phetchuay et al. (2014) studied the viability of using calcium carbide residue as an alkali activator and FA as a precursor to stabilize problematic silty clay as a bound pavement material whose compressive strength meets the strength requirement, specified by the local national road authority of Thailand. Zhang et al. (2013) illustrated the feasibility of using geopolymer as an effective soil stabiliser for clayey soils based on an experimental study. Arulrajah et al. (2015) recently used spent coffee ground as an aggregate and FA-based geopolymer as a binder to develop a green engineering fill material.

This research aims to investigate the possibility of using high calcium FA-based geopolymer to stabilise a marginal LS to be a sustainable bound pavement material. Unconfined compressive strength (UCS) was used as an indicator for this investigation. The microstructural development of marginal LS–FA geopolymer was observed through scanning electron microscope (SEM) analysis for understanding the role of influential factors, controlling the strength development. The influential factors studied in this paper include  $\text{Na}_2\text{SiO}_3:\text{NaOH}$  ratio and curing time at ambient room temperature. This study is significant from engineering, economical and environmental perspectives.

## **3.2 Materials and methods**

### **3.2.1 Soil sample**

The marginal LS was collected from a borrow pit in Rayong province, Thailand. The specific gravity is 2.58. The liquid limit (LL), plastic limit (PL), and plastic index (PI) undertaken according to ASTM D4318 (2010) are 27.72%, 21.65%, and 6.07%, respectively. Grain size distribution of this soil obtained from sieve analysis (ASTM D422–63, 2007) is shown in **Figure 3.1**. This soil is classified as silty clayey sand according to the Unified Soil Classification System and A-2-4(0) according to the AASHTO system (ASTM D3282–09, 2009). The mineral and chemical compositions of the marginal LS determined by X-ray fluorescence (XRF) analysis are summarized in **Table 3.1**. The compaction characteristics under modified Proctor energy (ASTM D1557–12, 2012), are Optimum Moisture Content (OMC) of 8.0%, and maximum dry unit weight ( $\gamma_{d,max}$ ) of 20.85 kN/m<sup>3</sup>. California Baring Ratio (CBR) value is 14.7% at 95% of maximum dry unit weight. Los Angeles (LA) abrasion described by ASTM C131 (2006) and C535 (2012a) is 52.9%. With low CBR and high LA abrasion compared to the specification of the Department of Highways (DOH) and Department of Rural Roads (DRR), Thailand (required CBR and LA abrasion are greater than 25% and less than 60% for subbase materials, located below the base course, respectively), this LS is classified as a marginal soil.

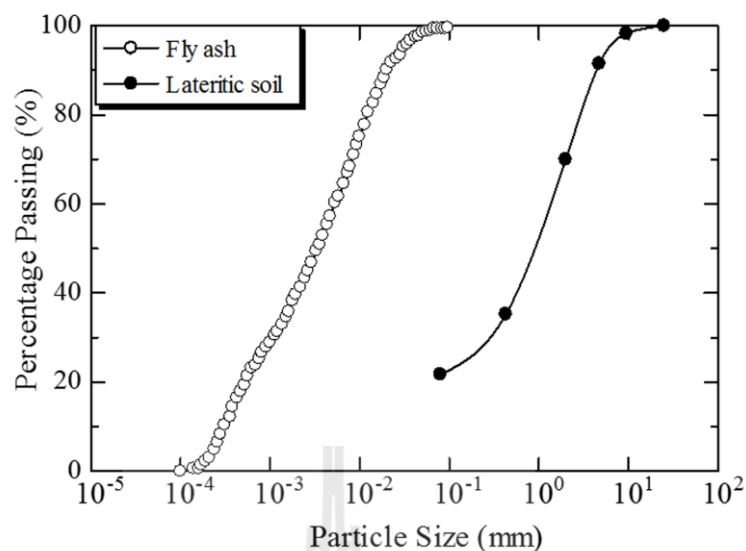


**Figure 3.1** Particle size distributions of the LS and FA.

**Table 3.1** Chemical compositions of FA and marginal LS.

Chemical composition (%)	FA	Marginal LS
SiO <sub>2</sub>	36.00	77.81
Al <sub>2</sub> O <sub>3</sub>	16.80	4.42
Fe <sub>2</sub> O <sub>3</sub>	17.64	10.93
CaO	26.73	1.13
SO <sub>3</sub>	N.D.	1.36
K <sub>2</sub> O	1.83	2.33
TiO <sub>2</sub>	0.48	1.33
MnO <sub>2</sub>	0.15	0.55
Br <sub>2</sub> O	N.D.	0.38

Note: N.D. = not detected

### 3.2.2 Fly ash

FA used in this study was obtained from Mae Moh power plant in Northern Thailand, which is the largest lignite power plant in Thailand. The chemical compositions of FA were determined using XRF technique and are shown in **Table 3.1**. The XRF spectrometer is an instrument used for routine, relatively non-destructive chemical analyses of rocks, minerals, sediments and fluids. It works on wavelength-dispersive spectroscopic principles. The major and trace elements in geological materials are analysed by the behaviour of atoms when they interact with X-radiation. The major components are 36.00% SiO<sub>2</sub>, 26.73% CaO, 17.64% Fe<sub>2</sub>O<sub>3</sub>, and 16.80% Al<sub>2</sub>O<sub>3</sub>. According to ASTM C 618-12a (2012b), it is categorized as class C high-calcium fly ash (CaO > 10%). It has been shown that this FA is suitable as a precursor for making good geopolymer (Chindapasirt et al., 2007; Rattanasak et al., 2011). The high calcium content of FA leads to the formation of Calcium Silicate Hydrate (C-S-H), which coexists with the geopolymerization product (Sodium Alumino Silicate Hydrate, N-A-S-H) (Guo et al., 2010; Somna et al., 2011). The coexistence of C-S-H phase with N-A-S-H phase has been proved to improve the mechanical properties of final products (Temuujin and van Riessen, 2009). The particle size distribution and SEM image of FA are shown in **Figures 3.1** and **3.2**, respectively. The FA particles are generally fine and spherical while the LS particles are irregular in shape.

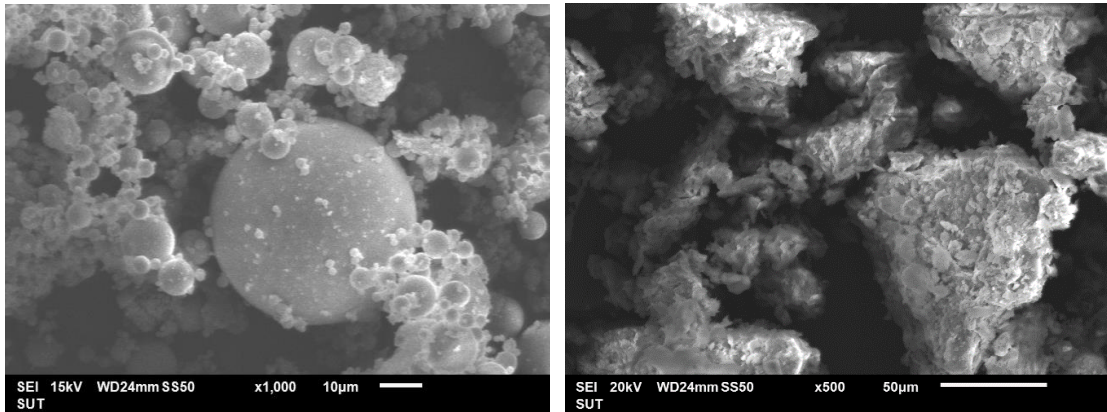


**Figure 3.2** SEM images of: (a) FA and (b) LS.

### 3.2.3 Liquid alkali activator

The liquid alkali activator was a mixture of sodium silicate ( $\text{Na}_2\text{SiO}_3$ , NS) solution, composed of 15.50%  $\text{Na}_2\text{O}$ , 32.75%  $\text{SiO}_2$ , and 51.75% water by weight, and sodium hydroxide ( $\text{NaOH}$ , NH) solution with 5 molar. The suitable concentration is generally between 4.5 and 18 molar (Andini et al., 2008; Chindaprasirt et al., 2009; Hanjitsuwan et al., 2014; Rattanasak and Chindaprasirt, 2009; Somna et al., 2011). The low NH concentration of 5 molar was considered in this study to avoid health harm of workers and to have cost-effectiveness.

### 3.2.4 LS– FA geopolymer

The NH and NS solutions were first mixed together and used as the liquid alkali activator. The LS and FA were air-dried and mixed thoroughly at soil to FA ratio of 70:30. The liquid alkali activator was mixed with a mixture of LS and FA for 10 min to develop LS–FA geopolymer at various NS:NH ratios of 100:0, 90:10, 80:20 and 50:50. This mixing procedure has been done by previous researchers

(Suksun Horpibulsuk et al., 2010; Sukmak, Horpibulsuk, and Shen, 2013; Suksiripattanapong et al., 2015). The  $\text{SiO}_2:\text{Al}_2\text{O}_3$  ratios in this study range from 4.5 to 5.8 as summarized in **Table 3.2**. The mixtures with different ingredients were compacted in a standard mold of 101.6 mm in diameter and 116.4 mm in height (the ratio of height to diameter equals 1.15) under modified Proctor energy according to the specification of the DOH (ASTM, 2012c). All the compacted samples were then dismantled and wrapped with vinyl sheet to prevent the moisture loss. They were next cured at ambient temperature (27–30°C) until the various pre-planned curing times lapsed. Although the geopolymerisation reaction is significantly accelerated by the heat curing, the LS–FA geopolymer samples in this study were cured at ambient temperature to simulate the average field temperature. The samples were submerged under water for 2 h and were air-dried for 1 h prior to UCS test according to the specification of the (DH-S 204/2000) (DOH, 2000), Thailand. UCS tests on the soaked samples at the four different NS:NH ratios were undertaken after 7, 28, 60 and 90 days. The results were reported using mean UCS values of at least three samples to assure test result consistency. In most cases, the results under the same testing condition were reproducible with low mean standard deviation,  $SD/\bar{x}$  ( $< 10\%$ , where  $\bar{x}$  is mean strength value).

Scanning electron microscopic (SEM) images were undertaken on the LS–FA geopolymer samples to analyse the microstructural changes with NS:NH ratio and curing time. The small fragments from the centre of specimens were frozen at  $-195^\circ\text{C}$  by immersion in liquid nitrogen for 5 min and coated with gold before SEM (JEOL JSM-6400 device) analysis (Du et al., 2014; Horpibulsuk et al., 2010; S.

Horpibulsuk et al., 2009; Sukmak, Horpibulsuk, and Shen, 2013; Sukmak, Horpibulsuk, Shen, et al., 2013).

**Table 3.2** Initial molar ratios of LS-FA geopolymer.

Sample	Na <sub>2</sub> O: SiO <sub>2</sub>	SiO <sub>2</sub> : Al <sub>2</sub> O <sub>3</sub>	H <sub>2</sub> O: Na <sub>2</sub> O	Na <sub>2</sub> O: Al <sub>2</sub> O <sub>3</sub>	SiO <sub>2</sub> :Al <sub>2</sub> O <sub>3</sub> : Na <sub>2</sub> O
1	0.174	5.800	11.250	1.008	5.798: 1: 1.008
2	0.179	5.535	11.818	0.993	5.535: 1: 0.993
3	0.183	5.258	12.375	0.963	5.258: 1: 0.963
4	0.188	4.500	13.985	0.845	4.501: 1: 0.845

### 3.3 Results

#### 3.3.1 Compaction characteristics

**Figure 3.3** shows the relationships between dry unit weight and liquid alkali activator content with various NS:NH ratios of LS-FA geopolymer. The compaction curves of LS-FA geopolymer are different and depend on the NS:NH ratio. For a particular NS:NH ratio, the dry unit weight of LS-FA geopolymer increases with increasing liquid alkali activator content until  $\gamma_{d,max}$  is attained at an optimum alkali activator content. Beyond this optimum value, the unit weight decreases as the alkali activator content increases. This characteristic is similar to a typical compaction behavior of coarse-grained materials. The effect of NS:NH ratio is also noticed in this figure in that  $\gamma_{d,max}$  is 20.3 kN/m<sup>3</sup> at NS:NH ratio of 50:50, decreases to 19.2 kN/m<sup>3</sup> when NS:NH ratio increases to 80:20, increases to 20.4 kN/m<sup>3</sup> when NS:NH ratio increases to 90:10 and then decreases to 20.0 kN/m<sup>3</sup> at NS:NH ratio of 100:0. The optimum NS:NH ratio exhibiting the highest  $\gamma_{d,max}$  was

found at 90:10. Based on a linear regression analysis of the test result, the optimum liquid alkali activator for each NS:NH ratio is summarised in **Table 3.3**.

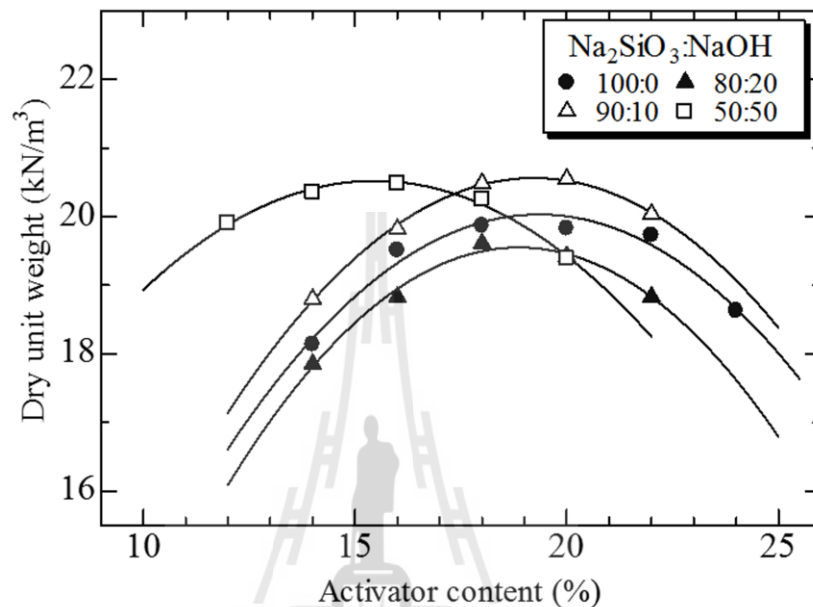


**Figure 3.3** Compaction curves of LS – FA geopolymer at different ingredients.

**Table 3.3** Optimum liquid alkali activator and maximum dry unit weight.

Sample	NS:NH	Optimum activator content (%)	Maximum dry unit weight, $\gamma_{d,max}$ (kN/m <sup>3</sup> )	Activator: FA ratio (g/g)
1	100:0	19.60	20.21	0.653
2	90:10	19.13	20.56	0.638
3	80:20	18.38	19.56	0.613
4	50:50	15.68	20.45	0.523

Note: Activator:FA ratio is the ratio of optimum liquid alkali activator that used in

each mix (NS:NH = 100:0, 90:10, 80:20 and 50:50) to FA by weight.

### 3.3.2 Unconfined compressive Strength

The UCS of geopolymers is attributed to the reaction between silica and alumina in the presence of alkali ions and in age of specimens (Somna et al., 2011). The UCS values of the LS-FA geopolymer for various NS:NH ratios (100:0 to 50:50) and curing times (7-90 days) are presented in **Figure 3.4**. It is evident that the UCS values for all NS:NH ratios increase as the curing time increases. At early stage of geopolymerization, the maximum 7-day UCS is found at NS:NH ratio of 90:10 (about 7,100 kPa), which is greater than the strength requirement specified by the national road authority in Thailand (UCS > 1,724 kPa for light traffic and UCS > 2,413 kPa for high traffic) (DOH, 2000; DRR, 2013). The light traffic roads infer to collector roads or rural roads, which are predominantly designed and constructed by the DRR. The designed equivalent single axle (ESA) load on the light traffic roads is not more than  $1 \times 10^6$ . The heavy traffic roads refer to highways under the responsibility of the DOH. The designed ESA load on the heavy traffic roads is more than  $1 \times 10^6$ . The 7-day UCS at NS:NH ratio of 100:0 (no NH) is approximately 5,800 kPa. This moderately high UCS at NS:NH ratio of 100:0 is contributed from the C-S-H, which is the cementitious product from the reaction between silica from NS and calcium from FA. In presence of  $\text{Ca}^{2+}$ , NS forms soluble calcium silicate, which polymerises further to form gels that bind soil particles together and fills voids as the following equation (Brykov et al., 2002):

$\text{Ca}^{2+} + \text{Na}_2\text{SiO}_3 + m\text{H}_2\text{O} \rightarrow \text{CaO} \cdot 3\text{SiO}_2 \cdot m\text{H}_2\text{O} + 2\text{Na}^+$ . The effect of C-S-H is minimal when the curing time is greater than 28 days as seen that the UCS of sample at NS:NH ratio of 100:0 is essentially constant when the curing time is greater than 28 days.

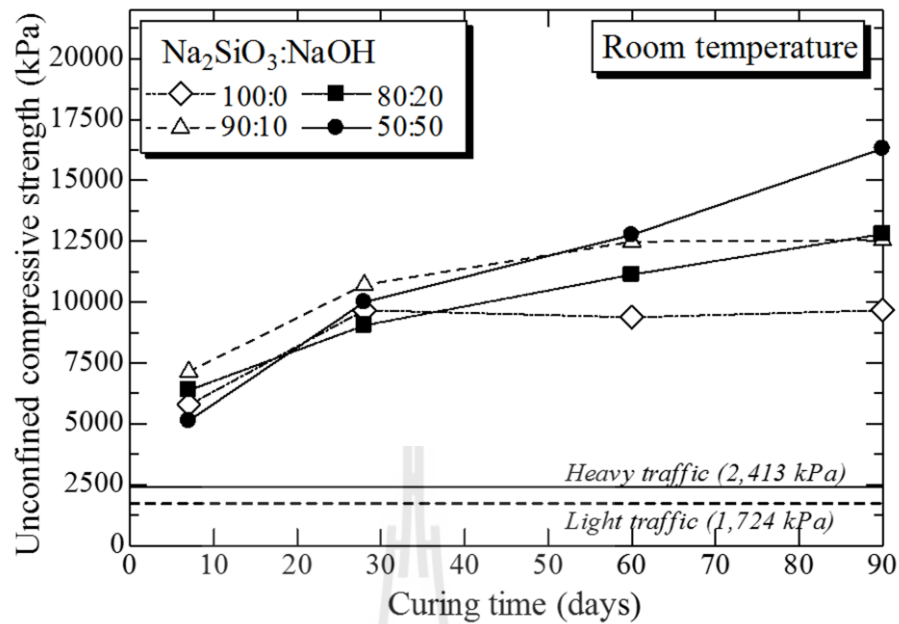


**Figure 3.4** Effect of curing time on UCS of LS – FA geopolymer.

The geopolymerization reaction occurs when NH is mixed together with NS, which causes the pH of the pore liquid to be higher than 10.5. The silica and alumina in amorphous phase of the high calcium FA are dissolved and the NS acts as a binder to develop N-A-S-H. As such, the reactions of high calcium FA, NH and NS results in the coexistence of C-S-H and sodium aluminosilicate geopolymer (N-A-S-H) products. Since the N-A-S-H products are time-dependent, the UCS of geopolymer samples with the presence of NH (NS:NH ratios of 90:10, 80:20, 70:30 and 50:50) increases with curing time even after 28 days of curing.

Due to the coexistence of C-S-H and N-A-S-H products, the geopolymer samples with NS:NH ratios of 90:10 and 80:20 exhibit higher 7-day UCS than the geopolymer sample with NS:NH ratios of 100:0 (its UCS is mainly contributed from C-S-H). The optimum coexistence of C-S-H and N-A-S-H products at 7 days of curing (providing the highest UCS) is found at NS:NH ratio of 90:10.

Since the geopolymerisation process at ambient temperature is time-consuming, the N-A-S-H products at the early state are minimal compared to the C-S-H products, which are from the faster reaction between NS and high calcium FA. Consequently, the 7-day UCS decreases with the reduction in NS:NH ratio and the lowest UCS is found at NS:NH ratio of 50:50 and is about 5,100 kPa, which still meets strength requirement for heavy traffic bound/stabilised base.

At 28 days curing, the NS:NH ratio of 90:10 still exhibits the highest UCS. However, the UCS development rate (slope of UCS versus time relationship) is greater for samples with lower NS:NH ratio (higher NH content). This is attributed to the growth of N-A-S-H products over time. For curing times longer than 60 days, the UCS of geopolymer increases with decreasing NS:NH ratio (increasing NH content); i.e., NS:NH ratios of 50:50 and 100:0 exhibit the maximum and minimum UCS after 60 days of curing, respectively.

Based on the strength data, it is suggested that the NS:NH ratio of 50:50 is the best ingredient whose UCS is greater than 2,413 kPa (required for heavy traffic). The highest rate of UCS development of the geopolymer at this ingredient is also observed. This ingredient also provides the most economical because NH is much cheaper than NS.

### 3.4 Microstructural analysis

Microstructural development of LS-FA geopolymer is explained via the SEM image, which is an advantageous tool for monitoring the growth of cementation matrix over time. **Figure 3.5** shows the microstructure of the four NS:NH ratios of 100:0, 90:10, 80:20, and 50:50 at 7 days of curing (early stage of geopolymerization

process) at ambient temperature. The cementitious (C-S-H and N-A-S-H) products on the high calcium FA surface are clearly observed at NS:NH ratios of 90:10 and 80:20 when compared to those at NS:NH ratios of 50:50 and 100:0, respectively. Many holes on the FA surface are clearly observed for NS:NH ratios of 50:50 due to strong alkaline reaction from NH while the least etched holes on FA surface are observed at NS:NH ratios of 100:0.

**Figure 3.6** shows SEM images of the LS-FA geopolymer samples at NS:NH ratios of 90:10 and 50:50 cured at ambient temperature for 7 and 60 days of curing to illustrate the role of curing time. Comparing **Figures 3.6a – 3.6b** for samples with different NS:NH ratios of 90:10 and 50:50 at the same 7 days of curing, the etched holes on the FA surfaces are clearly observed for both NS:NH ratios but more cementitious products around FA particles and in the pores are detected at NS:NH ratio of 90:10. At longer curing time of 60 days, some holes on the surface of FA are partially filled with other smaller FA particles and the cementitious products form a dense matrix for both NS:NH ratios. In contrast to the SEM images at 7 days of curing, more cementitious products at 90 days of curing are detected at NS:NH ratio of 50:50 (**Figures 3.6c and 3.6d**). Consequently, the sample at NS:NH ratio of 90:10 exhibits the highest early UCS while the sample at NS:NH ratio of 50:50 exhibits the highest long-term UCS (*vide Figure 3.4*).

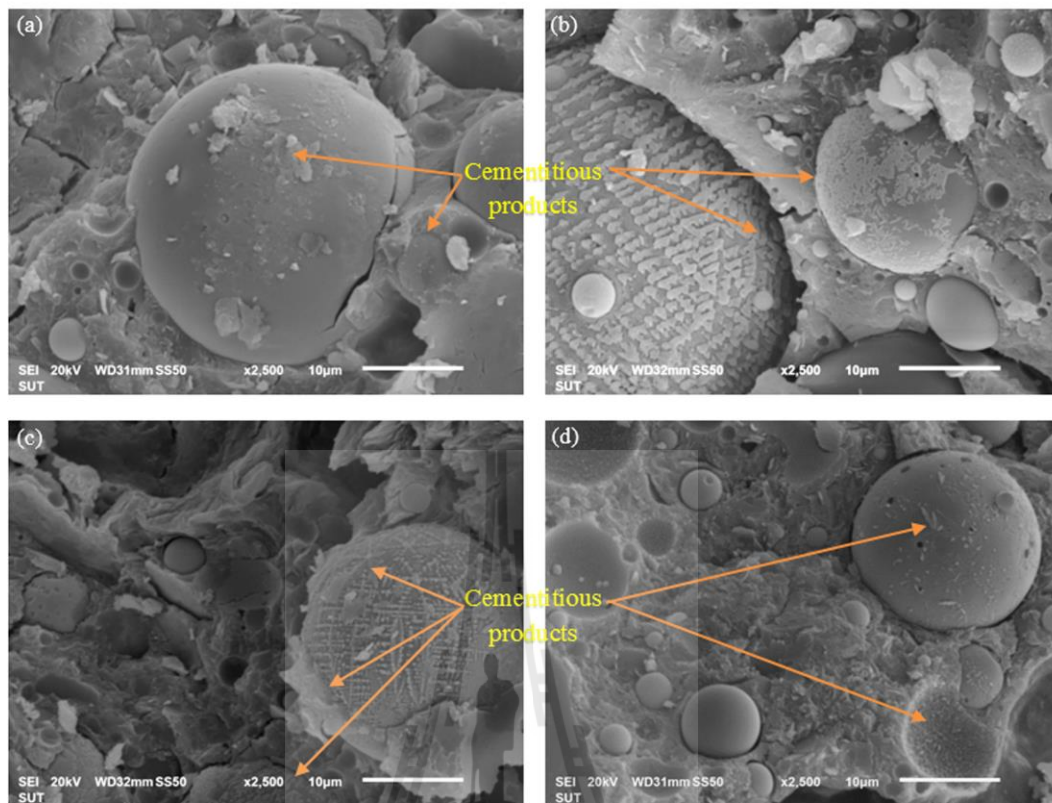


**Figure 3.5** SEM images of LS – FA geopolymer cured at 7 days of curing at ambient temperature for different NS:NH ratios of (a) 100:0, (b) 90:0, (c) 80:20 and (d) 50:50.

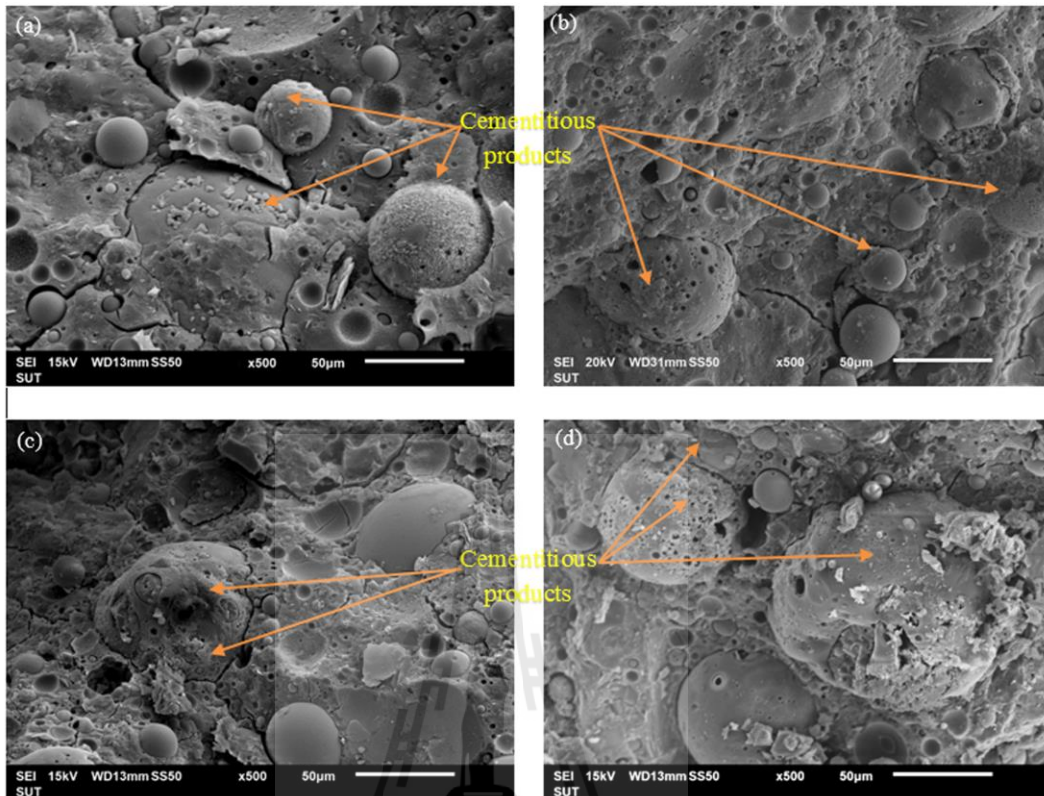


**Figure 3.6** SEM images of LS-FA geopolymer cured at ambient temperature for NS:NH ratio of 90:10 and 50:50 for (a) 90:10 cured at 7 days, (b) 50:50 cured at 7 days, (c) 90:10 cured at 60 days and (d) 50:50 cured at 60 days.

The effect of NS:NH ratio on the growth of geopolymerization products is illustrated by comparing **Figures 3.7a–3.7d**, which show SEM images of the LS–FA geopolymer samples at various NS:NH ratios of 100:0, 90:10, 80:20, and 50:50 after 90 days of curing. For NS:NH ratio of 100:0 (no NH), the FA surface is approximately smooth and spherical with traces of C-S-H products. This indicates that the silica and alumina in FA was insignificantly leached out and the UCS of the samples is contributed from C-S-H (reaction of NS and CaO from FA) (**Figure 3.7a**).

The NH content is not sufficient for leaching silica and alumina from FA for the sample at NS:NH ratio of 90:10 as seen by the small amount of cementitious products on FA surface (**Figure 3.7b**) when compared to the samples at NS:NH ratios of 80:20 and 50:50 (**Figures 3.7c and 3.7d**). For both samples at NS:NH ratios of 80:20 and 50:50, the etched holes are mostly filled with other smaller size ash particles and the cementitious products fill up the pore space, resulting in a dense matrix. The cementitious products are more for the sample at NS:NH ratio of 50:50. As such, the maximum UCS is found at NS:NH ratio of 50:50 at 60 and 90 days of curing (*vide* **Figure 3.4**).

The present study on the improvement of marginal LS by FA-based geopolymer has significant impacts on sustainable pavement applications. The green geopolymer stabilised LS is proved as suitable where the 7-day UCS meets the specification for heavy traffic and the UCS increases with increasing curing time even after 28 days of curing due to the growth of geopolymerisation product (N-A-S-H) over time. The field construction can begin with roller-compacting underlying subgrade in accordance with the specifications of the road authority. The marginal LS was mixed with FA at construction site or in a ready mixer from a plant. Then, a mixture of LS and FA is activated by the liquid alkali activator at the optimum content. Next, the LS-FA geopolymer is compacted to attain at least 95% modified Proctor density. Finally, the field density and UCS of the cored pavement samples are measured for confirming the quality of construction. A life cycle analysis study is recommended for further study on the environmental aspect.

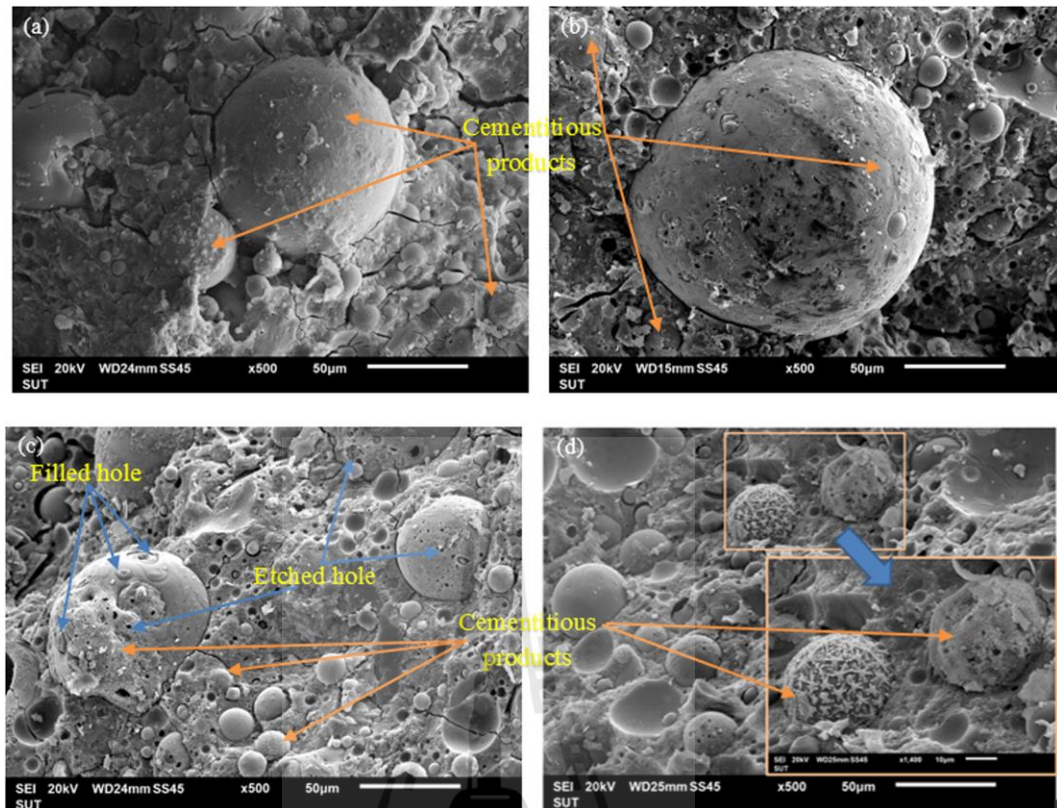


**Figure 3.7** SEM images of LS – FA geopolymer cured at 90 days at ambient temperature for different ingredients of NS: NH (a) 100:0, (b) 90:10, (c) 80:20 and (d) 50:50.

### 3.5 Conclusions

This study investigates UCS and microstructural characteristics of the marginal LS stabilized with high calcium FA based geopolymer as low-carbon alternative green bound pavement material. It is evident from this study that the strength of LS-FA geopolymer meets the standard requirements for heavy and light traffic bound base materials specified by DOH and DRR, Thailand. The following conclusions are drawn.

(1) The optimum liquid alkali activator content of the LS-FA geopolymer is dependent upon the NS:NH ratio. As the NS:NH ratio increases, the optimum liquid alkali activator content increases. The maximum dry unit weight decreases as the increase in optimum liquid alkali activator content.

(2) The maximum 7-day soaked UCS of LS-FA geopolymer samples is found at NS:NH ratio of 90:10 and is 7,143 kPa while the minimum UCS is found at NS:NH ratio of 50:50 and is 5,126 kPa. The UCS values of the samples at all NS:NH ratios tested meet the strength requirement for both light and heavy traffic, specified by DOH and DRR, Thailand.

(3) The coexistence of calcium silicate hydrate (C-H-S) and sodium aluminosilicate hydrate (N-A-S-H) products contributes to the UCS values of LS-FA geopolymer. The C-S-H is resulted from the reaction of CaO from FA and NS while N-A-S-H is the time-dependent geopolymer products.

(4) The results of alkaline activated dissolution on the FA particles of LS-FA geopolymer at NS:NH ratio of less than 100:0 are clearly shown by several etched holes. For longer curing, the holes on FA particles are filled by smaller reactive FA particles and welded by the cementitious products, resulting in a condensed geopolymer matrix. Insignificant amount of etched holes on FA surface are found for the sample at NS:NH ratio of 100:0 for all curing times tested while the traces of C-S-H products on the FA surface are observed and imparts the UCS. The most cementitious products are found at NS:NH ratio of 90:10 for early stage (7 days) and 50:50 for long-term stage (>60 days). As such, the early and long-term UCS are found at NS:NH ratios of 90:10 50:50, respectively.

(5) FA based geopolymer can be used as an alternative binder to PC for sustainable pavement applications. This study indicates that the marginal LS can be stabilized by the high calcium FA based geopolymer to be a bound pavement material for both light and heavy traffic. This will leads to a usage reduction of PC and develop a possible environmentally sustainable material. The economical ingredient is suggested to be NS:NH of 50:50.

### 3.6 References

- Alvarez-Ayuso, E., Querol, X., Plana, F., Alastuey, A., Moreno, N., Izquierdo, M., . . . Barra, M. (2008). **Environmental, physical and structural characterisation of geopolymer matrixes synthesised from coal (co-) combustion fly ashes.** *Journal of Hazardous Materials*, 154(1-3), 175-183.
- Andini, S., Cioffi, R., Colangelo, F., Grieco, T., Montagnaro, F., and Santoro, L. (2008). **Coal fly ash as raw material for the manufacture of geopolymer-based products.** *Waste Management*, 28(2), 416-423. doi: 10.1016/j.wasman.2007.02.001
- Arulrajah, A., Kua, T.-A., Phetchuay, C., Horpibulsuk, S., Maghoolpilehrood, F., and Disfani, M. M. (2015). **Spent coffee grounds-fly ash geopolymer used as an embankment structural fill material.** *Journal of Materials in Civil Engineering*. doi: 10.1061/(ASCE)MT.1943-5533.0001496
- ASTM. (2006). ASTM C131-06. Standard Test Method for Resistance to Degradation of Small-Size Coarse Aggregate by Abrasion and Impact in the Los Angeles Machine. West Conshohocken, PA, USA: ASTM International.

- ASTM. (2007). ASTM D422–63. Standard Test Method for Particle-Size Analysis of Soils<sup>1</sup>. West Conshohocken, PA, USA: ASTM International.
- ASTM. (2009) ASTM D3282–09. Standard Practice for Classification of Soils and Soil-Aggregate Mixtures for Highway Construction Purposes. West Conshohocken, PA, USA: ASTM International.
- ASTM. (2010). ASTM D4318-10. Standard Test Methods for Liquid Limit, Plastic Limit, and Plasticity Index of Soils. West Conshohocken, PA, USA: ASTM International.
- ASTM. (2012a). ASTM C535–12. Standard Test Method for Resistance to Degradation of Large-Size Coarse Aggregate by Abrasion and Impact in the Los Angeles Machine. West Conshohocken, PA, USA: ASTM International.
- ASTM. (2012b). ASTM C618–12a. Standard Specification for Coal Fly Ash and Raw or Calcined Natural Pozzolan for Use in Concrete. West Conshohocken, PA, USA: ASTM International.
- ASTM. (2012c). ASTM D1557. Standard Test Methods for Laboratory Compaction Characteristics of Soil Using Modified Effort (56,000 ft-lbf/ft<sup>3</sup> (2,700 kN-m/m<sup>3</sup>)). West Conshohocken, PA, USA: ASTM International.
- Brykov, A. S., Danilov, V. V., Korneev, V. I., and Larichkov, A. V. (2002). **Effect of hydrated sodium silicates on cement paste hardening**. *Russian Journal of Applied Chemistry*, 75(10), 1577-1579.
- Chindaprasirt, P., Chareerat, T., Hatanaka, S., and Cao, T. (2011). **High-Strength Geopolymer Using Fine High-Calcium Fly Ash**. *Journal of Materials in Civil Engineering*, 23(3), 264-270. doi: 10.1061/(asce)mt.1943-5533.0000161

- Chindaprasirt, P., Chareerat, T., and Sirivivatnanon, V. (2007). **Workability and strength of coarse high calcium fly ash geopolymer**. *Cement and Concrete Composites*, 29(3), 224-229. doi: 10.1016/j.cemconcomp.2006.11.002
- Chindaprasirt, P., Jaturapitakkul, C., Chalee, W., and Rattanasak, U. (2009). **Comparative study on the characteristics of fly ash and bottom ash geopolymers**. *Waste Management*, 29(2), 539-543.
- Chinkulkijniwat, A., and Horpibulsuk, S. (2002). **Field strength development of repaired pavement using the recycling technique**. *Quarterly Journal of Engineering Geology and Hydrogeology*, 45(2), 221-229.
- Davidovits, J. (1991). **Geopolymer: inorganic polymeric new materials**. *Journal of Thermal Analysis*, 37, 1633-1656.
- Davidovits, J. (1994a). **Geopolymers: Man-Made Rock Geosynthesis And The Resulting Development of Very Early High Strength Cement**. *Journal of Materials Education*, 16(2&3), 91-139.
- Davidovits, J. (1994b). **Global Warming Impact on the Cement and Aggregates Industries**. *World Resource Review*, 6(2), 263-278.
- Davidovits, J. (1994c). **Properties Of Geopolymer Cements**. *Alkaline Cements and Concretes, KIEV Ukraine*.
- Davidovits, J. (2002). *Environmentally Driven Geopolymer Cement Applications*.  
Paper presented at the Geopolymer 2002 Conference, Melbourne, Australia.
- Davidovits, J. (2013). **Geopolymer Cement**. *Geopolymer Cement, a review*.
- DOH. (2000). DH-S204/2000 Standard of soil cement base: Department of Highways.
- DRR. (2013). DRR244-2013 Standard of soil cement base: Department of Rural Roads.

- Du, Y. J., Jiang, N. J., Liu, S. Y., Jin, F., Singh, D. N., and Puppala, A. (2014). **Engineering properties and microstructural characteristics of cement-stabilized zinc-contaminated kaolin.** *Canadian Geotechnical Journal*, 51, 289–302.
- Ebrahimi, A., Edil, T. B., and Son, Y.-H. (2012). **Effectiveness of Cement Kiln Dust in Stabilizing Recycled Base Materials.** *Journal of Materials in Civil Engineering*, 24(8), 1059-1066. doi: 10.1061/(asce)mt.1943-5533.0000472
- Guo, X., Shi, H., and Dick, W. A. (2010). **Compressive strength and microstructural characteristics of class C fly ash geopolymer.** *Cement and Concrete Composites*, 32(2), 142-147.
- Hanjitsuwan, S., Hunpratub, S., Thongbai, P., Maensiri, S., Sata, V., and Chindaprasirt, P. (2014). **Effects of NaOH concentrations on physical and electrical properties of high calcium fly ash geopolymer paste.** *Cement and Concrete Composites*, 45, 9-14. doi: 10.1016/j.cemconcomp.2013.09.012
- Horpibulsuk, S., Phetchuay, C., Chinkulkijniwat, A., and Cholaphatsorn, A. (2013). **Strength development in silty clay stabilized with calcium carbide residue and fly ash.** *Soils and Foundations*, 53(4), 477-486.
- Horpibulsuk, S., Rachan, R., Chinkulkijniwat, A., Raksachon, Y., and Suddeepong, A. (2010). **Analysis of strength development in cement-stabilized silty clay from microstructural considerations.** *Construction and Building Materials*, 24(10), 2011-2021. doi: 10.1016/j.conbuildmat.2010.03.011
- Horpibulsuk, S., Rachan, R., and Raksachon, Y. (2009). **Role of fly ash on strength and microstructure development in blended cement stabilized silty clay.** *Soils and Foundations*, 49(1), 85-98.

- Jamsawang, P., Voottipruex, P., and Horpibulsuk, S. (2015). **Flexural strength characteristics of compacted cement-polypropylene fiber sand.** *Journal of Materials in Civil Engineering*, 27(9), 04014243.
- Kampala, A., and Horpibulsuk, S. (2013). **Engineering Properties of Silty Clay Stabilized with Calcium Carbide Residue.** *Journal of Materials in Civil Engineering*, 25(5), 632-644. doi: 10.1061/(asce)mt.1943-5533.0000618
- Kampala, A., Horpibulsuk, S., Chinkullijniwat, A., and Shen, S.-L. (2013). **Engineering properties of recycled Calcium Carbide Residue stabilized clay as fill and pavement materials.** *Construction and Building Materials*, 46, 203-210. doi: 10.1016/j.conbuildmat.2013.04.037
- Kampala, A., Horpibulsuk, S., Prongmanee, N., and Chinkulkijniwat, A. (2014). **Influence of Wet-Dry Cycles on Compressive Strength of Calcium Carbide Residue–Fly Ash Stabilized Clay.** *Journal of Materials in Civil Engineering*, 26(4), 633-643. doi: 10.1061/(asce)mt.1943-5533.0000853
- Nath, S. K., and Kumar, S. (2013). **Influence of iron making slags on strength and microstructure of fly ash geopolymer.** *Construction and Building Materials*, 38, 924-930. doi: 10.1016/j.conbuildmat.2012.09.070
- Phetchuay, C., Horpibulsuk, S., Suksiripattanapong, C., Chinkulkijniwat, A., Arulrajah, A., and Disfani, M. M. (2014). **Calcium carbide residue: Alkaline activator for clay–fly ash geopolymer.** *Construction and Building Materials*, 69, 285-294. doi: 10.1016/j.conbuildmat.2014.07.018
- Puppala, A. J., Wattanasanticharoen, E., and Punthutaecha, K. (2003). **Experimental evaluations of stabilisation methods for sulphate-rich expansive soils.** *Ground Improvement*, 7(1), 25-35.

- Rashad, A. M. (2014). **A comprehensive overview about the influence of different admixtures and additives on the properties of alkali-activated fly ash.** *Materials and Design*, 53, 1005-1025. doi: 10.1016/j.matdes.2013.07.074
- Rattanasak, U., and Chindapasirt, P. (2009). **Influence of NaOH solution on the synthesis of fly ash geopolymer.** *Minerals Engineering*, 22(12), 1073-1078. doi: 10.1016/j.mineng.2009.03.022
- Rattanasak, U., Pankhet, K., and Chindapasirt, P. (2011). **Effect of chemical admixtures on properties of high-calcium fly ash geopolymer.** *International Journal of Minerals, Metallurgy, and Materials*, 18(3), 364-369. doi: 10.1007/s12613-011-0448-3
- Silva, P. D., and Sagoe-Crenstil, K. (2008). **The Effect of Al<sub>2</sub>O<sub>3</sub> and SiO<sub>2</sub> On Setting and Hardening of Na<sub>2</sub>O-Al<sub>2</sub>O<sub>3</sub>-SiO<sub>2</sub>-H<sub>2</sub>O Geopolymer Systems.** *Journal of the Australian Ceramic Society*, 44(1), 39-46.
- Silva, P. D., and Sagoe-Crenstil, K. (2009). **The Role of Al<sub>2</sub>O<sub>3</sub> - SiO<sub>2</sub> and Na<sub>2</sub>O Amorphous → Crystalline Phase Transformation in Geopolymer Systems.** *Journal of the Australian Ceramic Society*, 45(1), 63-71.
- Somna, K., Jaturapitakkul, C., Kajitvichyanukul, P., and Chindapasirt, P. (2011). **NaOH-activated ground fly ash geopolymer cured at ambient temperature.** *Fuel*, 90(6), 2118-2124. doi: 10.1016/j.fuel.2011.01.018
- Sukmak, P., De Silva, P., Horpibulsuk, S., and Chindapasirt, P. (2014). **Sulfate Resistance of Clay-Portland Cement and Clay High-Calcium Fly Ash Geopolymer.** *Journal of Materials in Civil Engineering*, 04014158. doi: 10.1061/(asce)mt.1943-5533.0001112

- Sukmak, P., Horpibulsuk, S., and Shen, S.-L. (2013). **Strength development in clay–fly ash geopolymer**. *Construction and Building Materials*, 40, 566-574. doi: 10.1016/j.conbuildmat.2012.11.015
- Sukmak, P., Horpibulsuk, S., Shen, S.-L., Chindaprasirt, P., and Suksiripattanapong, C. (2013). **Factors influencing strength development in clay–fly ash geopolymer**. *Construction and Building Materials*, 47, 1125-1136. doi: 10.1016/j.conbuildmat.2013.05.104
- Suksiripattanapong, C., Horpibulsuk, S., Chanprasert, P., Sukmak, P., and Arulrajah, A. (2015). **Compressive strength development in fly ash geopolymer masonry units manufactured from water treatment sludge**. *Construction and Building Materials*, 82, 20-30. doi: 10.1016/j.conbuildmat.2015.02.040
- Temuujin, J., and van Riessen, A. (2009). **Effect of fly ash preliminary calcination on the properties of geopolymer**. *Journal of Hazardous Materials*, 164(2-3), 634-639. doi: 10.1016/j.jhazmat.2008.08.065
- Van Jaarsveld, J. G. S., Van Deventer, J. S. J., and Lorenzen, L. (1998). **Factors Affecting the Immobilization of Metals in Geopolymerized Flyash**. *Metallurgical and Materials Transactions B*, 29, 283-291.
- Zhang, M., Guo, H., El-Korchi, T., Zhang, G., and Tao, M. (2013). **Experimental feasibility study of geopolymer as the next-generation soil stabilizer**. *Construction and Building Materials*, 47, 1468-1478. doi: 10.1016/j.conbuildmat.2013.06.017

# **CHAPTER IV**

## **STRENGTH AND MICROSTRUCTURE OF MARGINAL LATERITIC SOIL STABILIZED WITH CALCIUM CARBIDE RESIDUE AND FLY ASH GEOPOLYMER**

### **4.1 Statement of problem**

Quarry materials are becoming increasingly scarce and difficult to obtain for road infrastructure projects. The construction cost of pavement base and subbase is often exorbitant, particularly when quarries are located far away from the construction site. The expansion of quarries furthermore results in significant environmental concerns. Ordinary Portland Cement (OPC) is commonly used as a cementing agent to improve the engineering properties of in-situ marginal soil. However, the production of OPC is an energy-intensive process and emits a significant amount of greenhouse gas into the atmosphere (Davidovits, 1991, 1994a, 1994b, 1994c, 2002). Generally speaking, the production of 1 ton of OPC releases about 1 ton of carbon dioxide (Davidovits, 2013), which is a significant environmental issue.

As a result, alternatives to OPC have been urgently sought in recent years. Geopolymer, a novel green cementing agent manufactured from various kinds of industrial by-products, has been investigated in recent years as an alternative soil stabilizer to OPC. Geopolymer is an inorganic aluminosilicate material synthesized by the alkaline activation of materials rich in alumina ( $\text{Al}_2\text{O}_3$ ) and silica ( $\text{SiO}_2$ ). It is formed through polycondensation of tetrahedral silica ( $\text{SiO}_4$ ) and alumina ( $\text{AlO}_4$ ),

which are linked with each other by the sharing of oxygen atoms (Davidovits, 1991; Gambrell et al., 2010). The chemical structure of geopolymer can be expressed as  $M_n - (Si-O)_z [ -Al-O ]_n \cdot wH_2O$  where M is the alkaline element, - indicates the presence of a bond, z is 1, 2, or 3, and n is the degree of polymerization (Davidovits, 1991).

It is vital that geopolymers possess significant performance properties not only in the laboratory scale but also in the real world-scale. This enables geopolymers to be applied with technological and commercial confidence (Duxson et al., 2007) and with evidence demonstrating: high compressive strength gain (Amnadhua et al., 2013; Bagheri and Nazari, 2014; Chen and Chang, 2007; Chindapasirt et al., 2011; Davidovits, 1994a; Komljenovic et al., 2010; Lee and Van Deventer, 2002; Nugteren et al., 2009), rapid controllable setting and hardening (Lee and Van Deventer, 2002), fire resistance (Cheng and Chiu, 2003; Lyon et al., 1997; Sakkas et al., 2014; Sarker et al., 2014), high level of resistance to a range of different acids and salt solutions (Palomo et al., 1999), not subject to deleterious alkali–aggregate reactions, low shrinkage (Zhang et al., 2013), high surface definition that replicates mold patterns (Davidovits, 1991) and so on.

Recently, many research works have reported on the usage of geopolymer as a sustainable soil stabilizer, especially for building materials. Sukmak et al. (2013) carried out a pioneering work on the strength and microstructure of silty clay-FA geopolymer masonry units. It was found that the developed masonry units have a strength greater than 7 MPa and can be used as a bearing unit according to the Thailand Industrial Standards. Furthermore, the factors controlling the strength development (Sukmak, Horpibulsuk, Shen, et al., 2013) and sulfate resistance of soil stabilized with high - calcium FA geopolymer were investigated (Sukmak et al.,

2014). Zhang et al. (2013) illustrated the feasibility of using geopolymer as an effective soil stabilizer for clayey soils based on an experimental study. Suksiripattanapong et al. (2015) and Horpibulsuk et al. (2015) successfully used FA based geopolymer as a cementing agent and used water treatment sludge as aggregates to develop sustainable geopolymer masonry bearing units.

Besides geopolymer, Calcium Carbide Residue (CCR), a by-product of acetylene production process through the hydrolysis of calcium carbide ( $\text{CaC}_2$ ) is regarded as a sustainable cementing agent. CCR is mainly composed of calcium hydroxide in a slurry form (Amnadhua et al., 2013; Horpibulsuk et al., 2012; Horpibulsuk et al., 2013; Kampala et al., 2013). The production of CCR is described in the following equation:



From Eq. (1), it is evident that 64 g of calcium carbide ( $\text{CaC}_2$ ) generates 26 g of acetylene gas ( $\text{C}_2\text{H}_2$ ) and 74 g of CCR in term of  $\text{Ca}(\text{OH})_2$  (Kampala et al., 2013). In Thailand, the demand of  $\text{CaC}_2$  for producing acetylene gas is about 18,500 tons/year, consequently this implies that more than 21,500 tons/year of CCR is released (Amnadhua et al., 2013; Kampala et al., 2013; Vichan and Rachan, 2013). The demand for acetylene gas is increasing annually, driven by the growing demand from the metal cutting and welding industry. Presently, the CCR is mainly disposed in landfills, which causes various environmental problems due to its high alkalinity.

Many researchers have used CCR for partial or full replacement of OPC in concrete application. Makaratat et al. (2010) used both CCR and FA as a concrete

binder without OPC. The Unconfined Compressive Strengths (UCS) of tested CCR-FA concretes were 28.4 and 33.5 MPa after 28 and 90 days, respectively. Somna et al. (2011) studied the chemical reaction and the microstructures of CCR and CCR-Ground Fly Ash (CCR-GFA) pastes. Silica oxides from GFA could be reacted with  $\text{Ca(OH)}_2$  from CCR and formed Calcium Silicate Hydrate (C-S-H). The UCS of samples increased with age and was nearly constant after 42 days. Amnadhua et al. (2013) successfully used the mixture of ground CCR, GFA and OPC as a new cementing material to produce a high strength concrete having a compressive strength of over 50 MPa. The compressive strength of ground CCR-GFA concrete containing 20% OPC could be as high as 67 MPa or 95% of OPC concrete at 28 days. Jaturapitakkul and Roongreung (2013) used the mixture of CCR and Rice Husk Ash (RHA) as a new cementitious material. The mortar with a CCR to RHA ratio of 50:50 by weight provided a high UCS of 15.6 MPa at 28 days of curing. Rattanasotinunt et al. (2013) studied a possibility of using CCR and bagasse ash as a cementing agent to substitute OPC in concrete. The CCR and bagasse ash mixtures with  $90 \text{ kg/m}^3$  of OPC provided a concrete with a 28-day UCS of 32.7 MPa. Horpibusuk et al. (2014) used CCR and FA as a cementing agent for manufacturing masonry units without OPC. The UCS of masonry units was greater than 20 MPa, which met the requirements for non-bearing masonry unit, according to the Thailand Industrial Standards.

Besides building material applications, CCR can be used to improve engineering properties of problematic soil. Du et al. (2011) studied the use of CCR as a binder to treat over-wetted clays for filling embankment material in China highway engineering practice. It was revealed that CCR stabilized soil performed better than lime stabilized soil, in agreement with the test results previously reported by Kampala

and Horpibulsuk (2013). Vichan and Rachan (2013) demonstrated that the CCR and Biomass Ash (BA) blend can be employed to improve strength and compressibility of soft Bangkok clay. Horpibulsuk et al. (Horpibulsuk et al., 2012; 2013) reported on the UCS development of CCR-FA stabilized silty clay in northeast Thailand. Kampala et al. (2013) showed that the recycled CCR stabilized clay can be used as fill and embankment materials, which possessed satisfactorily high strength and low compressibility. The unreactive CCR can react with silica and alumina in FA after recycling. Kampala et al. (2014) investigated the durability against wetting and drying cycles of the CCR and FA stabilized silty clay to ascertain its performance in pavement applications. Recently, Phetchuay et al. (2014) investigated the possibility of using CCR, sodium silicate ( $\text{Na}_2\text{SiO}_3$ ) solution and water as an alkaline activator for a FA geopolymer binder. This geopolymer binder can improve the engineering properties of problematic silty clay as a stabilized subgrade material.

Most of research work on CCR stabilization is on the usage of a blend of CCR and pozzolanic material. The investigation of CCR as a promoter in FA based geopolymer stabilized soil is however still limited. In this study, CCR is used as a promoter in alkaline activator (a mixture of  $\text{Na}_2\text{SiO}_3$  and  $\text{NaOH}$ ) to enhance the strength of marginal lateritic soil (LS). UCS is used to investigate strength development. The microstructural development is observed via Scanning Electron Microscope (SEM) analysis to understand the role of influential factors, controlling the strength development. The influential factors studied in this research include CCR content,  $\text{Na}_2\text{SiO}_3:\text{NaOH}$  ratio, and curing time at room temperature. This study enables the usage CCR, a industrial by-product traditionally destined for landfill, to be used in a sustainable manner as a promoter in FA-based geopolymer pavement

bases/subbases, which is significant from engineering, economical and environmental perspectives.

## 4.2 Materials and methods

### 4.2.1 Soil sample

The marginal LS was obtained from a borrow pit in Rayong province, Thailand. The specific gravity is 2.58. Liquid Limit (LL), Plastic Limit (PL), and Plastic Index (PI) undertaken according to ASTM D4318 (2010) are 27.72%, 21.65%, and 6.07%, respectively. The grain size distribution of the marginal LS determined by a sieve analysis test (ASTM, 2007a) is shown in **Figure 4.1**. This soil is classified as Silty clayey sand (SC-SM) according to the Unified Soil Classification System (USCS) [42] and A-2-4(0) according to the AASHTO (ASTM, 2009). The compaction characteristics under modified Proctor energy (ASTM, 2012b) are optimum moisture content (OMC) of 8.0%, and maximum dry unit weight ( $\gamma_{dmax}$ ) of 20.85 kN/m<sup>3</sup>. California Baring Ratio (CBR) value is 14.7% at 95% of  $\gamma_{dmax}$ . Los Angeles abrasion described by ASTM C131 (2006) and C535 (2012a) is 52.9%. With low CBR, poor gradation, and high LA abrasion compared to the specification of the Department of Highways, Thailand for pavement subbase materials (DOH, 1989) (**Table 4.1**), this LS is classified as a marginal soil targeted for landfill. Chemical composition of the LS obtained from X-ray Fluorescence (XRF) analysis is shown in **Table 4.2**. The LS is irregular shape as shown in **Figure 4.2a**.

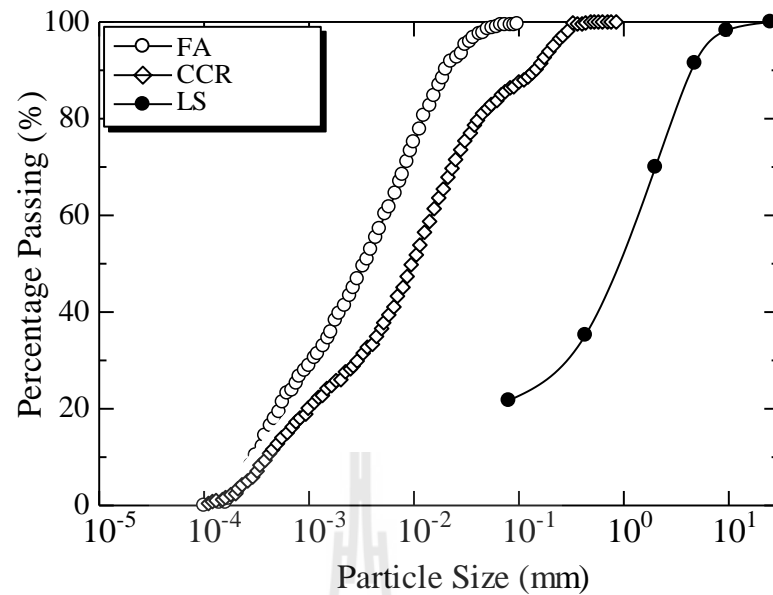


**Figure 4.1** Particle size distributions of FA, CCR and LS.

**Table 4.1** The engineering properties of the soil sample and subbase specifications.

Engineering properties	Soil sample	Subbase specifications by road authority of Thailand
Liquid limit (LL) (%)	27.72	< 35
Plastic index (PI) (%)	6.07	< 11
California Bearing Ratio (CBR) at 95% of $\gamma_{dmax}$ (%)	14.70	> 25
Los Angeles abrasion (percent of wear) (%)	52.90	> 60

### 4.2.2 Fly ash

Fly Ash (FA) used in this study was obtained from Mae Moh power plant in Northern Thailand, which is the largest lignite power plant in Thailand. The chemical composition obtained from X-Ray Fluorescence (XRF) of FA is shown in **Table 4.2**. The major components of FA are 36.00% SiO<sub>2</sub>, 26.73% CaO, 17.64% Fe<sub>2</sub>O<sub>3</sub>, and 16.80% Al<sub>2</sub>O<sub>3</sub>. FA is thus classified as high calcium. Particle size distribution and microstructure of FA are shown in **Figure 4.1** and **Figure 4.2b**, respectively. The FA particles are generally fine and spherical in shape.

**Table 4.2** The chemical compositions of the marginal LS, FA and CCR.

Chemical composition (%)	LS	FA	CCR
SiO <sub>2</sub>	77.81	36.00	6.49
Al <sub>2</sub> O <sub>3</sub>	4.42	16.80	2.55
Fe <sub>2</sub> O <sub>3</sub>	10.93	17.64	3.25
CaO	1.13	26.73	70.78
MgO	N.D.	N.D.	0.69
SO <sub>3</sub>	1.36	N.D.	0.66
K <sub>2</sub> O	2.33	1.83	7.93
TiO <sub>2</sub>	1.33	0.48	N.D.
MnO <sub>2</sub>	0.55	0.15	N.D.
Br <sub>2</sub> O	0.38	N.D.	N.D.

N.D. = not detected

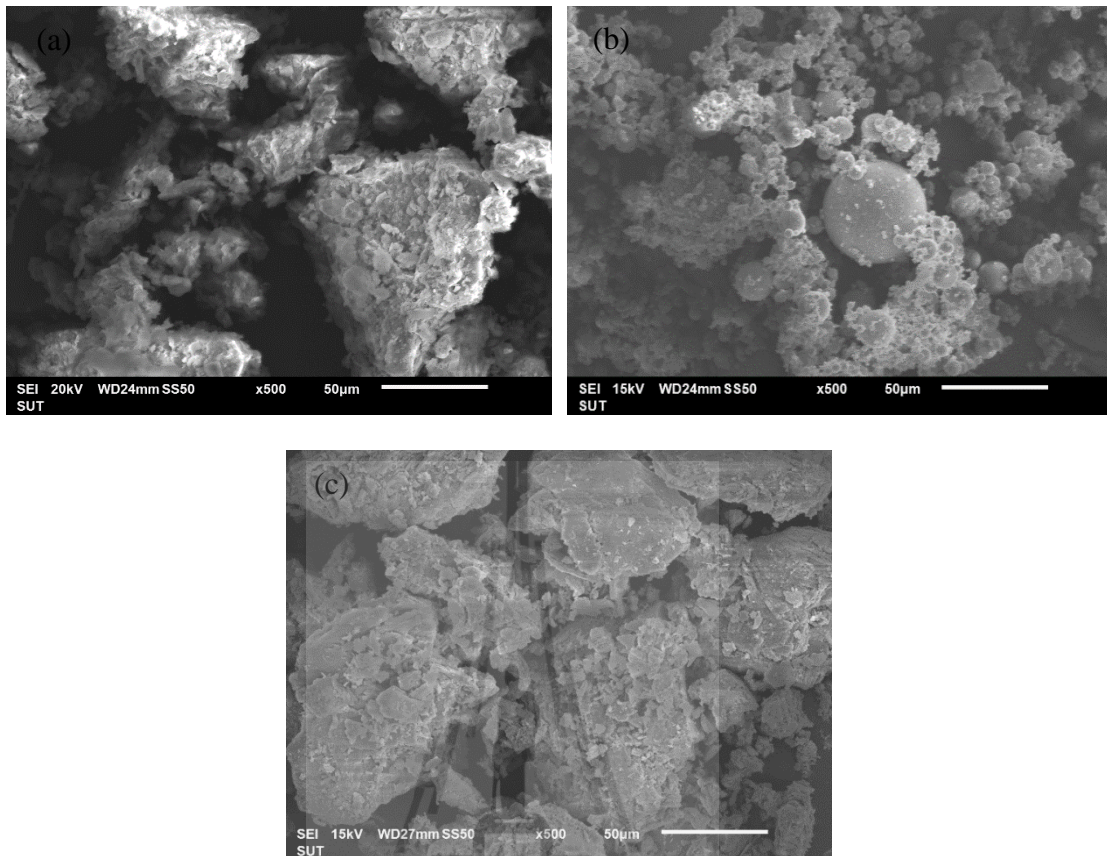


**Figure 4.2** SEM images of: (a) LS, (b) FA and (c) CCR.

#### 4.2.3 Calcium carbide residue

Calcium Carbide Residue (CCR) was obtained from Sai 5 Gas Product Co., Ltd. The CCR was oven-dried at 100°C for 24 hours and was also pulverized with a Los Angeles abrasion machine. The CCR was passed through a sieve No. 40 (425 µm). The specific gravity of CCR is 2.32. The chemical composition of CCR is shown in **Table 4.2**. The major component of CCR is 70.78% CaO while the minor components are pozzolanic materials (SiO<sub>2</sub>, Al<sub>2</sub>O<sub>3</sub> and Fe<sub>2</sub>O<sub>3</sub>) of about 12.29%. The high Ca(OH)<sub>2</sub> and CaO contents of the CCR indicate that it can react with FA and produce a cementitious products (CSH) (Kampala et al., 2013). The particle size

distribution of CCR obtained from laser particle size analysis is shown in **Figure 4.1**. The microstructure of CCR is shown in **Figure 4.2c**, indicating that the particles are generally irregular in shape. **Figure 4.3** shows the X-Ray Diffraction (XRD) pattern of CCR indicating that it is composed of about 76.7%  $\text{Ca}(\text{OH})_2$  as the main composition, which is similar to that of the hydrated lime (Horpibulsuk et al., 2014).

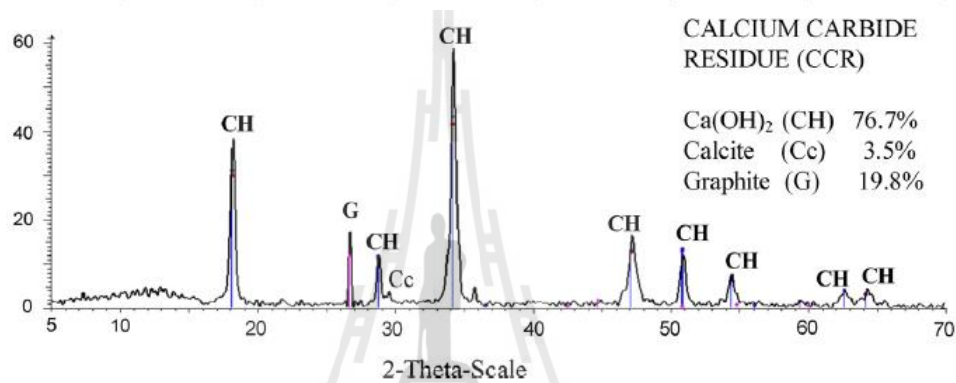


**Figure 4.3** XRD pattern of CCR.

#### 4.2.4 Liquid alkali activator

The liquid alkaline activator was a mixture of sodium silicate ( $\text{Na}_2\text{SiO}_3$ , NS) solution and sodium hydroxide (NaOH, NH) solution with a concentration of 5 molar. NS solution was composed of 15.50%  $\text{Na}_2\text{O}$ , 32.75%  $\text{SiO}_2$ , and 51.75  $\text{H}_2\text{O}$  by weight. Distilled water was used throughout the experiments for producing the NH solution.

#### 4.2.5 LS – FA – CCR geopolymer

The LS-FA-CCR geopolymer is a mixture of the LS, FA, CCR and liquid alkaline activator (NS and NH). In this study, the FA content was fixed at 30% of the total mix while the soil and CCR contents were varied. The soil: FA: CCR

ratios were 60:30:10, 50:30:20, and 40:30:30. The NS:NH ratios were 100:0, 90:10, 80:20 and 50:50. The LS, CCR, and FA were first mixed together to ensure homogeneity and then mixed with liquid alkaline activator for an additional 5 minutes. The mixtures were next compacted under modified Proctor energy according to the specification of the Department of Highways, Thailand. After 24 hours, the compacted samples were demolded, wrapped with plastic sheet and cured at room temperature between 27 to 30°C.

UCS of the soaked LS-CCR-FA geopolymer samples was measured (ASTM, 2007b) after curing periods of 7, 28, 60 and 90 days. The samples were submerged under water for 2 hours and then air-dried for 1 h prior to UCS testing according to the specification of the Department of Highways (DOH, 2000) and Department of Rural Roads (DRR, 2013), Thailand. The results were reported using mean compressive strength values of at least three specimens to check for consistency.

Microstructural characterizations of the geopolymer stabilized soil were measured using SEM. The small fragments from the center of samples were frozen at -195°C by immersion in liquid nitrogen for 5 min and coated with gold before SEM (JEOL JSM-6400 device) analysis (Sukmak, Horpibulsuk, and Shen, 2013).

## 4.3 Results

### 4.3.1 Compaction characteristics

**Figure 4** shows the relationships between dry unit weight and liquid alkaline activator content of the LS-CCR-FA geopolymer for various CCR contents and NS:NH ratios. The compaction curves of the LS-CCR-FA geopolymer are evidently dependent on the CCR content and NS:NH ratio. For a particular NS:NH

ratio and CCR content, the dry unit weight of the LS-CCR-FA geopolymer increases with increasing liquid alkaline activator content until the maximum dry unit weight is attained at an Optimum Liquid Content (OLC). Beyond this optimum value, the unit weight decreases as the alkaline activator content increases. This characteristic is typical of compaction behavior of coarse-grained materials (Horpibulsuk et al., 2009). For a particular NS:NH ratio, the  $\gamma_{d,max}$  decreases (associated with an increase in OLC) with increasing the CCR content due to low specific gravity of CCR. For 10% and 20% CCR, the NS:NH ratio of 50:50 exhibits the highest  $\gamma_{d,max}$ . For 30% CCR, the  $\gamma_{d,max}$  changes insignificantly while the OLC decreases with increasing the NH content. The highest  $\gamma_{d,max}$  is found at 10% CCR and NS:NH = 50:50 (Soil:FA:CCR = 60:30:10). The relationship between OLC and NS contents for various CCR contents can be represented by linear function as shown in **Figure 4.5**.

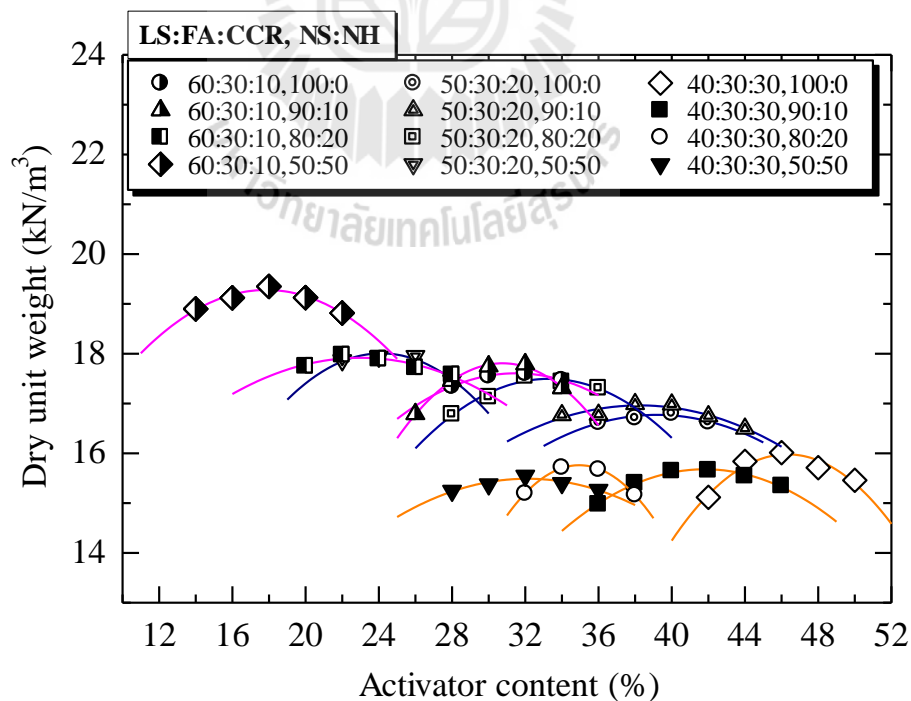


**Figure 4.4** Compaction curves of the LS – CCR – FA geopolymer.

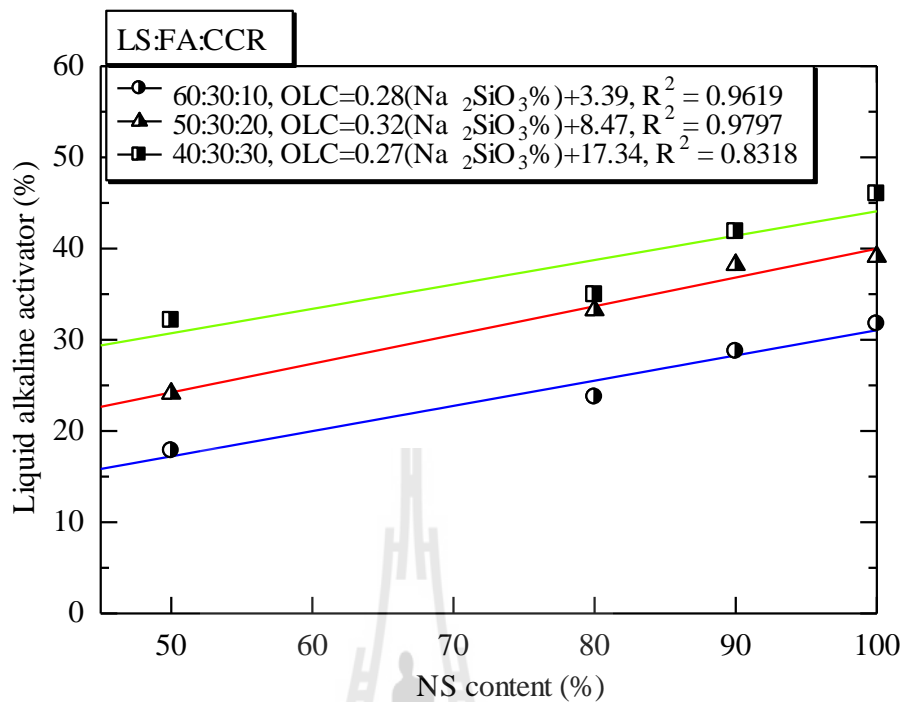


**Figure 4.5** Prediction of optimum liquid alkaline activator for each proportion.

### 4.3.2 Unconfined compressive Strength

The relationships between UCS and CCR replacement ratio of the LS-FA-CCR geopolymer specimens at different curing times and NS:NH ratios are shown in **Figure 4.6**. The 7-day UCS values for geopolymer samples with and without CCR are greater than the strength requirement specified by the national road authority in Thailand for light traffic (> 1,724 kPa) and for heavy traffic (> 2,413 kPa) (DOH, 2000; DRR, 2013). It is evident from the test results that without CCR, the 7-day UCS is essentially the same for all NS:NH ratios and NH improves long-term UCS. For instance, the UCS of samples at NS:NH = 100:0 increases minimally after 28 days of curing (**Figure 4.6a**) while the significant UCS development is observed for the sample at NS:NH = 50:50 (**Figure 4.6d**).

The role of CCR on the UCS development of geopolymer sample is evident in **Figure 4.6** in that the CCR replacement increases 7-day UCS for all NS:NH ratios; i.e., the higher CCR content results in the greater 7-day UCS and the highest 7-day UCS is found at 30% CCR. For low NH content (NS:NH < 90:10), the long term 60-day and 90-day UCS increases with increasing CCR up to CCR = 20% and then decreases. The same is not evident for higher NH content (NS:NH > 80:20). The input CCR tends to slightly decrease the 28-day and 60-day UCS whereas significantly improves the long term 90-day UCS. It is noted that the optimum CCR content, which provides the highest long-term 90-day UCS for both low and high NH, is found at 20%. The CCR replacement is optimal at low NH; i.e., the maximum 90-day UCS is 18,800 kPa at NS:NH = 90:10 and CCR = 20%.

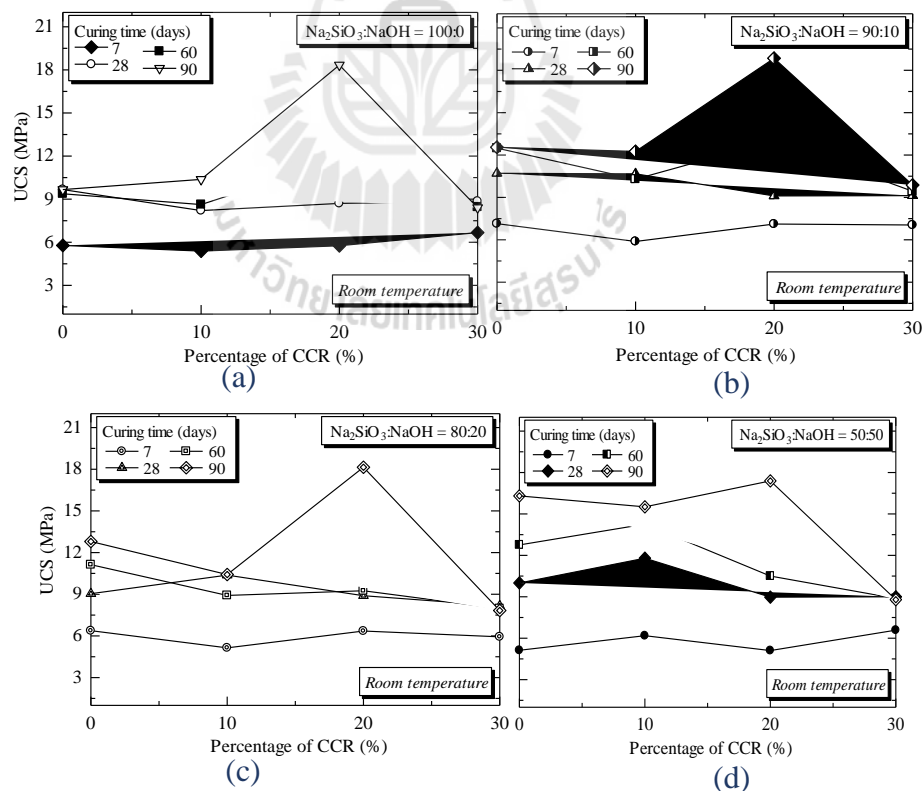


**Figure 4.6** The UCS of LS – CCR – FA geopolymer at various CCR contents cured at 7 to 90 days for different NS:NH ratios (a) 100:0, (b) 90:10,

(c) 80:20 and (d) 50:50.

It is of interest to note that the 30% CCR replacement improves the early strength significantly as seen by the highest 7-day UCS for a particular NS:NH ratio. However, this high CCR replacement ratio yields the negative long term response; i.e., UCS development after 28 days of curing is minimal and the long term 90-day UCS values are the lowest for all NS:NH ratios. This result is similar to the finding of geopolymer paste using a mixture of NH and  $\text{Ca}(\text{OH})_2$  as alkaline activators and fly ash as a precursor by De Vargas et al. (2014) that the geopolymer paste with high  $\text{Ca}(\text{OH})_2$  exhibited high UCS at early stage but the UCS decreased after 28 days of curing. To conclude, the CCR replacement in LS-FA geopolymer is advantageous on the enhancement of UCS at low NH and the optimum CCR content must be limited to 20%. The CCR replacement is not recommended for high NH where despite very early and long-term UCS improvement, the UCS between 28 days and 90 days decreases significantly.

#### 4.4 Microstructural analysis

Investigation of microstructural development of LS-FA-CCR geopolymer via SEM analysis is advantageous for monitoring the chemical reaction among alkaline activator, FA and CCR and the growth of cementation matrix over time. **Figures 4.7a-4.7d** and **Figures 4.8a-4.8d** show the SEM images of 7-day cured sample at low NH (NS:NH = 90:10) and high NH (NS:NH = 50:50) for four different CCR replacement ratios, respectively. More etched holes, which indicate the stronger chemical reaction, are observed at greater CCR replacement ratio. The etched holes

indicate the leaching of silica and alumina oxides from FA by alkaline dissolution. The leached silica and alumina ions react with  $\text{Ca}^{2+}$  and  $\text{Na}^+$  ions and result in the formation of geopolymerization products (Sodium Alumino Silicate Hydrate, N-A-S-H) coexisted with Calcium Silicate Hydrate (C-S-H) and/or Calcium Alumino Silicate hydrate (C-A-S-H). Furthermore, the reaction between  $\text{Ca}^{2+}$  from CCR and water generates heat and an exothermal process, which accelerates the geopolymerization process. The similar formation of C-S-H and/or C-A-S-H within the geopolymer matrix was previously reported by Phoo-ngernkham et al. (2013) for geopolymer paste containing Portland cement. Hence, the 7-day UCS of LS-FA-CCR geopolymer increases with the increased CCR replacement ratio.

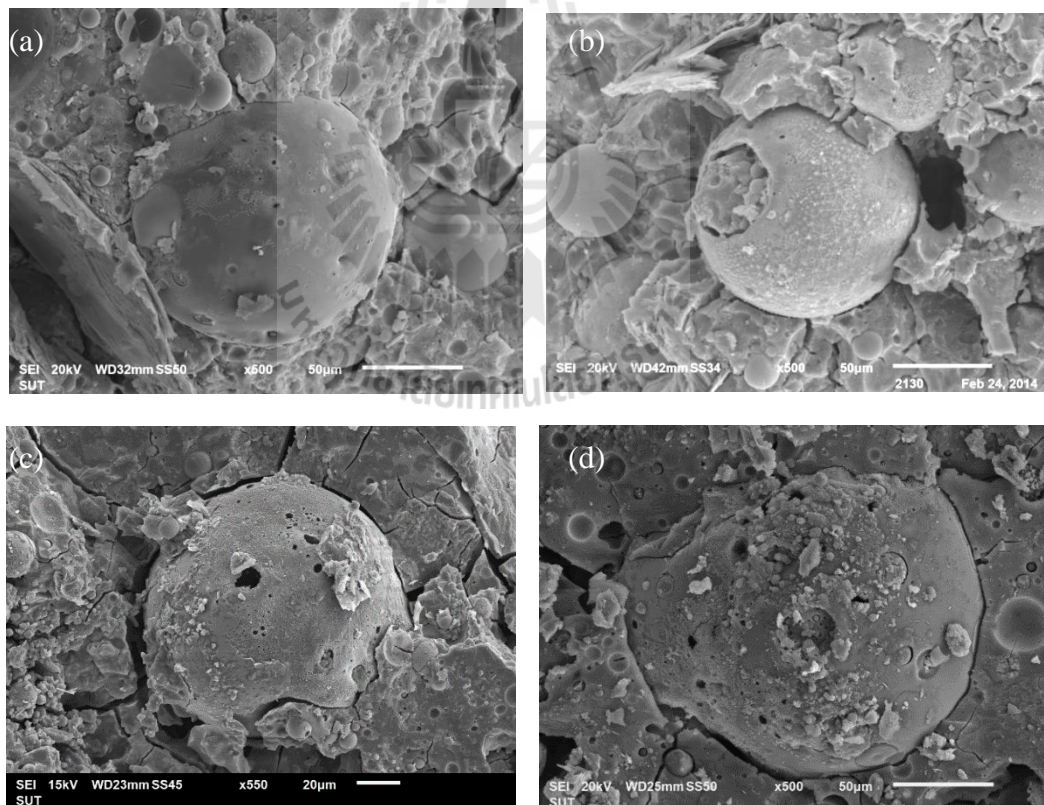


**Figure 4.7** SEM images of samples at NS:NH ratio of 90:10 cured 7 days at room temperature for different CCR contents: (a) 0%, (b) 10%, (c) 20% and (d) 30%.

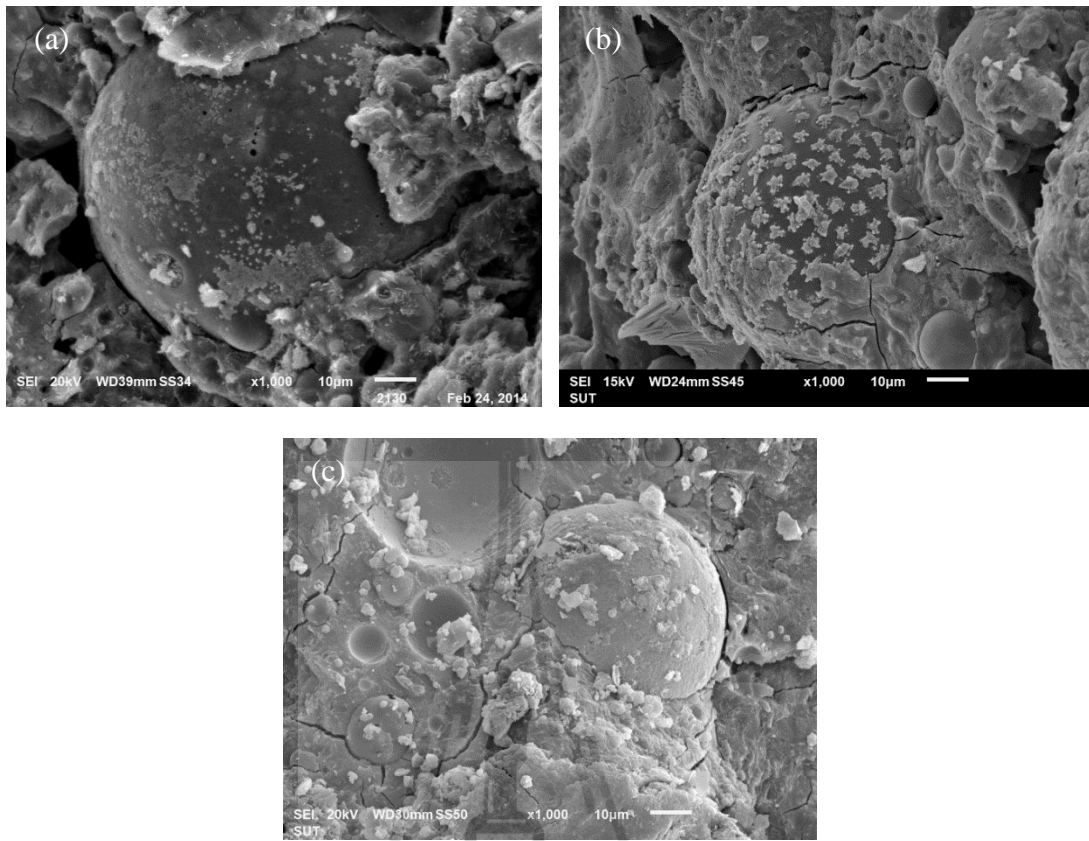


**Figure 4.8** SEM images of samples at NS:NH ratio of 90:10 cured 7 days at room temperature for different CCR contents: (a) 10%, (b) 20% and (c) 30%.

The role of CCR replacement on the high NH samples is presented in **Figure 4.8**, which shows SEM images of 7-day cured samples at NS:NH ratio of 50:50 and for 10% to 30% CCR. The SEM images of the high NH sample are similar to that of the low NH samples in that the growth of cementitious products is mainly dependent upon CCR replacement ratio and the significant cementitious products are observed at CCR = 30% where the maximum 7-day UCS is attained.

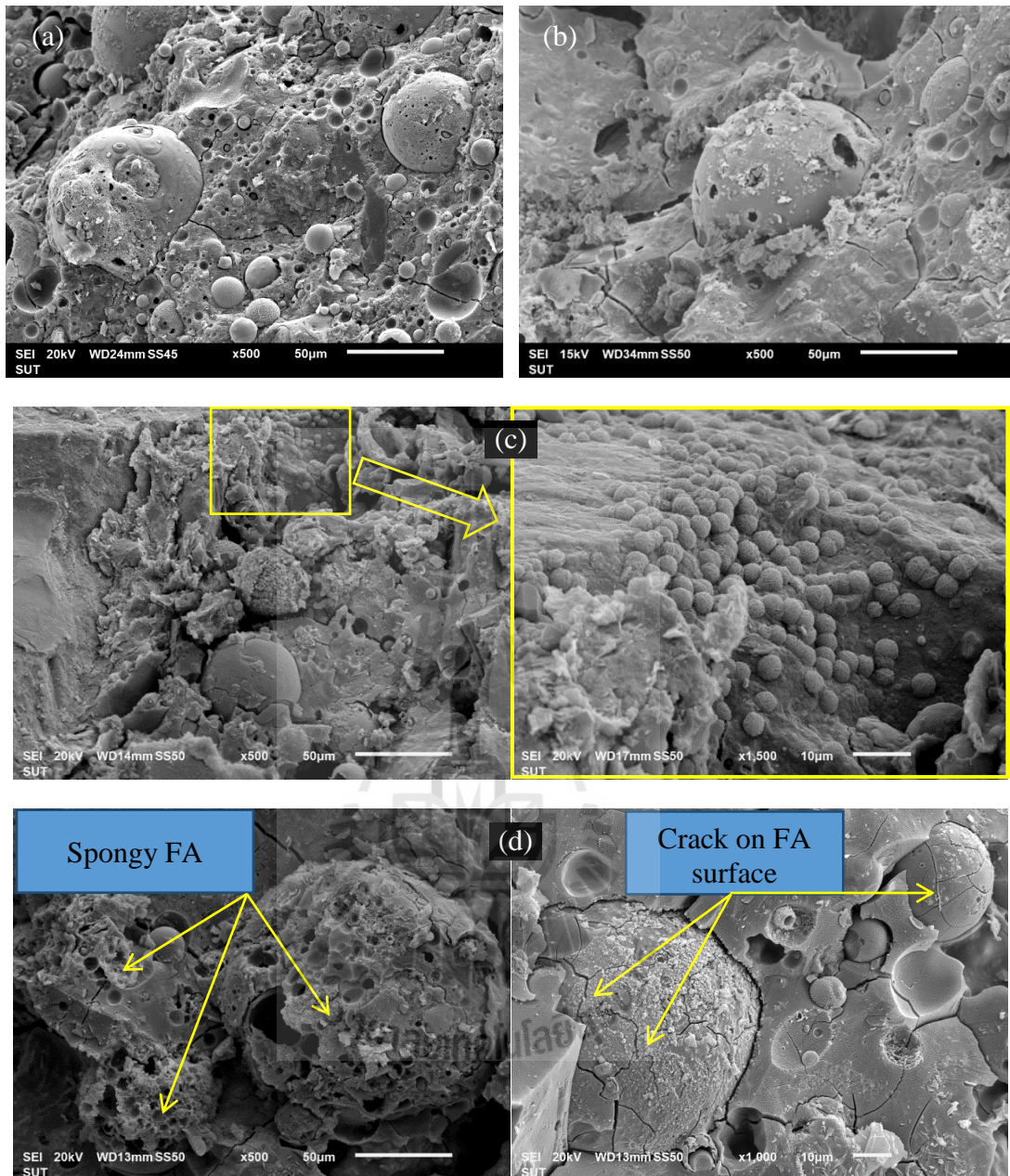


**Figure 4.9** SEM images of samples at NS:NH ratio of 80:20, cured for 90 days at room temperature for different CCR replacement ratios of (a) 0%, (b) 10%, (c) 20% and (d) 30%.

**Figure 4.9** shows SEM images of the LS-FA-CCR geopolymer at a high NH (NS:NH = 80:20) and cured for 90 days. The growth of geopolymerization products is

demonstrated by comparing **Figures 4.9a–4.9d**. For the samples with 0% and 10% CCR replacement ratio, the FA surface characteristics are more or less the same; however, 10% CCR sample indicates fewer non-reacted and/or partially reacted FA particles. The etched holes on FA surface indicate that the chemical reaction still continues even after a long curing time of 90 days (**Figures 4.9a** and **4.9b**). A lot of geopolymerization products on the FA surface and soil particles with fewer non-reacted FA particles are clearly observed at 20% CCR (**Figure 4.9c**). As such, the highest 90-day UCS is observed at this CCR replacement ratio.

For the high CCR replacement ratio of 30%, the polycondensation is hindered and the excessive OH<sup>-</sup> ion concentration causes early aluminosilicate gel precipitation. This phenomenon was also observed in the geopolymer paste with high NH (Phoo-ngernkham et al., 2013). The early aluminosilicate gel precipitation causes the spongy FA particles and the fast setting and the high heat temperature generated from alkali solutions due to high CCR content results in cracks on FA particles (**Figure 4.9d**). These spongy FA and cracked FA particles result in a weak material and hence the reduction in UCS. Yip and Van Deventer (2002) have also reported on the spongy and cracked FA particles in high calcium geopolymer paste. Moreover, the UCS reduction is possibly caused by the formation of calcite (CaCO<sub>3</sub>) over time. The formation of calcite after 28 days is attributed to a chemical reaction of Calcium Hydroxide (Ca(OH)<sub>2</sub>) from CCR and Calcium Silicate Hydrate (C-S-H) from hydration products with Carbon Dioxide (CO<sub>2</sub>) in the presence of moisture (Yip and Van Deventer, 2003). This carbonation is the most common causes of concrete deterioration (Lo et al., 2008).

Similarly, **Figure 4.10** presents the SEM images of very high NH samples (NS:NH = 50:50) at various CCR replacement ratios. The cementitious matrix around the FA particles for 10% CCR and 20% CCR samples are clearly observed (**Figures 4.10a** and **4.10b**). However, for 30% CCR, the cracked FA surface is clearly evident, which is similar to that of NS:NH ratio of 80:20 at 30% CCR (**Figure 4.9d**). This confirms that a high CCR replacement of 30% causes the early aluminosilicate gel precipitation at various NH contents tested and thus lowers the UCS of LS-FA geopolymer.

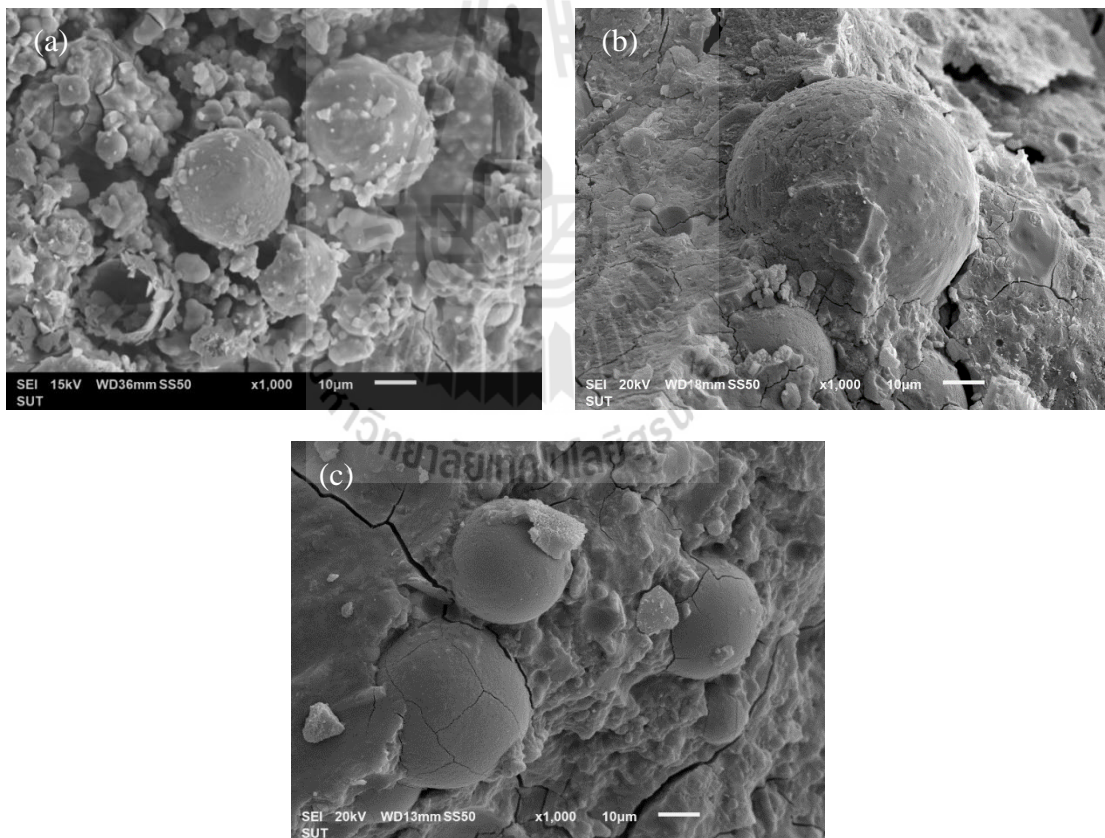


**Figure 4.10** SEM images of LS-FA- geopolymer cured for 90 days at high NH (NS:NH ratio of 50:50) for: (a) 10% CCR, (b) 20% and (c) 30% CCR.

## 4.5 Conclusions

This paper studies the influences of CCR as a promoter, NS:NH ratio and curing time on UCS and microstructural development of marginal LS-FA geopolymer. The measured 7-day UCS of the LS-FA geopolymer at different NS:NH ratios and CCR replacement ratios is compared to the specification for light and heavy traffic pavement of local national authorities. It is evident from this research that the high calcium FA based geopolymer with CCR as a promoter can be used as a green stabilizer of marginal LSs alternative to conventional PC for developing a sustainable bound pavement material. The conclusions arising from this research are drawn as follows.

(1) The soaked 7-day UCS of marginal LS-FA geopolymer with and without CCR at various NS:NH ratios meets the strength requirement for both light and heavy traffic pavement.

(2) The soaked 7-day UCS of marginal LS-FA geopolymer is essentially similar for all NS:NH ratios tested. The NH improves the long-term UCS of marginal LS-FA geopolymer and the NS:NH ratio of 50:50 exhibits the highest long-term UCS after 28 days of curing.

(3) The CCR improves early 7-day UCS of marginal LS-FA geopolymer for all NS:NH ratios tested. The higher CCR replacement ratio results in the higher 7-day UCS; i.e., the 30% CCR provides the highest 7-day UCS. The 28-day and 60-day UCS of marginal LS-FA geopolymer tends to decrease with increasing CCR replacement ratio especially for very high NH content (NS:NH < 80:20). On the other hand, the 90-day UCS increases with increasing CCR replacement ratio where the maximum 90-day UCS values are found at an optimum CCR replacement ratio of

20% for all NS:NH ratios tested. Beyond this optimum value, the 90-day UCS decreases.

(4) The CCR replacement ratio is not recommended for the high NH samples; i.e., even though very early and long-term UCS is improved, the service UCS between 28 days and 90 days significantly decreases. The CCR replacement is more advantageous at low NH; i.e., the maximum 90-day UCS is found to be 18,800 kPa at NS:NH = 90:10 and CCR = 20%.

(5) For both low and high NH contents, the clear cementitious products on the FA particles are clearly observed via SEM images of 7-day cured LS-FA-geopolymer samples. The most cementitious products are detected at higher CCR replacement ratio; i.e., the 30% CCR sample shows the most cementitious products. The cementitious products are attributed to the coexistence of C-S-H and N-A-S-H.

(6) The optimum CCR replacement ratio providing the highest 90 day UCS of LS-FA geopolymer is found at 20% for all NS:NH ratios tested. The significant cementitious products are clearly observed via SEM images at this CCR replacement ratio. The negative effect of excessive CCR replacement ratio of 30% on the 90-day UCS is evident. The spongy and cracked FA particles due to early aluminosilicate gel precipitation and high heat temperature are clearly observed via SEM images and hence the UCS reduction. The UCS reduction is also caused by the carbonation.

## 4.6 References

Amnadnua, K., Tangchirapat, W., and Jaturapitakkul, C. (2013). **Strength, water permeability, and heat evolution of high strength concrete made from the**

**mixture of calcium carbide residue and fly ash.** *Materials and Design*, 51, 894-901. doi: 10.1016/j.matdes.2013.04.099

ASTM. (2006). ASTM C131. Standard Test Method for Resistance to Degradation of Small-Size Coarse Aggregate by Abrasion and Impact in the Los Angeles Machine. West Conshohocken, PA, USA: ASTM International.

ASTM. (2007a). ASTM D422-63. Standard Test Method for Particle-Size Analysis of Soils<sup>1</sup>. West Conshohocken, PA, USA: ASTM International.

ASTM. (2007b). ASTM D1633. Standard Test Methods for Compressive Strength of Molded Soil-Cement Cylinders. West Conshohocken, PA, USA: ASTM International.

ASTM. (2009). ASTM D3282. Standard Practice for Classification of Soils and Soil-Aggregate Mixtures for Highway Construction Purposes. West Conshohocken, PA, USA: ASTM International.

ASTM. (2010). ASTM D4318. Standard Test Methods for Liquid Limit, Plastic Limit, and Plasticity Index of Soils. West Conshohocken, PA, USA: ASTM International.

ASTM. (2012a). ASTM C535. Standard Test Method for Resistance to Degradation of Large-Size Coarse Aggregate by Abrasion and Impact in the Los Angeles Machine. West Conshohocken, PA, USA: ASTM International.

ASTM. (2012b). ASTM D1557. Standard Test Methods for Laboratory Compaction Characteristics of Soil Using Modified Effort (56,000 ft-lbf/ft<sup>3</sup> (2,700 kN-m/m<sup>3</sup>)): ASTM International.

Bagheri, A., and Nazari, A. (2014). **Compressive strength of high strength class C fly ash-based geopolymers with reactive granulated blast furnace slag**

- aggregates designed by Taguchi method.** *Materials and Design*, 54, 483-490. doi: 10.1016/j.matdes.2013.07.035
- Chen, J.-W., and Chang, C.-F. (2007). **High-Strength Ecological Soil Materials.** *Journal of Materials in Civil Engineering*, 19, 149-154.
- Cheng, T. W., and Chiu, J. P. (2003). **Fire-resistant geopolymer produced by granulated blast furnace slag.** *Minerals Engineering*, 16(3), 205-210. doi: 10.1016/s0892-6875(03)00008-6
- Chindaprasirt, P., Chareerat, T., Hatanaka, S., and Cao, T. (2011). **High-Strength Geopolymer Using Fine High-Calcium Fly Ash.** *Journal of Materials in Civil Engineering*, 23(3), 264-270. doi: 10.1061/(asce)mt.1943-5533.0000161
- Davidovits, J. (1991). **Geopolymer: inorganic polymeric new materials.** *Journal of Thermal Analysis*, 37, 1633-1656.
- Davidovits, J. (1994a). **Geopolymers: Man-Made Rock Geosynthesis And The Resulting Development Of Very Early High Strength Cement.** *Journal of Materials Education*, 16(2&3), 91-139.
- Davidovits, J. (1994b). **Global Warming Impact on the Cement and Aggregates Industries.** *World Resource Review*, 6(2), 263-278.
- Davidovits, J. (1994c). **Properties of Geopolymer Cements.** *Alkaline Cements and Concretes, KIEV Ukraine.*
- Davidovits, J. (2002). *Environmentally Driven Geopolymer Cement Applications.*  
Paper presented at the Geopolymer 2002 Conference, Melbourne, Australia.
- Davidovits, J. (2013). **Geopolymer Cement.** *Geopolymer Cement, a review.*
- De Vargas, A. S., Dal Molin, D. C. C., Masuero, Â. B., Vilela, A. C. F., Castro-Gomes, J., and de Gutierrez, R. M. (2014). **Strength development of alkali-**

**activated fly ash produced with combined NaOH and Ca(OH)<sub>2</sub> activators.**

*Cement and Concrete Composites*, 53, 341-349.

DOH. (1989). DH-S205/1989 Standard of soil aggregate subbase: Department of Highways.

DOH. (2000). DH-S204/2000 Standard of soil cement base: Department of Highways.

DRR. (2013). DRR244-2013 Standard of soil cement base: Department of Rural Roads.

Du, Y., Zhang, Y., and Liu, S. (2011). *Investigation of Strength and California Bearing Ratio Properties of Natural Soils Treated by Calcium Carbide Residue*. Paper presented at the Proceedings of Geo-Frontiers 2011: Advances in Geotechnical Engineering, March 13-16, Dallas, Texas, USA.

Duxson, P., Provis, J. L., Lukey, G. C., and van Deventer, J. S. J. (2007). **The role of inorganic polymer technology in the development of 'green concrete'**. *Cement and Concrete Research*, 37(12), 1590-1597.

Gambrell, R. P., He, J., and Zhang, G. (2010). **Synthesis, Characterization, and Mechanical Properties of Red Mud-Based Geopolymers**. *Transportation Research Record: Journal of the Transportation Research Board*, 2167(-1), 1-9. doi: 10.3141/2167-01

Horpibulsuk, S., Katkan, W., and Naramitkornburee, A. (2009). **Modified Ohio's Curves: A Rapid Estimation of Compaction Curves for Coarse- and Fine-Grained Soils**. *Geotechnical Testing Journal* 32(1), 101659.

Horpibulsuk, S., Munsrakest, V., Udomchai, A., Chinkulkijniwat, A., and Arulrajah, A. (2014). **Strength of sustainable non-bearing masonry units**

- manufactured from calcium carbide residue and fly ash.** *Construction and Building Materials*, 71, 210-215. doi: 10.1016/j.conbuildmat.2014.08.033
- Horpibulsuk, S., Phetchuay, C., and Chinkulkijniwat, A. (2012). **Soil Stabilization by Calcium Carbide Residue and Fly Ash.** *Journal of Materials in Civil Engineering*, 24(2), 184-193. doi: 10.1061/(asce)mt.1943-5533.0000370
- Horpibulsuk, S., Phetchuay, C., Chinkulkijniwat, A., and Cholaphatsorn, A. (2013). **Strength development in silty clay stabilized with calcium carbide residue and fly ash.** *Soils and Foundations*, 53(4), 477-486.
- Horpibulsuk, S., Suksiripattanapong, C., Samingthong, W., Rachan, R., and Arulrajah, A. (2015). **Durability against Wetting–Drying Cycles of Water Treatment Sludge–Fly Ash Geopolymer and Water Treatment Sludge–Cement and Silty Clay–Cement Systems.** *Journal of Materials in Civil Engineering*, 04015078. doi: 10.1061/(asce)mt.1943-5533.0001351
- Kampala, A., and Horpibulsuk, S. (2013). **Engineering Properties of Silty Clay Stabilized with Calcium Carbide Residue.** *Journal of Materials in Civil Engineering*, 25(5), 632-644. doi: 10.1061/(asce)mt.1943-5533.0000618
- Kampala, A., Horpibulsuk, S., Chinkullijniwat, A., and Shen, S.-L. (2013). **Engineering properties of recycled Calcium Carbide Residue stabilized clay as fill and pavement materials.** *Construction and Building Materials*, 46, 203-210. doi: 10.1016/j.conbuildmat.2013.04.037
- Kampala, A., Horpibulsuk, S., Prongmanee, N., and Chinkulkijniwat, A. (2014). **Influence of Wet-Dry Cycles on Compressive Strength of Calcium Carbide Residue–Fly Ash Stabilized Clay.** *Journal of Materials in Civil Engineering*, 26(4), 633-643. doi: 10.1061/(asce)mt.1943-5533.0000853

- Komljenovic, M., Bascarevic, Z., and Bradic, V. (2010). **Mechanical and microstructural properties of alkali-activated fly ash geopolymers.** *Journal of Hazardous materials*, 181(1-3), 35-42. doi: 10.1016/j.jhazmat.2010.04.064
- Lee, W. K. W., and Van Deventer, J. S. J. (2002). **The effect of ionic contaminants on the early-age properties of alkali-activated fly ash-based cements.** *Cement and Concrete Research*, 32, 577–584.
- Lo, T. Y., Tang, W. C., and Nadeem, A. (2008). **Comparison of carbonation of lightweight concrete with normal weight concrete at similar strength levels.** *Construction and Building Materials*, 22(8), 1648-1655. doi: 10.1016/j.conbuildmat.2007.06.006
- Lyon, R. E., Balaguru, P. N., Foden, A., Sorathia, U., Davidovits, J., and Davidovics, M. (1997). **Fire Resistant Aluminosilicate Composites.** *Fire and Materials* 21, 67-73.
- Makaratat, N., Jaturapitakkul, C., and Laosamathikul, T. (2010). **Effects of Calcium Carbide Residue–Fly Ash Binder on Mechanical Properties of Concrete.** *Journal of Materials in Civil Engineering*, 22, 1164-1170. doi: 10.1061//ASCE/MT.1943-5533.0000127
- Nugteren, H. W., Butselaar-Orthlieb, V. C. L., Izquierdo, M., Witkamp, G.-J., and Kreutzer, M. T. (2009). *High Strength Geopolymers from Fractionated and Pulverized Fly Ash.* Paper presented at the 2009 World of Coal Ash (WOCA) Conference, Lexington, KY, USA.

- Palomo, A., Blanco-Varela, M. T., Granizo, M. L., Puertas, F., Vazquez, T., and Grutzeck, M. W. (1999). **Chemical stability of cementitious materials based on metakaolin.** *Cement and Concrete Research*, 27(7), 997-100.
- Phetchuay, C., Horpibulsuk, S., Suksiripattanapong, C., Chinkulkijniwat, A., Arulrajah, A., and Disfani, M. M. (2014). **Calcium carbide residue: Alkaline activator for clay-fly ash geopolymer.** *Construction and Building Materials*, 69, 285-294. doi: 10.1016/j.conbuildmat.2014.07.018
- Phoo-ngernkham, T., Chindaprasirt, P., Sata, V., Pangdaeng, S., and Sinsiri, T. (2013). **Properties of high calcium fly ash geopolymer pastes with Portland cement as an additive.** *International Journal of Minerals, Metallurgy, and Materials*, 20(2), 214-220. doi: 10.1007/s12613-013-0715-6
- Rattanashotinunt, C., Thairit, P., Tangchirapat, W., and Jaturapitakkul, C. (2013). **Use of calcium carbide residue and bagasse ash mixtures as a new cementitious material in concrete.** *Materials and Design*, 46, 106-111. doi: 10.1016/j.matdes.2012.10.028
- Sakkas, K., Panyas, D., Nomikos, P. P., and Sofianos, A. I. (2014). **Potassium based geopolymer for passive fire protection of concrete tunnels linings.** *Tunnelling and Underground Space Technology*, 43, 148-156. doi: 10.1016/j.tust.2014.05.003
- Sarker, P. K., Kelly, S., and Yao, Z. (2014). **Effect of fire exposure on cracking, spalling and residual strength of fly ash geopolymer concrete.** *Materials and Design*, 63, 584-592. doi: 10.1016/j.matdes.2014.06.059

- Somna, K., Jaturapitakkul, C., and Kajitvichyanukul, P. (2011). **Microstructure of Calcium Carbide Residue–Ground Fly Ash Paste**. *Journal of Materials in Civil Engineering*, 23, 298-304. doi: 10.1061/
- Sukmak, P., De Silva, P., Horpibulsuk, S., and Chindaprasirt, P. (2014). **Sulfate Resistance of Clay-Portland Cement and Clay High-Calcium Fly Ash Geopolymer**. *Journal of Materials in Civil Engineering*, 04014158. doi: 10.1061/(asce)mt.1943-5533.0001112
- Sukmak, P., Horpibulsuk, S., and Shen, S.-L. (2013). **Strength development in clay–fly ash geopolymer**. *Construction and Building Materials*, 40, 566-574. doi: 10.1016/j.conbuildmat.2012.11.015
- Sukmak, P., Horpibulsuk, S., Shen, S.-L., Chindaprasirt, P., and Suksiripattanapong, C. (2013). **Factors influencing strength development in clay–fly ash geopolymer**. *Construction and Building Materials*, 47, 1125-1136. doi: 10.1016/j.conbuildmat.2013.05.104
- Suksiripattanapong, C., Horpibulsuk, S., Chanprasert, P., Sukmak, P., and Arulrajah, A. (2015). **Compressive strength development in fly ash geopolymer masonry units manufactured from water treatment sludge**. *Construction and Building Materials*, 82, 20-30. doi: 10.1016/j.conbuildmat.2015.02.040
- Vichan, S., and Rachan, R. (2013). **Chemical stabilization of soft Bangkok clay using the blend of calcium carbide residue and biomass ash**. *Soils and Foundations*, 53(2), 272-281. doi: 10.1016/j.sandf.2013.02.007
- Yip, C. K., and Van Deventer, S. (2003). **Microanalysis of calcium silicate hydrate gel formed within a geopolymeric binder**. *Journal of materials science*, 38, 3851–3860.

Zhang, M., Guo, H., El-Korchi, T., Zhang, G., and Tao, M. (2013). **Experimental feasibility study of geopolymer as the next-generation soil stabilizer.** *Construction and Building Materials*, 47, 1468-1478.



# **CHAPTER V**

## **STRENGTH AND MICROSTRUCTURE ANALYSIS OF LATERITIC SOIL STABILIZED WITH FLY ASH AND GROUND GRANULATED BLAST FURNACE SLAG PRECUSORS**

### **5.1 Statement of problem**

Ordinary Portland Cement (OPC) is the most widely used cementing agent in civil construction and infrastructure projects. The production of OPC, however, is an energy-intensive process and emits a large amount of greenhouse gases, notably CO<sub>2</sub> into the atmosphere. Cement production worldwide discharges up to 4.0 billion tons of CO<sub>2</sub> annually (Davidovits, 1994; Part et al., 2015; Yusuf et al., 2014). The production of just 1 ton of OPC releases about 1 ton of carbon dioxide (Davidovits, 2013).

Pollution and global warming coupled with growing public environmental awareness has been increasing rapidly in many countries. Alternative and environmental friendly materials are therefore increasingly sought (Part et al., 2015). Geopolymer, a novel green cementing agent manufactured from various industrial waste by-products, is considered as an alternative materials to OPC. Geopolymer is an inorganic aluminosilicate material synthesized by mixing source materials rich in silica (SiO<sub>2</sub>) and alumina (Al<sub>2</sub>O<sub>3</sub>) such as Fly Ash (FA), metakaolin, Granulated Blast

Furnace Slag (GBFS) and Silica Fume (SF), with alkali activators (De Silva et al., 2007). It is formed through poly-condensation of tetrahedral silica ( $\text{SiO}_4$ ) and alumina ( $\text{AlO}_4$ ), which are linked by the sharing of oxygen atoms (Davidovits, 1991; Gambrell et al., 2010). The chemical structure of geopolymer can be expressed as  $M_n -(\text{Si-O}_2)_z[-\text{Al-O}]_n \cdot w\text{H}_2\text{O}$  where M is the alkaline element, - indicates the presence of a bond, z is 1, 2, or 3, and n is the degree of polymerization (Davidovits, 1991).

The engineering properties of geopolymers that are sought for civil applications include: high compressive strength (Amnadhua et al., 2013; Bagheri and Nazari, 2014; Duxson et al., 2007), rapid controllable setting and hardening (Lee and Van Deventer, 2002), fire resistance (Cheng and Chiu, 2003; Sakkas et al., 2014; Sarker et al., 2014), different acids and salt solution resistance (Palomo et al., 1999), lack of deleterious alkali–aggregate reactions and low shrinkage (Zhang et al., 2013).

The commonly used activators for geopolymerization include alkaline metal and alkaline earth metal compounds (Komnitsas and Zaharaki, 2007). Generally, the most effective activator providing the best performance for high strength and other advantageous properties is a mixture combining sodium hydroxide (NaOH) and sodium silicate ( $\text{Na}_2\text{SiO}_3$ ) (Rashad, 2013).

The precursor extensively used for geopolymer system is Fly Ash (FA). However, several researchers reported that the FA geopolymer exhibits low to moderate strength gain at ambient temperature (Palomo et al., 2007; Temuujin et al., 2009). Mechanical properties and microstructure of FA geopolymer at ambient temperature could be improved when incorporated with calcium-rich GBFS (Kumar et al., 2010; Puertas et al., 2000). The FA-GBFS geopolymer system will form

aluminum-modified calcium silicate hydrate (CASH) gel coexisting with sodium aluminosilicate hydrate (NASH) gel (geopolymer gel) (Bernal et al., 2013; Ismail et al., 2014). The coexistence of CASH and NASH was also evident for other FA and calcium-rich additive based geopolymers (Guo et al., 2010; Somna et al., 2011).

A number of researchers have used geopolymer in concrete applications. However, a few researchers have studied geopolymer improved problematic soil (Arulrajah et al., 2015; Horpibulsuk et al., 2013; Mohammadinia et al., 2016; Phetchuay et al., 2014; Phummiphan et al., 2016; Sukmak et al., 2013; Suksiripattanapong et al., 2015). GBFS is commonly used as an additive in FA geopolymer concrete, yet its usage as an additive in FA based geopolymer stabilized soil is very limited. In this study, GBFS is used as an additive in alkaline activator to enhance the strength of FA geopolymer stabilized lateritic soil to develop a sustainable pavement base material. Unconfined Compression Strength (UCS) is used as an indicator to investigate strength development. The microstructural development is also investigated via Scanning Electron Microscope (SEM) and X-ray Diffraction (XRD) analyses to understand the role of influential factors, controlling the strength development. The influential factors include GBFS content,  $\text{Na}_2\text{SiO}_3:\text{NaOH}$  (NS:NH) ratio, and curing time at room temperature. The outcome of this study will enable GBFS, an industrial by-product, to be used as an additive in FA geopolymer pavement applications.

## **5.2 Materials and methods**

### **5.2.1 Soil sample**

Lateritic Soil (LS) samples were obtained from a borrow pit in Rayong province, Eastern Thailand. The specific gravity is 2.58. Liquid Limit (LL), Plastic Limit (PL), and Plastic Index (PI) undertaken according to ASTM D4318 (ASTM, 2010) are 27.72%, 21.65%, and 6.07%, respectively. The grain size distribution determined by a sieve analysis test (ASTM, 2007a) is shown in **Figure 5.1** and is compared to that specified for base/subbase materials of AASHTO and Department of Highways (DH), Thailand (AASHTO, 2012; DOH, 1989). It is noted that the gradation of LS is within the boundary. This soil is classified as silty clayey sand (SC-SM) according to the Unified Soil Classification System (USCS) (ASTM, 2011) and as A-2-4(0) according to the AASHTO (ASTM, 2009). The compaction characteristics under modified Proctor energy (ASTM, 2012b) are optimum moisture content (OMC) of 8.0%, and maximum dry unit weight ( $\gamma_{d,max}$ ) of 20.85 kN/m<sup>3</sup>. California Bearing Ratio (CBR) value is 14.7% at 95% of  $\gamma_{d,max}$ . Los Angeles (LA) abrasion followed by ASTM C131 (ASTM, 2006) and C535 (ASTM, 2012a) is 52.9%. When comparing the CBR and LA abrasion results to the specification of DH for subbase and engineering fill materials (DOH, 1989) (**Table 5.1**), LS does not meet the subbase requirement but however meets the requirements of an engineering fill material. In remote construction sites, located far away from high quality quarry materials, chemical stabilized LS can be used as base and subbase materials. The usage of chemically stabilized LS in such a sustainable manner will lead to savings on haulage costs and will furthermore minimize negative environmental impacts. Chemical composition of LS obtained from X-ray Fluorescence (XRF) analysis is shown in **Table 5.2**. SEM image (**Figure 5.2a**) shows that LS is irregular shape.

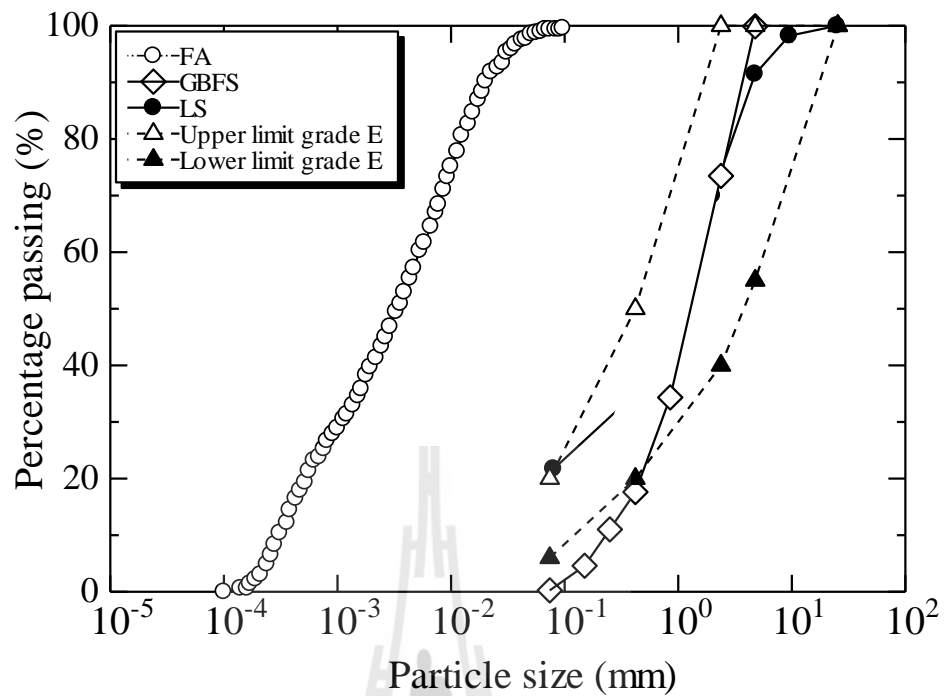


**Figure 5.1.** Particle size distributions of FA, LS and GBFS.

**Table 5.1.** The engineering property comparisons of the soil sample and subbase specifications.

Engineering properties	Soil sample	Subbase	Engineering fill material
Liquid limit (LL) (%)	27.72	< 35	< 40
Plastic index (PI)	6.07	< 11	< 20
California Baring Ratio (CBR) at 95% of $\gamma_{d,max}$ (%)	14.70	> 25	> 10
Los Angles abrasion (percent of wear) (%)	52.90	< 60	< 60

### 5.2.2 Fly ash

Fly Ash (FA) used in this study was obtained from Mae Moh power plant in Northern Thailand, which is the largest lignite power plant in Thailand. The chemical composition obtained from XRF of FA is shown in **Table 5.2**. The main components of FA are 36.00% SiO<sub>2</sub>, 26.73% CaO, 17.64% Fe<sub>2</sub>O<sub>3</sub>, and 16.80% Al<sub>2</sub>O<sub>3</sub>. FA is therefore classified as high calcium class C. Particle size distribution and microstructure of FA are shown in **Figure 5.1** and **Figure 5.2b**, respectively. The FA particles are normally fine and spherical in shape. The XRD pattern of FA shows that FA consists mainly of glassy phase materials with some crystalline additions of anhydrite, quartz, calcite and maghemite (**Figure 5.3**).

**Table 5.2** The chemical compositions of LS, FA, and GBFS.

Chemical composition (%)	LS	FA	GBFS
SiO <sub>2</sub>	77.81	36.00	26.78
Al <sub>2</sub> O <sub>3</sub>	4.42	16.80	6.96
Fe <sub>2</sub> O <sub>3</sub>	10.93	17.64	18.65
CaO	1.13	26.73	30.38
MgO	N.D.	N.D.	9.70
SO <sub>3</sub>	1.36	N.D.	1.74
K <sub>2</sub> O	2.33	1.83	N.D.
TiO <sub>2</sub>	1.33	0.48	0.89
MnO <sub>2</sub>	0.55	0.15	3.56
Br <sub>2</sub> O	0.38	N.D.	N.D.
Cr <sub>2</sub> O <sub>3</sub>	N.D.	N.D.	0.85
ZnO	N.D.	N.D.	0.48

N.D. = not detected

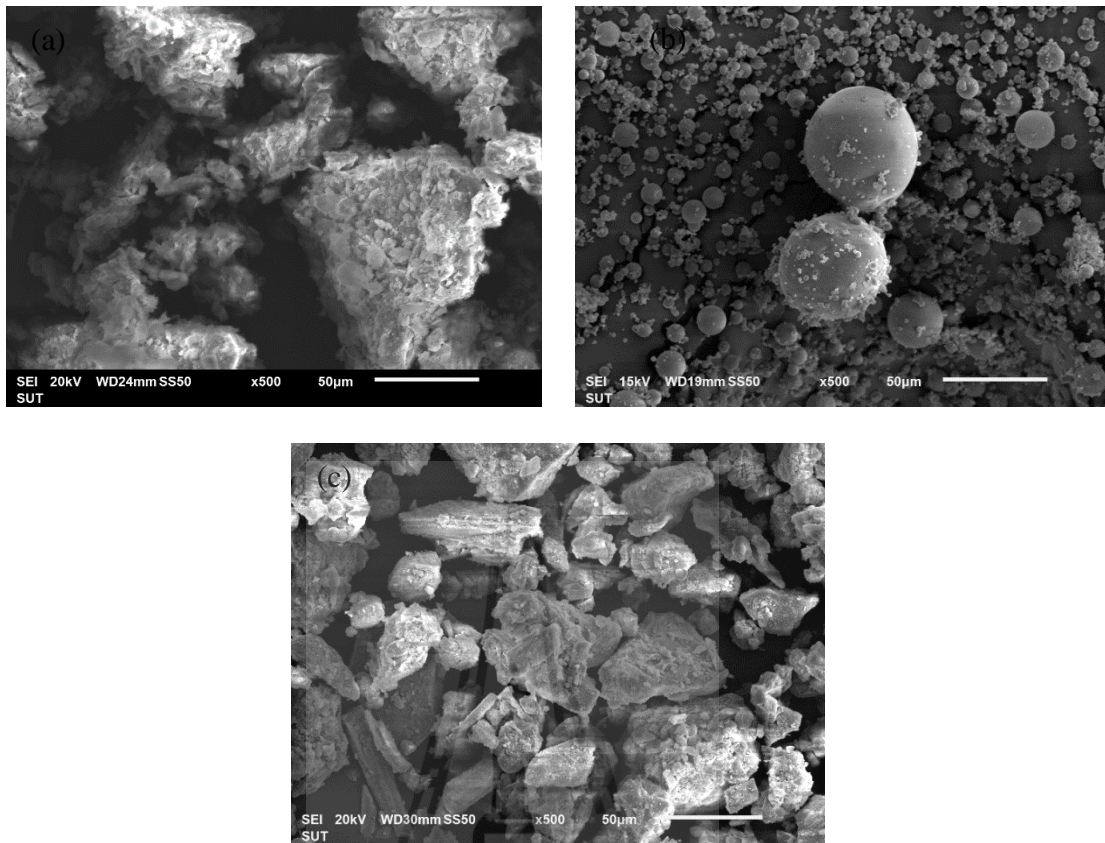


**Figure 5.2** SEM images of: (a) LS, (b) FA and (c) GBFS.

### 5.2.3 Ground granulated blast furnace slag

Ground Granulated Blast Furnace Slag (GBFS) samples were obtained from Siam Steel Mill Services Co., Ltd., Chonburi Thailand. The GBFS was fine aggregates, passing through a 2.00-mm (No.10) sieve, and air-dried at room temperature. GBFS is non-plastic with its specific gravity of 3.54. The main chemical compositions are 30.38% CaO, 26.78% SiO<sub>2</sub>, 18.65% Fe<sub>2</sub>O<sub>3</sub>, 9.70% MgO and 6.96% Al<sub>2</sub>O<sub>3</sub> as shown in **Table 5.2**. The particle size distribution is also shown in **Figure 5.1**. The SEM image (**Figure 5.2c**) indicates that the particles are generally irregular

in shape. The XRD pattern shows that GBFS contains phases of calcite, calcium silicate, gehlenite and calcium aluminium oxide (**Figure 5.3**).

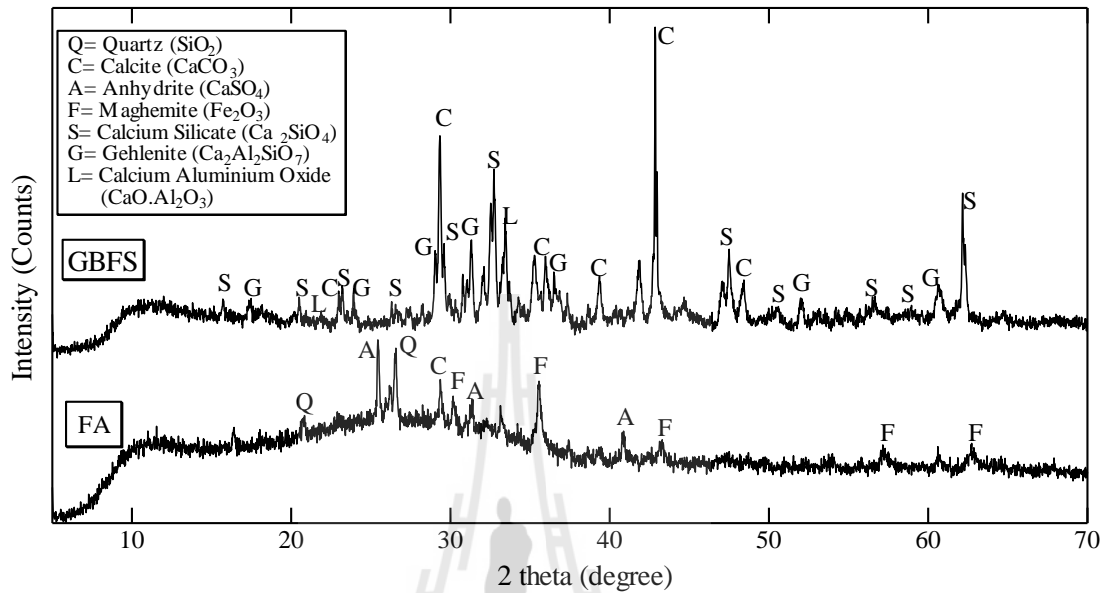


**Figure 5.3** XRD pattern of GBFS and FA.

#### 5.2.4 Liquid alkali activator

The liquid alkaline activator (L) used was a mixture of sodium silicate ( $\text{Na}_2\text{SiO}_3$ , NS) solution and sodium hydroxide ( $\text{NaOH}$ , NH) solution with a concentration of 5 molar. NS solution was composed of 15.50%  $\text{Na}_2\text{O}$ , 32.75%  $\text{SiO}_2$ , and 51.75%  $\text{H}_2\text{O}$  by weight. Distilled water was used throughout the experiments for producing the NH solution.

#### 5.2.5 Methods

In this study, the FA content was fixed at 30% of the total mix while the GBFS contents were varied to replace LS. The LS:FA:GBFS ratios investigated were 60:30:10, 50:30:20, and 40:30:30. The NS:NH ratios were 100:0, 90:10, 80:20, 50:50 and 40:60. The LS, FA and GBFS were firstly mixed together to ensure

homogeneity and then mixed with L for an additional 5 minutes. The mixtures were next compacted under modified Proctor energy according to ASTM (ASTM, 2012b). The compacted samples were demolded and immediately wrapped with plastic sheet and cured at room temperature between 27 to 30°C.

The UCS of soaked geopolymer samples was measured after curing periods of 7, 28, and 60 days. The samples were submerged under water for 2 hours and then air-dried for 1 h prior to UCS testing according to ASTM (ASTM, 2007b), the specification of DH (DOH, 2000) and Department of Rural Roads (DRR) (DRR, 2013), Thailand. The results were reported using mean compressive strength values of at least three specimens to check for consistency.

The growth of the geopolymer products was demonstrated using SEM and XRD analysis. The small fragments from the center of samples were frozen at -195°C by immersion in liquid nitrogen for 5 min and coated with gold before SEM (JEOL JSM-6400 device) analysis (Sukmak et al., 2013). The samples were also grounded to fine powder for XRD tests to obtain microstructural information of amorphous and crystalline phases. The XRD scans were performed at 0 – 90° 2 theta by Bruker D8 ADVANCE device.

## 5.3 Results

### 5.3.1 Compaction characteristics

**Figure 5.4** illustrates the relationships between  $\gamma_d$  and L content of the FA-GBFS geopolymer stabilized LS for various GBFS contents and NS:NH ratios. It is evident that the compaction curves of FA-GBFS geopolymer stabilized LS are dependent on the GBFS content and NS:NH ratio. For a particular NS:NH ratio and

GBFS content, the  $\gamma_d$  of the FA-GBFS geopolymer stabilized LS increases with increasing LA content until the  $\gamma_{d,max}$  reaches an Optimum Liquid Content (OLC). Beyond the OLC,  $\gamma_d$  decreases as the L content increases. This characteristic is typical of compaction behavior of coarse-grained materials. For all NS:NH ratios,  $\gamma_{d,max}$  increases with increasing the GBFS content due to high specific gravity of GBFS. For 20% and 30% GBFS,  $\gamma_{d,max}$  tends to increase with decreasing the NS content while the  $\gamma_{d,max}$  of 10% GBFS geopolymer stabilized LS shows an opposite trend. However, the change in  $\gamma_{d,max}$  for all GBFS contents are insignificant when compared to the change in OLC. The OLC significantly decreases with decreasing NS (increasing NH) because NH has lower viscosity than NS. In other words, NH lubricates the soil particles and hence improves the compactibility. The relationships between OLC and NS contents for various GBFS contents can be represented by linear functions as shown in **Figure 5.5**.

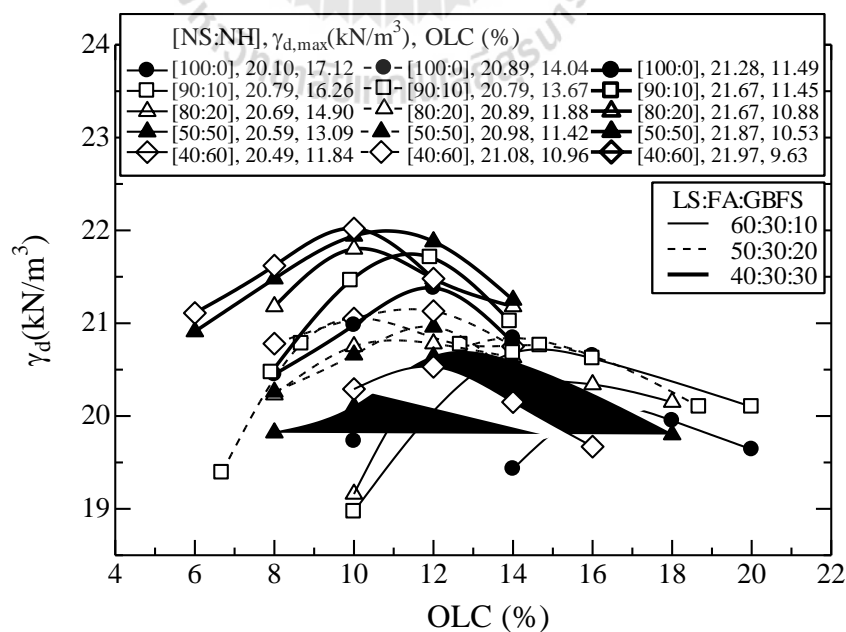


**Figure 5.4.** Compaction curves of the LS – FA – GBFS geopolymer.

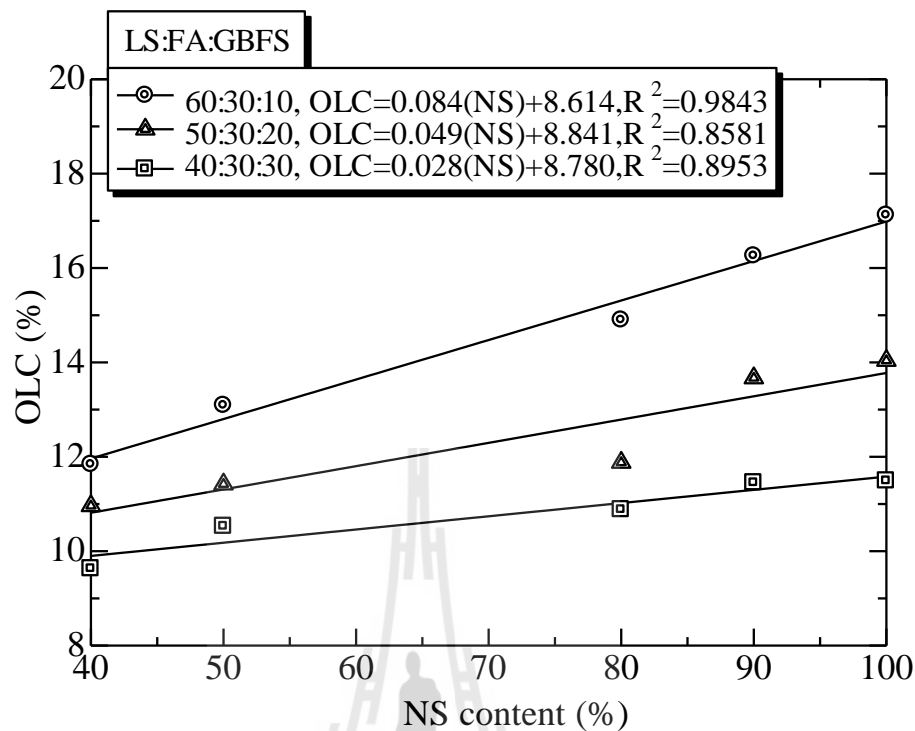


**Figure 5.5.** OLC versus NS relationships for various GBFS replacement ratios.

### 5.3.2 Unconfined compressive Strength

The relationships between UCS and GBFS content of the FA-GBFS geopolymer stabilized LS at different curing times and NS:NH ratios are shown in **Figure 5.6**. The 7-day UCS of all stabilized materials, with and without GBFS compacted at OLC, are greater than the required UCS specified by the national road authority in Thailand (> 1.724 MPa for light traffic and > 2.413 MPa for heavy traffic) (DOH, 2000; DRR, 2013) As shown in **Figures 5.6a – 5.6d**, the 7-day UCS development with GBFS content is dependent upon NS:NH ratio. For NS:NH ratios of 100:0, 90:10 and 80:20, the 7-day UCS values increase with increasing GBFS content until the maximum values at optimal GBFS content and then decrease. The

same is however not observed for NS:NH = 50:50; i.e., GBFS content does not affect the UCS development. The optimal GBFS contents decrease with decreasing NS:NH. The highest 7-day UCS is found at 20% GBFS (optimal) and NS:NH = 100:0, which is equal to 10.46 MPa.

For the long-term curing (28 to 60 days), two strength characteristics are noted for high NS:NH ratios (NS:NH = 100:0, 90:10 and 80:20) and low NS:NH ratio (NS:NH = 50:50). Referring to **Figures 5.6a – 5.6c** for the high NS:NH ratios, the 10% GBFS is regarded as optimal. The 60-day UCS values at 10% GBFS are 18.02 MPa, 20.21 MPa and 18.74 MPa for NS:NH = 100:0, 90:10 and 80:20, respectively. In other words, the highest long-term UCS is found at 10% and NS:NH = 90:10. For the low NS:NH of 50:50 (**Figure 5.6d**), GBFS does not affect the UCS development. Even though the 7-day UCS for 0% GBFS is lowest compared to that at the high NS:NH ratios, the 28-day and 60-day UCS values for 0% GBFS are the highest. In other words, without GBFS, NS:NH = 50:50 provides the highest long-term UCS.

It is of interest to mention that the effect of GBFS is noticed for the high NS:NH ratios; i.e., the optimal GBFS content can improve UCS of FA geopolymer stabilized LS both at early and long-term curings. The highest 7-day UCS is found at NS:NH = 100:0 and 20% GBFS while the highest 28-day and 60-day UCS values are found at NS:NH = 90:10 and 10% GBFS. However, the 7-day UCS at NS:NH = 90:10 and 10% GBFS is just slightly lower than that at NS:NH = 100:0 and 20% GBFS. As such, NS:NH = 90:10 and 10% GBFS are recommended in practice. The very high 30% GBFS must be avoided as it retards the UCS development

especially high NS:NH; i.e. the UCS development is insignificant after 28 days of curing.

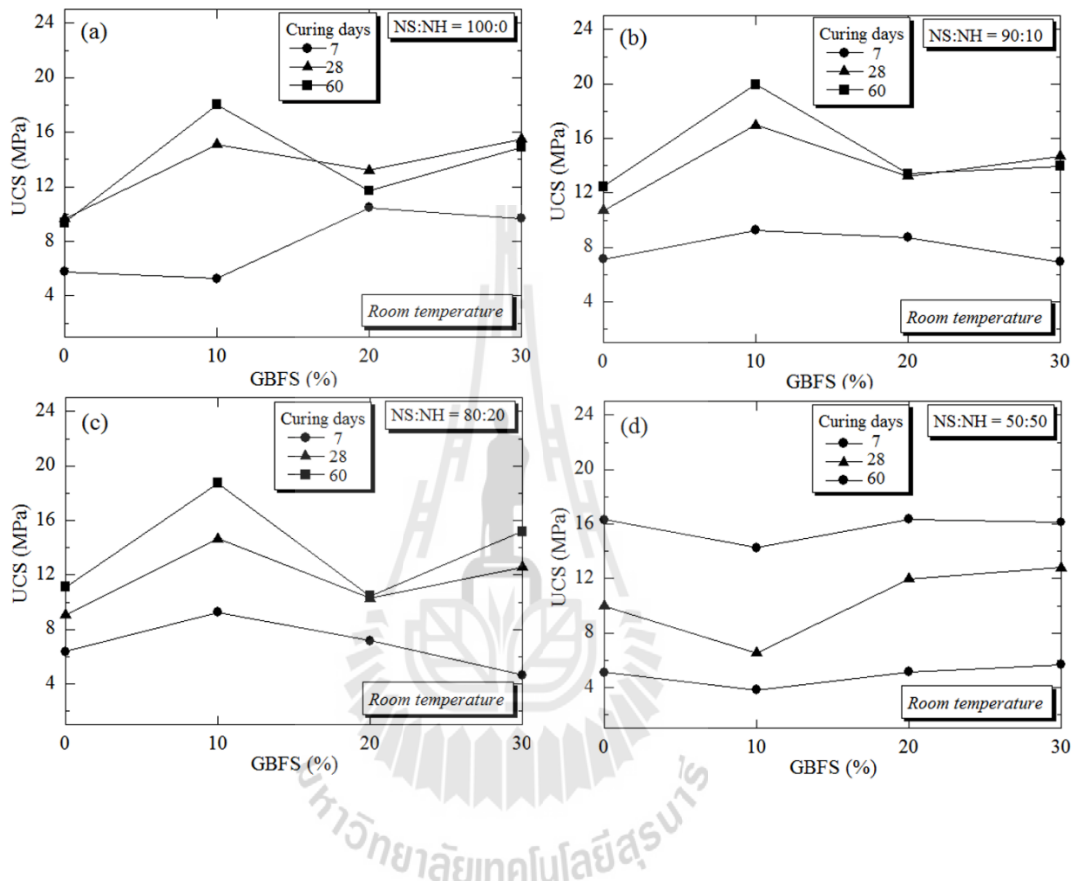


**Figure 5.6.** The UCS of FA-GBFS geopolymer stabilized LS at various GBFS replacement ratios, cured at 7 to 60 days for different NS:NH ratios (a) 100:0, (b) 90:10, (c) 80:20 and (d) 50:50.

## 5.4 SEM analysis

Investigation of microstructural development of FA-GBFS geopolymer stabilized LS via SEM analysis is advantageous for observing the chemical reaction and the growth of cementation matrix over the curing period. The 10% GBFS and

90:10 NS:NH are recommended in practice, which provide relatively high early 7-day UCS and the highest 28-day and 60-day UCS (**Figure 5.6**). The microstructural development with time (7, 28 and 60 days) of this sample is thus examined in **Figure 5.7**. For early curing time of 7 days, the chemical reaction occurs on the FA surface (**Figure 5.7a**). The etched holes and cementitious products on FA particles, which indicate the chemical reaction between L and FA, are observed after 28 days of curing (**Figure 5.7b**). More etched holes and cementitious products on the shell of FA particles after 60 days of curing are clearly detected (**Figure 5.7c**). This indicates the leaching of silica and alumina oxides from FA by alkaline dissolution with time. Hence, the UCS still develops even after 60 days of curing.

**Figure 5.8** shows SEM images of the FA-GBFS geopolymer stabilized LS at high 30% GBFS for both high and low NS:NH ratios of 90:10 and 50:50 and cured for 7, 14, 28 and 60 days to examine the negative impact of very high GBFS. For high NS:NH ratio of 90:10, the microstructures insignificantly change with increasing curing time (**Figures 5.8c, 5.8e and 5.8g**), which is different from those at 10% GBFS (**Figure 5.7**). This is probably because NH concentration is insufficient in the reaction system and hence the UCSs are essential the same after 28 days of curing. On the contrary, the microstructural change with time is noted for low NS:NH ratios of 50:50 (**Figure 5.8d, 5.8f and 5.8h**) due to the time-dependent leaching of silica and alumina from FA and GBFS for geopolymerization reaction. As a result, the UCS of low NS:NH increases continuously with curing time for all GBFS ratios.

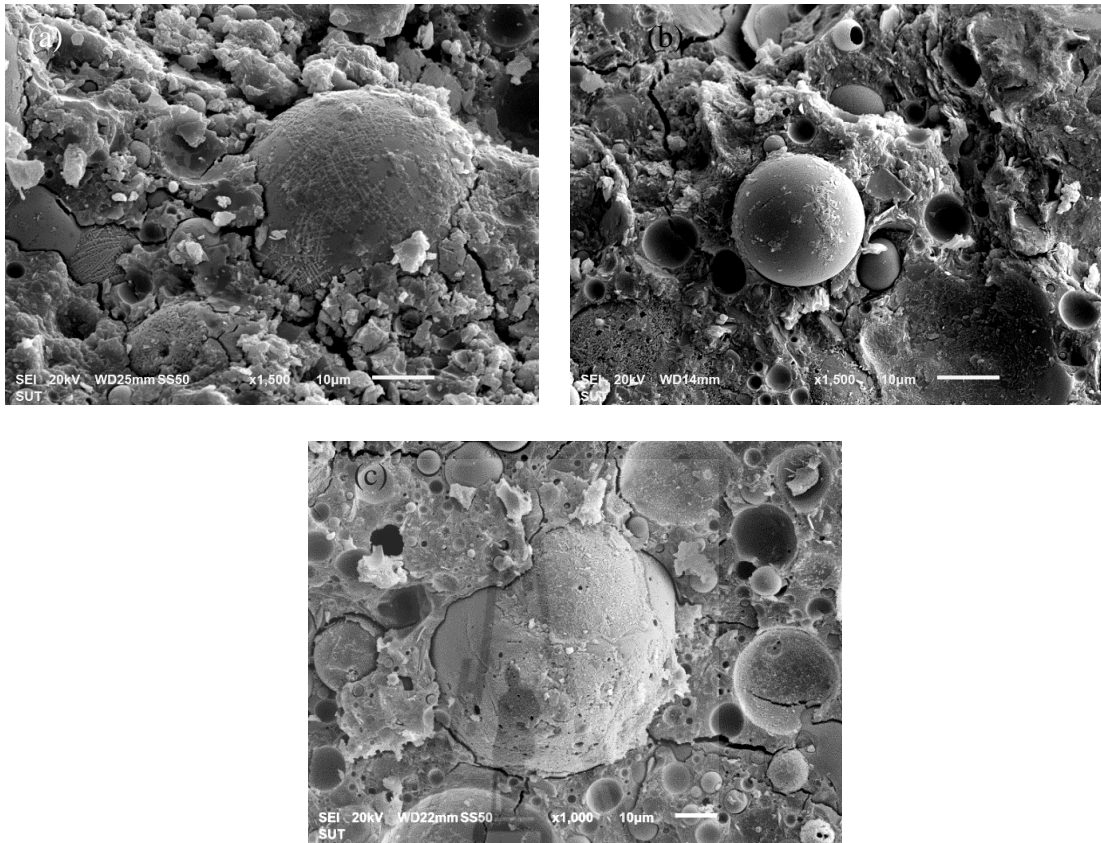


**Figure 5.7.** SEM images of stabilized geopolymer samples with NS:NH ratios of 90:10 and 10% GBFS after 7, 28 and 60 days of curing.

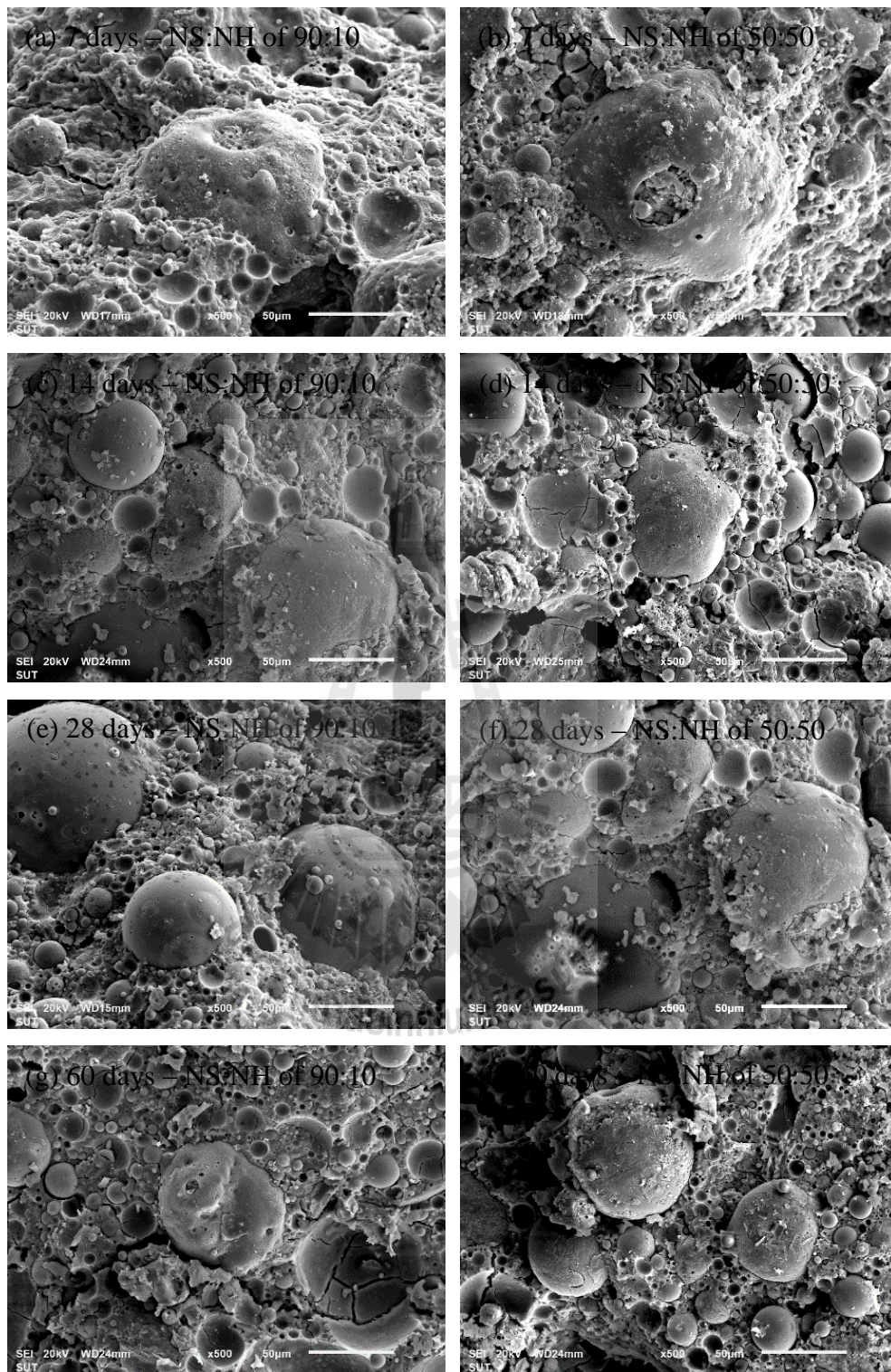


**Figure 5.8.** SEM images of 30% GBFS content samples at NS:NH ratio of 90:10 and 50:50.

## 5.5 XRD analysis

The XRD patterns of FA-GBFS geopolymer stabilized LS at 20% GBFS and at high and low NS:NH ratios of 90:10 and 50:50 are presented in **Figure 5.9** for 7 and 60 days of curing. The main phases consist of Quartz, Muscovite, Microcline and Albite. The Quartz phases were from the LS and the non-reacted elements from FA and GBFS. The presence of sodium alumino-silicate in the form of Albite and the potassium alumino-silicate in form of Muscovite and Microcline indicates the geopolymer products. Moreover, Ca and Fe elements, which are the main chemical composition of FA and GBFS (CaO from FA = 26.73% and from GBFS = 30.38%, Fe<sub>2</sub>O<sub>3</sub> from FA = 17.64% and from GBFS = 18.65%), are detected by XRD. For the sample with high NS:NH ratio of 90:10 at early stage (7 days – line A), the main phases are Calcium Silicate Hydrate (CSH), Anorthite, Goethite and Calcite while at a longer time (60 days) the main phases are Anorthite, Goethite, Calcite with little CSH. This shows the variation of cementitious products with curing times. The CSH phases in the 7 days cured sample are considerably higher than those in 60 days cured sample. This confirms that the significant CSH products happen in the early stage of the geopolymer system mainly due to the chemical reaction between high calcium FA and GBFS and NS.

On the other hand, for the sample with low NS:NH ratio of 50:50, the main phases are geopolymer products in the form of Anorthite, Goethite and Calcite with no appearance of CSH in early 7 days (see line C in **Figure 5.9**) whereas the 60-day phases are Anorthite, CSH, Goethite and Calcite. It is noted that CSH phases are detected in 60 days of curing but not in 7 days of curing while Anorthite, Goethite and Calcite in 60 days of curing are slightly more than those in 7 days of curing. This

implies that the CSH products in geopolymeric system are time-dependent for high calcium FA-S geopolymer with low NS:NH ratio.

To conclude, the chemical products for the stabilized samples at each curing time depend on the NS:NH ratio. The high CaO (from FA and GBFS) in the system is the contributor to develop the CSH in the early stage for high NS:NH ratio. Hence, the UCS of sample results from the coexistence of CSH, calcite and geopolymer gel. However, the excessive CaO will react with CO<sub>2</sub> and form Calcite (Phoo-ngernkham et al., 2015; Ravikumar et al., 2010) for both high and low NS:NH ratios; i.e., 30% GBFS and provides a negative effect on the UCS development.

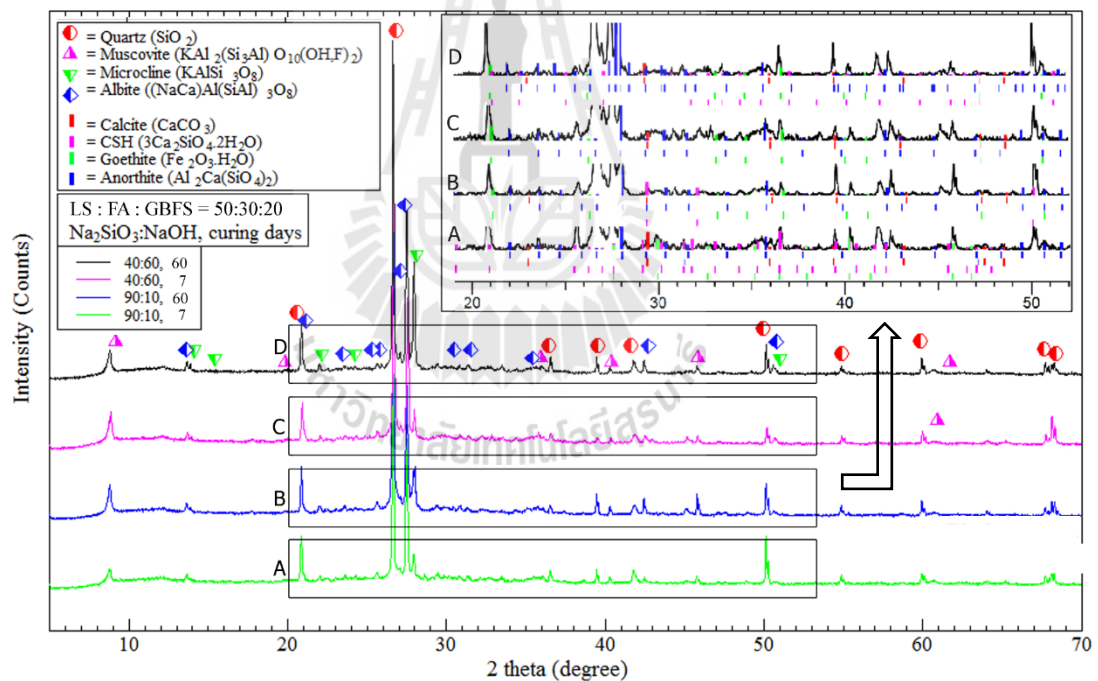


**Figure 5.9.** XRD of 20% GBFS content samples at NS:NH ratio of 90:10 and 40:60 for different curing times at room temperature.

## 5.6 Conclusions

This paper studies the effect of GBFS, NS:NH ratio and curing time on UCS and microstructural development of high calcium FA based geopolymer stabilized lateritic soil (LS). The 7-day UCS of the FA-S geopolymer stabilized LS at different NS:NH ratios and GBFS contents is comparable to the local national specifications for cement stabilized pavement material. It is illustrated that the FA-GBFS geopolymer can be used as a green stabilizer for LS improvement alternative to traditional OPC for developing a sustainable pavement base material. The conclusions arising from this research are drawn as follows.

(1) The soaked 7-day UCS of all FA-S geopolymer stabilized LS at various NS:NH ratios tested meets the strength requirement for both low and high volume roads specified by Department of Highways and Department of Rural Roads, Thailand.

(2) GBFS improves early 7-day UCS of FA geopolymer stabilized LS for the high NS:NH ratios tested (especially at  $NS:NH \geq 80:20$ ). The optimal GBFS content providing the highest 7-day UCS tends to decrease with decreasing NS:NH ratio. The GBFS insignificantly improves early and long-term UCS of FA geopolymer stabilized LS at low  $NS:NH = 50:50$ . The highest long term 28-day and 60-day UCS is found at 10% GBFS and 90:10 NS:NH, which are the recommended ingredient in practice.

(3) For high NS:NH ratios ( $> 80:20$ ), the SEM and XRD results show that the cementitious products increase with increasing curing time at optimal GBFS; i.e.,  $NS:NH = 90:10$  and  $GBFS = 10\%$ . The same is not observed at excessive GBFS of 30%; i.e., the cementitious products are essentially the same even with the increase in curing time; hence, insignificant UCS development with time.

(4) The coexistence of CSH and NASH for various NS:NH ratios is explained by XRD results. The significant CSH is detected at early stage of curing for high NS:NH while the significant CSH is detected at long curing time for low NS:NH. This confirms that the input of GBFS is useful when NS:NH is high. The excessive CaO will react with CO<sub>2</sub> and form Calcite for both high and low NS:NH ratios; i.e., 30% GBFS and provides a negative effect on the UCS development.

(5) The outcome of this research will enable GBFS to be used as an additive with FA geopolymer to stabilize LS in the development of a low carbon stabilized pavement base. 10% content of GBFS is recommended at high NS:NH ratios (> 80:20).

## 5.7 References

- AASHTO. (2012). "Standard specification for materials for aggregate and soil-aggregate subbase, base, and surface courses." AASHTO M147-65, American Association of State Highway and Transportation Officials.
- Amnadnua, K., Tangchirapat, W., and Jaturapitakkul, C. (2013). **Strength, water permeability, and heat evolution of high strength concrete made from the mixture of calcium carbide residue and fly ash.** *Materials and Design*, 51, 894-901. doi: 10.1016/j.matdes.2013.04.099
- Arulrajah, A., Kua, T.-A., Phetchuay, C., Horpibulsuk, S., Maghoolpilehrood, F., and Disfani, M. M. (2015). **Spent coffee grounds-fly ash geopolymer used as an embankment structural fill material.** *Journal of Materials in Civil Engineering*. doi: 10.1061/(ASCE)MT.1943-5533.0001496

- ASTM. (2006). ASTM C131. Standard Test Method for Resistance to Degradation of Small-Size Coarse Aggregate by Abrasion and Impact in the Los Angeles Machine. West Conshohocken, PA, USA: ASTM International.
- ASTM. (2007a). ASTM D422-63. Standard Test Method for Particle-Size Analysis of Soils<sup>1</sup>. West Conshohocken, PA, USA: ASTM International.
- ASTM. (2007b). ASTM D1633. Standard Test Methods for Compressive Strength of Molded Soil-Cement Cylinders. West Conshohocken, PA, USA: ASTM International.
- ASTM. (2009). ASTM D3282. Standard Practice for Classification of Soils and Soil-Aggregate Mixtures for Highway Construction Purposes. West Conshohocken, PA, USA: ASTM International.
- ASTM. (2010). ASTM D4318. Standard Test Methods for Liquid Limit, Plastic Limit, and Plasticity Index of Soils. West Conshohocken, PA, USA: ASTM International.
- ASTM. (2011). ASTM D2487. Standard Practice for Classification of Soils for Engineering Purposes (Unified Soil Classification System). West Conshohocken, PA, USA: ASTM International.
- ASTM. (2012a). ASTM C535. Standard Test Method for Resistance to Degradation of Large-Size Coarse Aggregate by Abrasion and Impact in the Los Angeles Machine. West Conshohocken, PA, USA: ASTM International.
- ASTM. (2012b). ASTM D1557. Standard Test Methods for Laboratory Compaction Characteristics of Soil Using Modified Effort (56,000 ft-lbf/ft<sup>3</sup> (2,700 kN-m/m<sup>3</sup>)). West Conshohocken, PA, USA: ASTM International.

- Bagheri, A., and Nazari, A. (2014). **Compressive strength of high strength class C fly ash-based geopolymers with reactive granulated blast furnace slag aggregates designed by Taguchi method.** *Materials and Design*, 54, 483-490. doi: 10.1016/j.matdes.2013.07.035
- Bernal, S. A., Provis, J. L., Walkley, B., San Nicolas, R., Gehman, J. D., Brice, D. G., . . . van Deventer, J. S. J. (2013). **Gel nanostructure in alkali-activated binders based on slag and fly ash, and effects of accelerated carbonation.** *Cement and Concrete Research*, 53, 127-144. doi: 10.1016/j.cemconres.2013.06.007
- Cheng, T. W., and Chiu, J. P. (2003). **Fire-resistant geopolymer produced by granulated blast furnace slag.** *Minerals Engineering*, 16(3), 205-210. doi: 10.1016/s0892-6875(03)00008-6
- Davidovits, J. (1991). **Geopolymer: inorganic polymeric new materials.** *Journal of Thermal Analysis*, 37, 1633-1656.
- Davidovits, J. (1994). **Global Warming Impact on the Cement and Aggregates Industries.** *World Resource Review*, 6(2), 263-278.
- Davidovits, J. (2013). **Geopolymer Cement.** *Geopolymer Cement, a review.*
- De Silva, P., Sagoe-Crenstil, K., and Sirivivatnanon, V. (2007). **Kinetics of geopolymerization: Role of Al<sub>2</sub>O<sub>3</sub> and SiO<sub>2</sub>.** *Cement and Concrete*, 37(4), 512-518.
- DOH. (1989). DH-S205/1989 Standard of soil aggregate subbase: Department of Highways.
- DOH. (2000). DH-S204/2000 Standard of soil cement base: Department of Highways.

- DRR. (2013). DRR244-2013 Standard of soil cement base: Department of Rural Roads.
- Duxson, P., Provis, J. L., Lukey, G. C., and van Deventer, J. S. J. (2007). **The role of inorganic polymer technology in the development of 'green concrete'**. *Cement and Concrete Research*, 37(12), 1590-1597. doi: 10.1016/j.cemconres.2007.08.018
- Gambrell, R. P., He, J., and Zhang, G. (2010). **Synthesis, Characterization, and Mechanical Properties of Red Mud-Based Geopolymers**. *Transportation Research Record: Journal of the Transportation Research Board*, 2167(-1), 1-9. doi: 10.3141/2167-01
- Guo, X., Shi, H., Chen, L., and Dick, W. A. (2010). **Alkali-activated complex binders from class C fly ash and Ca-containing admixtures**. *Journal of Hazardous materials*, 173(1-3), 480-486. doi: 10.1016/j.jhazmat.2009.08.110
- Horpibulsuk, S., Phetchuay, C., Chinkulkijniwat, A., and Cholaphatsorn, A. (2013). **Strength development in silty clay stabilized with calcium carbide residue and fly ash**. *Soils and Foundations*, 53(4), 477-486. doi: 10.1016/j.sandf.2013.06.001
- Ismail, I., Bernal, S. A., Provis, J. L., San Nicolas, R., Hamdan, S., and Van Deventer, J. S. J. (2014). **Modification of phase evolution in alkali-activated blast furnace slag by the incorporation of fly ash**. *Cement and Concrete Composites*, 45, 125-135. doi: 10.1016/j.cemconcomp.2013.09.006
- Komnitsas, K., and Zaharaki, D. (2007). **Geopolymerisation: A review and prospects for the minerals industry**. *Minerals Engineering*, 20(14), 1261-1277. doi: 10.1016/j.mineng.2007.07.011

- Kumar, S., Kumar, R., and Mehrotra, S. P. (2010). **Influence of granulated blast furnace slag on the reaction, structure and properties of fly ash based geopolymer.** *Journal of Materials Science*, 45(3), 607-615. doi: 10.1007/s10853-009-3934-5
- Lee, W. K. W., and Van Deventer, J. S. J. (2002). **The effects of inorganic salt contamination on the strength and durability of geopolymers.** *Colloids and Surfaces A: Physicochemical and Engineering Aspects* 211, 115-126.
- Mohammadinia, A., Arulrajah, A., Sanjayan, J., Disfani, M. M., Win Bo, M., and Darmawan, S. (2016). **Stabilization of Demolition Materials for Pavement Base/Subbase Applications Using Fly Ash and Slag Geopolymers: Laboratory Investigation.** *Journal of Materials in Civil Engineering*, 04016033. doi: 10.1061/(asce)mt.1943-5533.0001526
- Palomo, A., Blanco-Varela, M. T., Granizo, M. L., Puertas, F., Vazquez, T., and Grutzeck, M. W. (1999). **Chemical stability of cementitious materials based on metakaolin.** *Cement and Concrete Research*, 27(7), 997-100.
- Palomo, A., Fernández-Jiménez, A., Kovalchuk, G., Ordoñez, L. M., and Naranjo, M. C. (2007). **Opc-fly ash cementitious systems: study of gel binders produced during alkaline hydration.** *Journal of Materials Science*, 42(9), 2958-2966. doi: 10.1007/s10853-006-0585-7
- Part, W. K., Ramli, M., and Cheah, C. B. (2015). **An overview on the influence of various factors on the properties of geopolymer concrete derived from industrial by-products.** *Construction and Building Materials*, 77, 370-395. doi: 10.1016/j.conbuildmat.2014.12.065

- Phetchuay, C., Horpibulsuk, S., Suksiripattanapong, C., Chinkulkijniwat, A., Arulrajah, A., and Disfani, M. M. (2014). **Calcium carbide residue: Alkaline activator for clay-fly ash geopolymer.** *Construction and Building Materials*, 69, 285-294. doi: 10.1016/j.conbuildmat.2014.07.018
- Phoo-ngernkham, T., Maegawa, A., Mishima, N., Hatanaka, S., and Chindaprasirt, P. (2015). **Effects of sodium hydroxide and sodium silicate solutions on compressive and shear bond strengths of FA-GBFS geopolymer.** *Construction and Building Materials*, 91, 1-8. doi: 10.1016/j.conbuildmat.2015.05.001
- Phummiphan, I., Horpibulsuk, S., Sukmak, P., Chinkulkijniwat, A., Arulrajah, A., and Shen, S.-L. (2016). **Stabilisation of marginal lateritic soil using high calcium fly ash-based geopolymer.** *Road Materials and Pavement Design*, 1-15. doi: 10.1080/14680629.2015.1132632
- Puertas, F., Martinez-Ramirez, S., Alonso, S., and Vazquez, T. (2000). **Alkali-activated fly ash/slag cement Strength behaviour and hydration products.** *Cement and Concrete Research*, 30, 1625-1632.
- Rashad, A. M. (2013). **A comprehensive overview about the influence of different additives on the properties of alkali-activated slag – A guide for Civil Engineer.** *Construction and Building Materials*, 47, 29-55. doi: 10.1016/j.conbuildmat.2013.04.011
- Ravikumar, D., Peethamparam, S., and Neithalath, N. (2010). **Structure and strength of NaOH activated concretes containing fly ash or GGBFS as the sole binder.** *Cement and Concrete Composites*, 32(6), 399-410. doi: 10.1016/j.cemconcomp.2010.03.007

- Sakkas, K., Panyas, D., Nomikos, P. P., and Sofianos, A. I. (2014). **Potassium based geopolymer for passive fire protection of concrete tunnels linings.** *Tunnelling and Underground Space Technology*, 43, 148-156. doi: 10.1016/j.tust.2014.05.003
- Sarker, P. K., Kelly, S., and Yao, Z. (2014). **Effect of fire exposure on cracking, spalling and residual strength of fly ash geopolymer concrete.** *Materials and Design*, 63, 584-592. doi: 10.1016/j.matdes.2014.06.059
- Somna, K., Jaturapitakkul, C., Kajitvichyanukul, P., and Chindaprasirt, P. (2011). **NaOH-activated ground fly ash geopolymer cured at ambient temperature.** *Fuel*, 90(6), 2118-2124. doi: 10.1016/j.fuel.2011.01.018
- Sukmak, P., Horpibulsuk, S., and Shen, S.-L. (2013). **Strength development in clay-fly ash geopolymer.** *Construction and Building Materials*, 40, 566-574. doi: 10.1016/j.conbuildmat.2012.11.015
- Suksiripattanapong, C., Horpibulsuk, S., Chanprasert, P., Sukmak, P., and Arulrajah, A. (2015). **Compressive strength development in fly ash geopolymer masonry units manufactured from water treatment sludge.** *Construction and Building Materials*, 82, 20-30. doi: 10.1016/j.conbuildmat.2015.02.040
- Temuujin, J., van Riessen, A., and Williams, R. (2009). **Influence of calcium compounds on the mechanical properties of fly ash geopolymer pastes.** *Journal of Hazardous Materials*, 167(1-3), 82-88. doi: 10.1016/j.jhazmat.2008.12.121
- Yusuf, M. O., Megat Johari, M. A., Ahmad, Z. A., and Maslehuddin, M. (2014). **Strength and microstructure of alkali-activated binary blended binder**

**containing palm oil fuel ash and ground blast-furnace slag.** *Construction and Building Materials*, 52, 504-510. doi: 10.1016/j.conbuildmat.2013.11.012

Zhang, M., Guo, H., El-Korchi, T., Zhang, G., and Tao, M. (2013). **Experimental feasibility study of geopolymer as the next-generation soil stabilizer.** *Construction and Building Materials*, 47, 1468-1478. doi: 10.1016/j.conbuildmat.2013.06.017



## CHAPTER VI

### CONCLUSIONS AND RECOMMENDATIONS

#### 6.1 Summary and conclusions

This thesis consists of three main objectives. The first is to investigate the possibility of using fly ash (FA) - based geopolymer to stabilize marginal lateritic soil (LS) to be a sustainable bound pavement material and to study the factors influencing strength and microstructure development of LS-FA geopolymer. The second is to study the effect of Calcium Carbide Residue (CCR) as an additive on strength and microstructure development of FA geopolymer stabilized marginal lateritic soil. The third is to study the effect of Ground Granulated Blast Furnace (GBFS) as an additive on strength and microstructure development of FA geopolymer stabilized LS. The conclusions can be drawn as follows:

##### 6.1.1 Stabilization of marginal lateritic soil using high calcium fly ash – based geopolymer

This chapter presents the effects of alkaline activator and curing time on UCS and microstructural characteristics of LS stabilized with high calcium FA based geopolymer. The possibility of using this stabilized LS as a bound pavement material was also examined and discussed. A liquid alkaline activator is a mixture of sodium silicate ( $\text{Na}_2\text{SiO}_3$ , NS) solution and sodium hydroxide (NaOH, NH) solution at various NS:NH ratios. The results show that the UCS increases with the curing time and the 7-day UCS for all NS:NH ratios tested meets the local national standard

as pavement bound material for both light and heavy traffic. The maximum early strengths at 7 days of curing are found at NS:NH of 90:10, where Calcium Silicate Hydrate (CSH), cementitious products from high calcium FA and NS plays a significant role. The development of geopolmerization products (Sodium Alumino Silicate Hydrate, NASH) come into play at longer duration as they are time-dependent. The maximum 90-day strength is thus found at NS:NH ratio of 50:50. This chapter indicates that LS can be stabilized by high calcium FA based geopolymer and used as environmental-friendly and sustainable material pavement materials, which will subsequently decrease amount of Portland cement (PC) consumption. The economical NS:NH ratio for both light and heavy traffic pavement materials is suggested to be 50:50.

### **6.1.2 Strength and microstructure of marginal lateritic soil stabilized with calcium carbide residue and fly ash geopolymer**

This chapter presents the evaluation of two waste by-products: FA and CCR as a precursor and an additive, respectively in the development geopolymer binder for stabilizing LS as sustainable pavement application. The liquid alkaline activator is a mixture of NS and NH solution at a concentration of 5 molars. UCS of LS-FA geopolymers at different influential factors (curing times, NS:NH ratios and CCR replacement ratios) is measured. Scanning Electron Microscopy (SEM) analysis was subsequently performed to investigate the effect of influential factors on UCS development. The soaked 7-day UCS of marginal lateritic soil-FA geopolymer with and without CCR at various NS:NH ratios tested meets the strength requirement for both light and heavy traffic pavement specified by the local national authorities. For all NS:NH ratios, the early 7-day UCS increases with increasing CCR replacement

ratio whereby the cementitious products increase with CCR replacement ratio and the significant cementitious products are observed at CCR = 30% (the highest CCR replacement ratio tested). However, the CCR replacement ratio providing the maximum 90-day strength is found at 20%. FA particles in lateritic soil-FA geopolymer at excessive CCR replacement ratio of 30% are evidently spongy and cracked due to early aluminosilicate gel precipitation and generated heat and hence the subsequent reduced strength. The CCR replacement is recommended for low NH geopolymer binder (NS:NH ratios  $\leq$  90:10) and the optimum CCR replacement ratio is found to be 20%. The maximum 90-day UCS is found to be 18.80 MPa at NS:NH = 90:10 and CCR = 20%. This research seeks to enable CCR traditionally destined for landfill to be used as a promoter in geopolymer binder, which is significant in addressing the sustainable usage of CCR from engineering, economical and environmental perspectives.

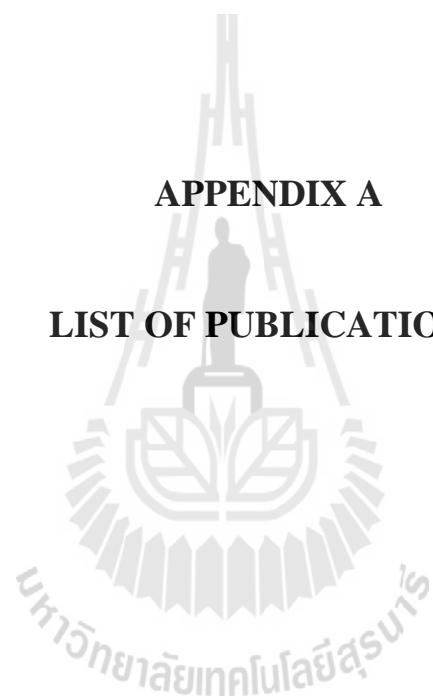
### **6.1.3 Strength and microstructure analysis of lateritic soil stabilized with fly ash and ground granulated blast furnace slag precursors**

This chapter presents the effect of GBFS as an additive on UCS and microstructure development of FA geopolymer stabilized LS. GBFS is used as an additive in alkaline activator to enhance the strength of FA based geopolymer stabilized LS as a pavement base material. The microstructural development is observed through SEM and XRD analysis to understand the role of influential factors, controlling the strength development. The significant factors studied consisted of GBFS content, NS:NH ratio, and curing time. The 7-day soaked UCS of FA- GBFS geopolymer stabilized LS at various NS:NH ratios tested meets the standard of national road authorities of Thailand. The GBFS replacement is recommended for

high NS:NH ratios because early and long-term UCS is significantly improved. The optimum GBFS replacement providing the highest 60-day UCS is found to be 19.97 MPa at NS:NH = 90:10 and GBFS = 10%. The cementitious products of FA – GBFS geopolymer stabilized LS are a coexisted NASH, CSH and calcite.

## 6.2 Recommendations for future work

- This study used FA as a precursor and used CCR and S as an additives. The other precursor such as rice husk ash, bagasse ash, metakaolin and other calcium-rich additives can be considered for further study.
- NS and NH were used as alkali activators for geopolymer system in this study. It is recommended to study other alkali activators in the further work.
- It is recommended to study durability against wetting–drying cycles of FA-CCR and FA-S geopolymers stabilized soil.
- It is recommended to study carbon foot prints and life cycle analysis of FA-CCR and FA-S geopolymers stabilized soil.



**APPENDIX A**

**LIST OF PUBLICATIONS**

## List of Publications

- Phummiphan, I., Horpibulsuk, S., Sukmak, P., Chinkulkijniwat, A., Arulrajah, A. and Shen, S-L. **Stabilisation of marginal lateritic soil using high calcium fly ash-based geopolymer**. Road Materials and Pavement Design. 2016:1-15.
- Arulrajah, A., Mohammadinia, A., Phummiphan, I., Horpibulsuk, S., and Samingthong, W. **Stabilization of recycled demolition aggregates with calcium carbide residue based geopolymers**. Construction and Building Materials. 2016 (To be published).
- Phummiphan, I., Horpibulsuk, S., and Sukmak, P. "**Strength and Microstructure of Marginal Lateritic Soil-Fly Ash Geopolymer**." Proceeding of the International Conference on Advances in Civil Engineering for Sustainable Development (ACESD 2014), 27-29 August 2014, Nakhon Ratchasima, 719 - 724.
- Phummiphan, I., Leelaphrapaporn, S., Wattana, K., Horpibulsuk, S., Kongkerd, C. and Namee, S. (2015), "**Stabilization of Marginal Lateritic Soil with Calcium Carbide Residue - Fly Ash Geopolymer**", Proceedings of the 10<sup>th</sup> National Transport Conference, 18 December 2015, Chiangmai, Thailand. CD Version, (in English).
- Kongkerd, C., Phummiphan, I., Horpibulsuk, S., Leelaphrapaporn, S. and Wattana, K. (2015), "**Strength Development of Marginal Lateritic Soil Stabilized with Slag-Fly Ash Geopolymer**", Proceedings of the 10<sup>th</sup> National Transport Conference, 18 December 2015, Chiangmai, Thailand. CD Version, (in English).

Leelapraphaporn, S., Phummiphan, I., Sukmak, P. and and Horpibulsuk, S., (2015),  
**“Strength and Microstructure Development of Crushed Rock Soil  
 Aggregate Stabilized with Fly Ash Geopolymer”**, Proceedings of the 20<sup>th</sup>  
 National Convention on Civil Engineering, 8-10 July 2015, Chonburi,  
 Thailand. CD Version, (in English).

Chareonwutirap, S., Chareonwutirap, K., Singhasanee, D., Kongkerd , C., and  
**Phummiphan, I.**, (2015), **“Strength and Microstructure Development of  
 Crushed Rock Soil Aggregate Stabilized with Fly Ash Geopolymer”**,  
 Proceedings of the 20<sup>th</sup> National Convention on Civil Engineering, 8-10 July  
 2015, Chonburi, Thailand. CD Version, (in English).

**Phummiphan, I.**, Cheonklang, P., Sukmak, P., Thiha, S., and Horpibulsuk, S.,  
 (2015), **“Geopolymer stabilized marginal lateritic soil”**, **Proceedings of the  
 5<sup>th</sup> Thailand symposium on rock mechanics**, 22-23 January 2015, Nakhon  
 Ratchasima, Thailand. (in English).

Phummiphan, I., Cheonklang, P. and Horpibulsuk, S., (2015), **“Strength and  
 Microstructure of Marginal Crushed Rock Soil Aggregate Stabilized by  
 Fly Ash Geopolymer”**, Proceedings of the 5<sup>th</sup> Thailand symposium on rock  
 mechanics, 22-23 January 2015, Nakhon Ratchasima, Thailand. (in English).

Phummiphan, I., Sukmak, P. and Wathana, K., (2014), **“Compressive Strength of  
 Marginal Lateritic Soil Stabilized with Fly Ash Geopolymer”**, Proceedings  
 of the 9<sup>th</sup> National Transport Conference, 20-21 November 2014, Bangkok,  
 Thailand. CD Version, (in English).

Phummiphan, I., Horpibulsuk, S., Kongkerd, C., Sukmak, P. and Chantra, W., (2014),  
**“The Strength Development of Lateritic Soil Stabilized with Slag - Fly**

**Ash Geopolymer**”, Proceedings of the 9<sup>th</sup> National Transport Conference, 20-21 November 2014, Bangkok, Thailand. CD Version., (in English).

Leelapraphaporn, S., Phummiphan, I., Sukmak, P., Siridaothong., S. and Sansri, P. (2014), “**The Strength Development of Crushed Rock Soil Aggregate Stabilized by Fly Ash Geopolymer**”, Proceedings of the 9<sup>th</sup> National Transport Conference, 20-21 November 2014, Bangkok, Thailand. CD Version, (in English).



## **BIOGRAPHY**

I, Mr. Itthikorn Phummiphan was born in September 1977 in Roi-et, Thailand. I received my Bachelor's degree in Civil Engineering from School of Civil Engineering, Suranaree University of Technology in 1999. After graduation, I have been working as a civil engineer in the Department of Rural Roads, Ministry of Transport. I obtained my Master's degree in Civil Engineering (Transportation) from Department of Civil Engineering, Prince of Songkla University in 2003. I have been granted a scholarship by Department of Rural Roads in 2014 to pursuing my Ph.D. study in Construction and Infrastructure Management, School of Civil Engineering, Suranaree University of Technology. During my Ph.D. study, I have had an opportunity to conduct my oversea research at Department of Civil and Construction Engineering, Swinburne University of Technology, Victoria, Australia from June 1, 2014 to October 31, 2015. So far, I have published 2 papers in reputed international journals, 1 paper in international conference and 9 papers in national conferences. I am currently interested in geopolymer application to pavement and geotechnical works.